Design and Experimental Evaluation of a Unidirectional Flow Collective Air Pumps Wave Energy Converter

by

Julio Cesar Rodriguez Macedo

B.Sc., ITESM, 2001

M.Sc., University of Victoria, 2006

A Dissertation Submitted in Partial Fulfillment of the

Requirements for the Degree of

DOCTOR OF PHILOSOPHY

in the Department of Mechanical Engineering

Design and Experimental Evaluation of a Unidirectional Flow Collective Air Pumps Wave Energy Converter

by

Julio Cesar Rodriguez Macedo

B.Sc., ITESM, 2001

M.Sc., University of Victoria, 2006

Supervisory Committee

Dr. Afzal Suleman , Supervisor

(Department of Mechanical Engineering)

Dr. Bradley Buckham , Departmental Member

(Department of Mechanical Engineering)

Dr. Nikitas Dimopoulos, Outside Member

(Department of Electrical and Computer Engineering)

Supervisory Committee

Dr. Afzal Suleman , Supervisor

(Department of Mechanical Engineering)

Dr. Bradley Buckham , Departmental Member

(Department of Mechanical Engineering)

Dr. Nikitas Dimopoulos, Outside Member

(Department of Electrical and Computer Engineering)

ABSTRACT

Commercial viability of Wave Energy Converters (WEC) depends on addressing not only the energetic efficiency, but also in solving the practical issues related to manufacturing methods, access to technology, handling, transportation and installation, operation and maintenance, impact on marine life and most importantly the cost per kW-h. The UFCAP WEC is one concept which has the potential to facilitate handling, manufacturing, and installation activities as well as to be able to lower the current wave energy cost per kW-h, however its feasibility had not been properly assessed nor proved. It consists of multiple interconnected Oscillating Water Columns (OWC) chambers, it is modular, and simple, with no-moving parts in contact with the water and can use a simpler one-direction turbine which is more economic, and more

efficient than self-rectifying turbines used in most of the OWCs devices. Testing of the device to fully assess its feasibility required an low pressure-drop/crack-pressure check-valve, and a customized turbine which were developed during the present work. Check-valves are widely used in the industry for medium or high-pressures, but were not available at all for large-flows with low-pressure-differences. A novel check-valve was devised for this application, along with the scaled UFCAP prototypes developed to be tested in a wave-flume and in the ocean to validate UFCAPs concept feasibility, and identify critical design parameters and features such as the conduit/air-chamber ratio. Ocean tests allowed to observe performance at component and assembly levels, learning new failure-modes and stablishing best-practices for future deployments. Testing confirmed the UFCAP WEC is not only an idea, but a concept which works and can generate electricity at a competitive cost.

Contents

List of Tables

List of Figures

ACKNOWLEDGEMENTS

I am surprised to have so many people to thank who somehow supported this work during these years. I would like to start with my supervisor Professor Afzal Suleman who is the person who encouraged me to pursue a PhD Degree. I am thankful for his unconditional support, encouragement, and advice during the last few years. Chronologically, my good friends from Continental, the brothers Ral and Ricardo Garca who support me filling my gaps in electronics, from testing generators and turbines with a few LEDs, creating preliminary handcrafted PCBs and selecting the pressure sensors, up to building and programing a full measurement device with multiple pressure sensors, couple to a DAQ and a computer which I could not be able to build by myself; and Jonathan Galindo who spend hours and hours helping me uninterestedly in building a huge prototype with conduits 80 meters long, and mooring so voluminous that could not fit in the building, and had to manage creative ways to solve it; along with his support during a complex installation in ocean, moving, advising, calibrating, driving or doing whatever activity was necessary plus motivating and encouraging in not giving up after the first unsuccessful trial. The team from CFE who supported with the marine installation and all the facilities, from the leadership Carlos Sanchez, to the whole local team of 9 people in Manzanillo whose supported from presenting the beach to performing the whole marine handling with ships and divers Nestor and Chaparrito who deserve a special mention for their perseverance hours and hours of trials below an intense sun until it finally worked. Special mention to Luis Perez Carlos from CFE, who became not only a colleague but a good friend who unexpectedly left us behind, whose experience in ocean waves, professionalism and commitment with the project, introducing and connecting me to people who finally open me doors to make possible the ocean deployments. My dear team of colleagues from RDZ Andrea, Carlos, Ricardo, Fernanda supporting aspects of the

Wave-Flume Prototype. A big thank to Erick, Rodolfo and Edgar, from UNAM for allowing me full access to the Wave-Flume, and their vast knowledge with the tests. My colleagues and friends from IIE, Ernesto Neri for all the hours working out giving it shape to a professional proposal, and Alonso Alvarado for supporting the initiative To my colleagues at UVic, Andre, Mario, Kerem, supporting me at a distance whenever I needed something at UVic, and Nicole, Rasoul, Elena, Jose, Ji, Barish, for their company, good talk, making my moments at Uvic more pleasant. Finally, but more important, to my wife Jany and kids Cristobal and Jos Pablo who suffered due to my absence whenever the peak workload happened, and now wisely understand and support this adventure as a future asset.

DEDICATION

to Jany, Cris, and little Jose Pa

Nomenclature

a	distance to max comb
a_w	amplitud ocean wave
a_{ch}	amplitud water level variation inside the air chamber
A_{cond}	conduit section area
α	angle of attack
β_1'	blade entry angle
β_1	air entry angle
β_2	air exit angle
c	cord
C_a	axial velocity
C_{amod}	modified axial velocity
C_d	drag coefficient
CD_A	losses due to wall, nose
CD_S	secondary losses
C_{DP}	losses due to airfoil
CD_T	total losses
C_l	lift coefficient
δ	deviation angle
ΔP_{avail}	available pressure
$\varnothing$	air chamber diameter
η	surface elevation
F	Energy flux
F_i	inertial force
F_r	Froude number
F_g	gravitational force

X_F	subscrit F for full size device's characteristic
Φ	volumetric flow
g	gravity
H	height (blade, or wave-height)
H_t	Pressure losses due to turbine
h_s	significant wave height
K_e	generator electric constant
L	representative legth scale
λ	wavelenght
m	proportionality constant
X_M	subscrit M for model's characteristic
$\dot{m}$	mass flow
μ_{air}	air absolute viscosity
n	number of blades
N	number of air chambers
ν	kinematic viscosity
ω	circular frequency
P_x	pressure at location x
r	ration wavelenght/airchamber
Re	Reynolds number
r_m	turbine median radius
ρ	density $[kg/m^3]$
ρ_w	salted water density
s	space between blades
sf	scale factor
$\dot{Q}$	volumetric Flow

sf	scaling factor
T	wave period (WEC)
Θ	comb angle
U_{tan}	tangent velocity
V	fluid velocity
$\mathcal{V}$	voltage
V_1	air entry velocity (blades)
V_2	air exit velocity (blades)
v_x	velocity at location x
$\dot{W}$	power (WEC)
x	aspect ratio (blade)
ξ	Xi similarity parameter
ζ	rotation angle
z	depth

Acronynms

BCs	Boundary Conditions
CFE	Comision Federal de Electricidad
GHG	Green House Gases
OWE	Ocean Wave Energy
OWC	Oscillating Water Column
RPM	Revolutions per Minute
TSR	Tip Speed Ratio
UFCAP	Unidirectional Flow Collective Air Pumps
WEC	Wave Energy Converter

Chapter 1

Introduction

1.1 Motivation

Despite Wave Energy Converters have been in intense R&D the last three decades, they cannot be considered a mature technology. When a concept is a clear winner, the community adopt it and work in optimizing it. However, in the case of WECs where many concepts have been patented so far, still new concepts rise every year, [1, 2] trying to make wave energy more competitive, and increase the efficiency. From the large number of devices, only a few of them have gotten to full size deployment, and even then, major accidents have occurred when they have gotten to 1 MW capacity and tested at the ocean [3, 4]. A reliable and competitive technology is needed and efforts are being done all over the world. Nonetheless, most of the research made so far was focused in academic modeling, attempting to optimize a component or improve the device hydrodynamically, but rarely an approach to face real commercialization issues which study integrally the problem has been taken. In this work, the problem of real implementation was envisioned integrally trying to prove the concept of a device which focus primarily in solving practical issues such as cost of energy, manufacturing,

handling, maintenance, and installation problems.

1.2 Background

1.2.1 Wave Energy Converters

It is mandatory to take care of the planet Earth better than has been done in the past. At the same time, it is necessary to satisfy the societal energetic needs. Renewable energies are an alternative to supply energy in a sustainable way reducing the use of fossil fuels and mitigating climate change [5, 6]. Ocean waves are a predominant form of renewable energy, they are formed mainly from wind, and offer some distinct characteristics. Ocean waves are a concentrated form of wind energy [7]. Their power is measured per length of crest, they normally reach 10-50 kW/m of crest [8], but could reach 2000 kW/m of crest during extreme conditions [3]. The wave resource assessment is the first step to define the correct strategy for its utilization and design of WECs [9]. For this reason, it has been included in different studies either per region e.g. the gulf of Mexico [10], US Coast [11], California [12], Vancouver Island , or per complete countries like Ireland, Portugal, UK [13], or Japan [8]. Worldwide wave power has been estimated to be 1-10 TW [14]. More important than the individual value, it is undoubtedly a large resource. Nevertheless, energy extraction from ocean waves is complex [7]. The slow (0.1 Hz), high force, random ocean waves, must be converted into smooth electricity connected to the grid at 60Hz. Devices to extract energy from ocean waves are called Wave Energy Converters (WECs). Due to the multiple combinations from the available variables, such as location (shore, near-shore, off-shore), height, position (underwater, interface water-air), pressure-driven, velocity-driven, ocean waves provide a wide range of possibilities to capture energy. Over a 1000 patents of WECs have been published [3, 7, 15], and a large number of

different prototypes have been built and tested [16, 3]. However as mentioned earlier, achieving long-term operability with competitive production cost-rates is complicated and then, from a long list of concepts, only a few devices have been tested connected to the grid and are close to commercial stage [17, 18]. Drew et al. includes UK developers [3]. In a review by the IEA, a list of developed WEC is provided [8]. An updated review of the available technologies is provided by Falcao [9]. There are important challenges that still need to be addressed to make wave energy converters a competitive technology for energy generation [19]:

- Handling manufacturing and installation is still an issue. WECs are large devices and their size limit manufacturing to shipyards increasing the cost, and make installation real complicated for enormous devices. There are examples of real pilot plants which have delayed installation for a few months waiting for calm weather, or crashed during installations maneuvers. Improving handling is a forgotten but real need.

- Impact on marine life, need to be minimized to get acceptance and compliance with environmental regulations.

- Inferior performance due to rapid variation and a wide range of incoming wave heights and wave periods. Rapid-tunability is one of the most important characteristics to elevate WECs efficiency. Phase-control needs to adjust the device's parameters rapidly enough for the incoming waves, if this is done slowly, part of the usable wave energy will be wasted. The inherent capacity of a device to be rapidly tunable is beyond a good phase-control strategy, depends on the physics of the device (specifically on the inertia of the controlled part, for example adjusting the angle of attack of a wells turbine has low inertia compared to adjusting a heavy point absorber going up and down).

- The ocean is a very inhospitable environment. Although WECs are designed for the most common sea estates, they need to be designed robust to survive the less frequent harsh environment and then cost is incremented. A mechanism or a design able to survive during storms without increasing the cost excessively is needed.

- The elevated cost is still a limitation. Wave energy selling price in Europe ranges 0.06-0.34 €/kWh , levelized-cost ranges from 0.06-0.64 €/kWh [20, 21]. The large variation can be explained in terms of the differences in available wave resource in the zone, the type of technology quoted, and the government subsidies in the country. A detailed and updated list of prices can be found at [22, 20] . O'Connor et al. [23] provides cost for different WEC scales, cost of infrastructure such as mooring, foundations, grid connection, etc., cable cost for different KV, installation cost and feed-in tariff. Dalton et al. [18] provide cost of electricity in different countries, cost of electricity reported from different sources, cost of cable, and more detailed the electricity tariff for the Pelamis WEC at different wave conditions. Dunnet and Wallace compare three WECs and detailed cost projections on Canada's coasts. Prest et al.[14] evaluate the cost of wave energy including interconnection cost with regards to proximity between population and wave resource. Wave energy cost has been reducing over the time as any other technology does. However, it is still not competitive against the more widespread wind-energy [24]. Making WECs competitive against other sources of renewable energy necessarily requires reducing the energy cost [25, 24].

Many WECs have been conceptualized trying to address the challenges and find an ultimate real solution for wave energy conversion. A first classification of WECs can be made by its type being these a) attenuators, b) point absorbers, and c) Ter-

minators. Attenuators are those which lie parallel to ocean waves, are large when compared to point-absorbers and ocean wave-lengths, they take some energy from the waves but still part of the wave may pass through. The Pelamis WEC [18] is the most representative of this category. A point-absorber is the WEC which is small when compared to the wavelength and then, wave direction is irrelevant to it. Most of the existing WECs belong to this category. Examples of this kind are the CETO [26], and Powerbuoy [27]. Finally, terminators are those WECs which receive the front wave and finish it extracting its energy virtually completely. Examples of this kind are the Salters Duck [28], and the Wave Dragon [29, 30, 31]. Another important feature to identify about WECs is *power take off (PTO)* which is the mechanics used to extract the energy and convert it into usable power. Despite the large variety of energy capture methods, power take off mechanisms are reduced in quantity and common among many WECs. At the end, WECs must generate some movement to drive either a linear-generator, or a rotary electrical generator, the most widespread. Among the most developed and efficient WECs power take off (PTO) methods are hydraulic motors, and air-turbines, both coupled to a rotary generator. Hydraulic pistons are a good fit with ocean waves since they both handle large forces at low frequencies (0.1 Hz), the high pressurized fluid can then, rotate a hydraulic motor at higher frequency which drive a generator [15]. Nevertheless, several of them require an arm with a fixed length, their efficiency is good for a given wave length, and decreases rapidly for other wavelengths (not point absorbers). A second interesting PTO is the turbine-generator which also make a precise fit converting low- frequency-large-forces from ocean waves into rapid rotary movement on the generator close to the desired 60 Hz for electricity production. Turbine-generator PTOs have a more natural way to handle a variety of wave sizes, and adjust for wave variations and hence, their range for reliable performance is wider. An additional WECs classification is made

by its mode of operation. They can be submerged-pressure-differential, oscillating-wave-surge converter, overtopping devices, and oscillating-water-column (OWC) [3]. In the present work, the OWC mode of operation was selected as the most reliable in the long term (see section 1.2.2), and then, only OWC mode of operation will be commented. Additional information about the others modes of operation is available in [3, 1, 32].

1.2.2 Oscillating Water Column

Oscillating Water Column (OWC) devices are the most mature WEC technology in terms of number of pilot plants around the world, and also in years of operations connected to the grid [33]. OWC plants operate or were in operation in Portugal, Scotland, Norway, Japan, India, Ireland, Australia, and Spain [8, 25] and performance records connected to the grid for more than 15 years [25, 28] for pilot plants, and more than 25 years if the research-tool period is included [34].

OWC WECs consist of a vertical container partially submerged, which is filled with water and air, having a large opening at the bottom part of the container which allows ocean waves to modify the pressure and then the water level at the containers interior. The water column at the containers interior is exited moving up and down creating the oscillating water column. Taking advantage of the change in height of the water level, the water-air interface is used as a reciprocating piston which pump the air above it and pass it through a second opening at the top of the container creating an oscillating airflow which turns a self-rectifying turbine which can rotate always in the same direction independently if the air is coming from one side or the other, and generate electricity [35, 36, 37]. OWC devices can be either on-shore such as the Limpet plant in the UK and the Azores in Portugal, or near/off-shore installations such as Energetech in Australia, or the Mighty Whale in Japan [38]. An

additional OWCs classification is provided by Falcao et. al according to its structure they can be *fixed structure OWC, breakwater-integrated OWCs, floating-structure, floating structure WECs with interior OWC, or multi-OWC devices* [16].

There are several types of OWC devices regarding its structure. The first kind are the *fixed structure* comprising those carved-on on-shore rock and built in concrete normally, and those built of steel usually and permanently fixed when installed on-shore or near-shore. The former has the advantage to have all the equipment on land with easy access for maintenance and relatively dry and safe, such as the Pico Azores in Portugal or the Islay in Scotland but their sites are limited since they are constrained to have the appropriated topography and soil, be close to populations with roads access for construction [25]. This kind of devices have proved very good survivability even with harsh environment. The later have a couple of the most distinguished accidents in WECs history, both made with large 1 MW *fixed structure* OWC devices, the first occurred in Scotland in 1995 and the second in Australia in 2014. The second type are the *breakwater-integrated* OWCs, they serve a multipurpose objective, a barrier (breakwater) for a port protection, and a WEC for electricity generation altogether. When a break-water investment is going to be made anyway for port protection, merging such an investment with a WEC results in an interesting project achieving savings using a single structure for two projects. It shares also the advantages of having all the delicate components in land for easy access and safety. Examples of this are the Sakata in Japan, and the Mutriku in Spain [25, 9]. The next type are the *floating structure* OWCs which are freely floating with 6 degrees of freedom, and might be either near-shore or off-shore structures. Location is less restrictive with respect to fixed-structure ones. This is the most frequently developed OWC with devices in Europe, Asia and America. One of the first known OWC devices was the Mighty Whale or the Masuda device on the 1950s, which is a floating OWC.

They offer better survivability characteristics versus the *fixed structur*e steel OWCs because they move along vs. resisting the water impact during storms, and they are less expensive to build. Another type of devices is the *floating structure with interior OWC*, which have an isolated fluid inside them, with the advantage of avoiding marine corrosion on the turbine due to sprayed salted water, and the disadvantage that their construction must be more complex than the simple *floating structure* with a double wall and then more expensive.

Finally, there are also the *multi-OWC* devices which consist in a multiple interconnected OWCs. The first record of this devices having a plurality of OWCs is the UFCAP WEC in 2006 which consist of several interconnected and independently floating cylindrical air-chambers with the ability of using a conventional wind-turbine by rectifying the airflow with double conduits and check-valves [39]. The Seabreath and Leancon consist of a plurality of rectangular air-chambers glued in a single block which are coupled also with check-valves and connected to high pressure and low-pressure ducts which rotate a conventional unidirectional air-turbine [32]. While they three *multi-OWC* are *floating-structures*, the UFCAP is clearly a point absorber, while the Seabreath and Leancon being larger devices, are one piece attenuators. The later two, must be considerably more robust and expensive than the UFCAP to ensure survivability during storms. The UFCAP air-chambers can move independently of each other which reduces the stresses imposed to the device. The aerodynamic efficiency of the UFCAP is expected to be better due to the soft transitions and curves along their conduits, and the circular section of their conduits versus sharp corners, rectangular ducts from the Seabreath and Leancon. The three *multi-OWC* devices are at initial stages of R&D and further work need to be done to prove their advantages and commercial viability. A complete list of OWC devices and further details on WECs other than the one covered in this work are described by Falcao et. al. in

[4] and Delmonte et al.[32].

Apart from the last three described *multi-OWC* devices, almost the rest of OWC WECs use self-rectifying turbines which accept airflow from either side. Over the last decades, several turbines capable of accepting oscillating flows have been designed, examples are the Dennis-Auld, Radial Flow Self Rectifying, Wells, Impulse, Hydro-air, Bi-radial, Savonious, and Cross-flow [40, 41, 42, 43, 16]. Among them the most commonly used turbine in OWC WECs is the Wells-turbine, followed by the impulse-turbine mainly due to their higher overall efficiency, being the former the best followed by the later. Additionally, most of the available OWC air turbines literature correspond to these two types of turbines. There are several reports which investigate their hydrodynamic performance in depth, compare them, optimize shapes, advise phase control strategies, for steady-state and irregular waves conditions.

Thakker & Abdulhadi investigated the performance of a Wells turbine with unsteady unidirectional, and bi-directional flow using 4 blade profiles and two different solidities [42]. Torresi et al. described numerically a 3D steady flow field for a high solidity Wells turbine [44]. Amundarain et al. analyzed the problem of Wells turbine stalling utilizing two different control strategies, rotational speed control, and airflow control [45]. Kim et al. investigated numerically the blade sweep impact on the performance of the Wells turbine, finding it has a large influence. [46]. Taha et al. [47] investigated the performance of a Wells turbine experimentally and show that its performance is influenced by tip clearance complemented with numerical studies which can provide flow details not possible to observe with the experiments. Folley et al. [48] compared the analytical vs. the experimental performance of the Limpet cotra-rotating Wells turbine. Ceballos et al. [49] studied several control strategies for generators powered with an OWC. Even though Wells turbine is leading the self-rectifying turbines, it is noisy, and overall efficiencies are still below equivalent uni-

directional turbines since their efficiencies drop more rapidly for air-velocities other than optimum [32]. In the Wells turbine, the airfoil must be symmetric, and cannot be twisted. On the contrary, unidirectional turbines can use non-symmetrical airfoils which maximize efficiencies over a wider range of air-velocities, and can be twisted which adjust the angle of attack along all the blade over the required range reducing the noise. The use of a unidirectional air turbine requires a check valve able to operate with very large airflows at very low pressure differences keeping good aerodynamic performance otherwise losing a great part of the available power. Such kind of check valves were not available before this work. An alternative for avoiding the use of self-rectifying turbines without the use of check-valves is the twin-turbine, however the increment in cost need to be considered in a real application since a second turbine is needed [43]. Another attempt to increase the efficiency of Wells turbine is the contra-rotating Wells turbine which also use a second set of blades that indeed improve efficiency but increase the cost of the turbine [48].

1.2.3 WECs R&D

Development of Wave Energy Converters is conducted basically through four different forms: Analytically (solving equations for a customized simplified model), Numerical Simulation (CFD, VOF meshed methods, meshless methods, etc.), Lab Tests (Wave Flume, and Wave Tank experiments), and Ocean Tests. Normally, due to economical and risk criteria, the research and development starts with the idea, followed by the exploration of the concept feasibility through theoretical and numerical simplified models, and later the scaled lab test, then larger, test in the lab or the field. Even though this is common for various technologies, the Sandia National Laboratories have designated a Technology Readiness Level classification specifically for WECs to denote the level of maturity of any WEC, depending on the type of work completed,

size, and duration of tests. The level 1 and 2, comprises the concept, level 3 includes the numerical model and concept exploration, level 4 includes the design of the basic component models where a medium scale concept verification is necessary, level 5 requires the development of specialized numerical models focused in full-scale concerns and some testing, level 6 focus on the system integration of the device and may include specialized numerical models as well as experiment in controlled conditions including other sub- assemblies. Level 7 contain the full testing in the ocean for a brief period. Level 8 is a long term full scale test, and level 9 means the device is ready and performs according to expectations [11].

During the last two decades Wave Energy Converters have been an area of active research [1]. Particularly, in the case of oscillating bodies and oscillating water columns, the most relevant theoretical hydrodynamic models correspond to Evans [50] where the oscillating water column was supposed to have a flat interface and operate as a reciprocating piston while interacting with the waves and a spring-like term was added to account for the damping, and Evans and Porter [35] who expanded the theory to a two-dimensional OWC assuming the air to be incompressible which is a reasonable assumption given the low pressure-difference, and the turbine to be linear. A transformation between the "pressure distribution" and the rigid-piston methods to describe OWC is presented by Brendmo et al. [51] where they included analog electric circuit diagrams to represent mass-spring loads. Sarmento and Falcao [52] presented a theory where the air is incorporated as compressible fluid, and Falnes and McIver [53] generalized the theory for floating OWCs. Evans and Porter further included the 3-dimenional case [54]. Deng et al. developed and analytical theory to improve the efficiency of an V-channel OWC [55].

While some efforts and progress has been made to understand theoretically the OWCs, numerical simulations are necessary to evaluate specifics of design and eval-

uate situations beyond the applicability range of the theories, such as real irregular wave conditions, or incorporation of non-linearities and transients effects where the theory does not apply. For example, the theory from Sarmento and Falcao, mentioned above, is valid for small wave-heights to wavelength ratios only.

Much of the WECs research has been done numerically. Examples of recent studies on OWC are that made by Kamath et al. [56] who studied the external damping effect on the OWC in a 2D numerical wave tank by including it in a form of a porous media. Luo et al. computed the efficiency of an OWC with CFD [57]. Senturk and Ozdamar investigated the energy extraction of an OWC with an opening on the wall using linear wave theory with matched eigenfunctions expansions [58]. They neglected compressibility effects. They found the bottom opening size has a substantial impact on the performance. It might be a similar effect on the submersion height in the UFCAP device.

As discussed earlier in de Sandia National Laboratories roadmap for development, the concepts are first evaluated numerically to determine if moving forward to the next stage of development is warranted. Therefore, the many concepts ready in the literature are evaluated numerically and many of them do not progress to the next stages of development. Additionally, the availability of Wave-Flume is limited and the resources needed to create a prototype and operate the Wave-Flume along with the measuring and peripherical equipment are large which limits access to testing. Conversely, numerical simulations are also useful to show fluid details that are not observable during the experiments, they can also be a complement of the tests.

Numerical simulations normally use a numerical wave tank which is the numerical representation of either a Wave-Flume or Wave-Tank [59, 60] which one of its boundaries act as the wave-maker, and also have a beach-like means to reduce wave reflection from the end of the numerical wave tank. This configuration allows to observe waves-

WEC interaction. Depending on the simulated WEC and conditions the approaches might vary. In the case of OWC, the turbine effects need to be considered. Turbines are simulated by porous media and small openings for linear and non-linear analysis respectively [56]. The other feature which demand special attention when simulating an OWC is the free surface where the water-air interface occurs. Usually, the Volume of Fluid model is utilized for meshed analysis [61] and enable the elements to handle water and air fluids. An additional advantage of numerical simulations is that test parameters can be completely controlled and results completely measured, which is not possible at the ocean. However, some characteristics from real conditions such as floor, currents, drops/separation, transients, or fauna effects among many others, are not easily replicable, or not replicable at all with numerical analysis. Only full size ocean test can effectively reveal converters behavior [32]. When the objective is optimization, numerical analyses are a powerful and appropriated tool since series of similar analysis can be created while varying the variable or variables of interest. Conversely, at the ocean it is not always easy to vary and control parameters.

Experimental development can be divided into Lab Test, and Ocean Tests. Lab tests are an additional and necessary step during the development process. Many WEC concepts are studied numerically, but only a portion of them are tested in a Wave Flume or a Wave tank/basin, and barely few concepts are tested at the ocean. The availability of wave-flume and wave-tanks is limited and require considerable sum of resources to build the prototypes and run the campaign. Lab tests provide valuable information for the development of WECs allowing to observe the device performance under a more real scenario where interactions and losses which are difficult to quantify in a CFD simulation due to accuracy, lack of information, or computational demand, such as floor-interaction impact, component losses due to friction, free-surface behavior, or full device with all details, among others, are assessed.

Many variables can be measured during a testing campaign, widening the possibilities to conduct experiments. The University of Edinburg was one of the pioneers in wave tank testing, stablishing practices and guidelines [62] which have been followed up in many further studies worldwide including variables to be measured, ways to be measured, start-up/steady conditions to begin measurements and length of measurements, waves generation, scaling models, materials and construction of models.

Besides to observe the full performance of the device, experimental campaigns allow to evaluate the efficacy of analytical theories, or numerical methods. Morris-Thomas et al. [63] studied the front wall geometry draught, thickness and aperture shape influence, and found high efficiencies occur nearby the natural frequency and the efficiency is not well captured by the theory of Evans and Porter. Wan et al. used a 1:50 scaled model of the spar torus concept to assess performance and compare with the numerical analysis [64]. Fairhurst et al. used experimental test to verify a time-domain simulation model of a submerged OWC [65]. Gomes et al. assessed wave power extraction and found lab test results may be affected by wave-flume walls which amplify the power capture up to a 15% for regular waves and 10% for irregular waves in a floating OWC during lab test [66]. Falcao et al. discuss similarity rules for OWC which are different from other WECs since the predominant forces on the OWC wetted area are different from those above the water level [67]. Ram et al. investigated experimentally a OWC in a 2D wave channel using PIV techniques varying water depth and wave frequency [68]. No turbine was included in the experiments. Rezanejad et al. used both numerical and experimental campaigns to evaluate the influence of the turbine damping and found damping has a large effect [69]. De-zhi et al. evaluated experimentally different geometric parameters in a fixed OWC finding the optimal opening ratio [70]. Correia et al. examined the motions and mooring forces of an OWC devices when placed in an array, the turbine damping was simulated also

with an orifice [71]. Patel et al. evaluated the effect of turbine orientation finding that the horizontal model presented better performance than the vertical oriented Savonious turbine [72]. Taha and Sawada investigated the performance of a Wells turbine computationally and experimentally [47]. Henriques et al. made experiments over an OWC device to validate the dynamic response from control algorithms, they found scaling-down the power-components such as turbine, generator or bearings during an experimental campaign, it is complicated, since they are scaled with $sf^{7/2}$ making friction losses to become important. The minimal realistic scaling factor to include power take off system is 1:4, and these scales must be performed at the ocean [73]. This is the reason why in many wave-flume experiments, turbine and power take off in general is simulated by an orifice or a porous wall. Henriques et al. analyzed latching control experimentally and assess the improvements [74]. Falcao et al. investigated a speed control of an OWC to maximize the produced electrical energy modelled as integrated process based on the linear wave theory [4].

Several state of the art developments on novel WEC designs tested in the laboratory has been made. Dai et al. [75] revealed a novel WEC composed of two oscillating bodies. Vyzikas et al. [76] made a preliminary comparison on different OWC geometries classic OWC and U-shape-OWC using regular and irregular waves, with and without power take off. Fleming and Macfarlane presented an analysis of different geometries of a forward-facing- bend-duct OWC using particle imaging velocimetry [77]. Kinoshita et al. [78] compared experimental and theoretical studies of and OWC using a prediction method and an equivalent electric circuit to account for the sum of compressibility effects, turbine, and generators inertia. Saadat et al. [79] studied a new concept of wave energy conversion that uses the Helmholtz resonance frequency amplifying the oscillation. Ogai et al. [80] created a novel pendulum WEC of high performance which is very simple. Instead generating electricity straightfor-

ward, this device compresses air, reaching high efficiencies according to wave flume's experiments. Brekken et al. presented a development of a novel point absorber WEC to improve performance and mooring [60].

Renzi and Dias [81] compared an Open Ocean test of a large flap type oscillating WEC with channel tests and theoretical solution. Ocean tests allow to observe behavior in full real conditions, and higher depths than those physically allowed in a wave flume. WEC's ocean tests are not common. Those available were performed with large prototypes or pilot plants. Conversely, testing small prototypes at the ocean requires short wavelengths and small wave-heights and those conditions are difficult to achieve. Almost no records on ocean tests with small prototypes like the described in Chapter 5 are available in the literature.

Despite the large amount of WEC R&D, most of it has an academic orientation only, focused on creating a mathematical model which explain behavior of idealized simple devices, or improving the performance of individual characteristics, predict the performance or energy capture of a device, or focus on some design aspect of a device [3]. Aspects as cost, manufacturability, handling, access, operation, maintenance, which are important for real applications are usually underestimated. For example, an excellent WEC in terms of energy capture with a larger generator than needed will have deficient performance. Even though selecting a proper generator is fundamental for WEC overall good performance, very little research has been done on it compared to the research made in WECs. Dorrel et al. compared permanent magnet generators for application in a WEC at low speed steady state [82]. Szabo et al. proposed and analyzed numerically a novel permanent magnet tubular linear generator for WECs [83]. Vermaak & Kamper presented an analytical model and optimization of a new topology air/cored permanent magnet linear generator for WECs which eliminate most of the end effects of iron cored machines [84]. Muller et al. highlight

the advantages and disadvantages of using different wave energy power take-off with conventional generators [85]. O'Sullivan & Lewis studied the annual performance of various generator configurations for typical wave climate [86].

The WEC to be used in the present work was chosen primarily through a literature review focused first in reliability, and simplicity. The OWC WECs group was considered the best for this criteria. Afterwards, including manufacturability, cost of materials, cost of turbine, the subgroup of OWC which used check-valves was chosen. Finally, from the 3 most important multi-chamber's subgroup, the UFCAP was chosen. It is more robust to support harsh weather, and the author had experience and access to the R&D information.

1.3 Research Objectives

The prime objective of this work is to experimentally investigate and proof the technical feasibility of a novel Wave Energy Converter for potential application in developing countries. The specific objectives of the present research include:

1. To experimentally assess the flow due to the addition of air-chambers (with one and two air-chambers);

2. To devise, design, and test a check-valve (low-crack-pressure) which can handle large volumes of air at low pressure-difference from low wave-height climates;

3. To design, and build a scaled WEC prototype and test different configurations in a wave-flume;

4. To design, and build a second scaled WEC prototype for ocean testing, and observe performance at the ocean;

5. To generate electricity from ocean waves;

6. To characterize the airflow in the central conduit as a function of the incoming waves; and

7. To identify design parameters to improve the performance of the OWC WEC device.

1.4 Contributions

The thesis makes an important contribution to the field of renewable energies, and more specifically to the development of wave energy converters.

1. Discovered the feasibility of a the UFCAP WEC.

2. Identified the relevant design parameters to improve performance of the UFCAP WEC.

3. Scaling approach-criterion which complements current Froude criterion, improves similarity and facilitate design decisions based on a variety of constrains.

4. A novel check-valve for application in OWC devices with low crack-pressure and low pressure-drop was proposed, tested and evaluated.

5. Development of a customized turbine for the UFCAP WEC.

6. Procedure for UFCAP WEC installation without heavy equipment to reduce installation cost.

7. Characterized UFCAP airflow from wave-flume experiments. Literature survey on the status, operation, performance, problems, and modelling of WEC.

8. New device failure-modes identified based on the ocean tests.

9. Identify design guidelines or recommendations for future UFCAP OWC designs

10. Prototype tests at the ocean to experimentally verify the future numerical simulations.

11. Software and hardware sensors for ocean measurements (integrated pressure, air-speed, water level several channels, generated voltage).

12. A wave channel prototype to perform tests.

13. An Ocean prototype device with measurement equipment.

14. Development of a numerical tool for sizing of the UFCAP WEC.

15. UFCAP WEC cost projection for ocean prototype, and ocean plants.

1.5 Thesis Layout

The feasibility and operation of a low-cost near-shore wave energy converter was investigated as well as its performance. First, a viable concept was selected (the UFCAP), and second it was necessary to solve some technical problems to be able to make it operable such as designing the check-valve and turbine for the specific application, and evaluate the effectiveness of the proposal (numerical and experimental work). Two experimental prototypes for wave channel tests were built and one prototype was built and deployed in the ocean.

Chapter 1 provides an overall framework including background, motivation, state of the Art and Research Contributions. Chapter 2, describes why the UFCAP was selected as the Wave Energy Converter which could better be implemented in a developing country and its mode of operation. Chapter 3 presents a new low-pressure check-valve, explains why none of the commercial check-valves were suitable for the present device, and presents the achievements, Chapter 4 depicts the turbine design

which is also a key component in the development of the present wave energy converter. Chapters 5 and 6 portray the wave channel and ocean tests and their results. Finally, Chapter 7 outlines the conclusions, recommendations, and future work.

Appendix 1 includes Turbine Design support information. Appendix 2 shares the ocean tests Installation Plan carried on during Ocean Deployment. Addendum 3 shares modifications made to the ocean prototype after the first deployment and in preparation for the second deployment. Addendum 4 includes a list of Lessons Learned which might be valuable for a further ocean test.

Chapter 2

UFCAP Wave Energy Converter

2.1 The Problem

Cost of wave-energy needs to get reduced to better compete in the renewable energy market. Chapter 1 introduced the state of the art, and complications faced by the technology. WEC devices are generally very large devices, and need to be very robust (expensive) to withstand harsh environment at the ocean. Handling during manufacturing, and installation is indeed an important problem often underestimated and not addressed by design teams, but real and responsible of several accidents and destruction of pilot plants and millions of dollars to date.

The UFCAP device is a WEC which was conceptualized to address handling problems and energy cost. It can incorporate plastic materials (more economic), off-the-shelf components (more economic), be built in relatively small components (modular) in regular facilities. However, the UFCAP was just a concept yet to prove good operation. Due to the flow path, and connections, it was not clear what would be the effect of the flow interactions at the manifold, and between the conduits; predicting the net result of generated/available energy was a complex problem. Validating the

device experimentally was also not possible because some needed technology did not exist. Scaled prototypes required check-valves with minuscule crack-pressure which was not available at all for the required flow regime. Additionally, other components such as the turbine were necessary customize in order to be able to have a usable prototype.

2.2 The Device

The device consists of multiple interconnected floating OWCs which share a single central-unidirectional-air-turbine. In the present work, such floating OWCs are called air pumps since they literally pump air in and out of the air-chamber. Its name UF-CAP stands for Unidirectional Flow Collective Air Pumps. Inside the air-chambers, the operating principle is the same described in Chapter 1 for OWC devices to create an airflow.

In Figure 2.1(a), a schematic representation of an air-chambers is depicted to explain the mode of operation of the pumping activity. Air-chambers are floating empty containers, completely passive with an opening at the bottom part, which are partially filled with air and water, and the air-water inter-phase act as a piston going up and down by the action of the surrounding ocean waves. Figures 2.1(b) and 2.1(c) displays the air-chamber at two different moments, Figure 2.1(b) displays when the wave crest is passing, at that instant the elevation of the surrounding pressure causes rising the water level inside the air chamber, pumping air toward the turbine through the supply-conduit. Figure 2.1(c) exhibits a different instant, when the wave trough is passing and the water level inside the air chamber decreases pumping air inside the air chamber though the return-conduits.

Air pumping is achieved using uniquely the water interface, without moving-parts which reduce stresses and wear of air-chambers [19]. Figure 2.2 [19], depicts the

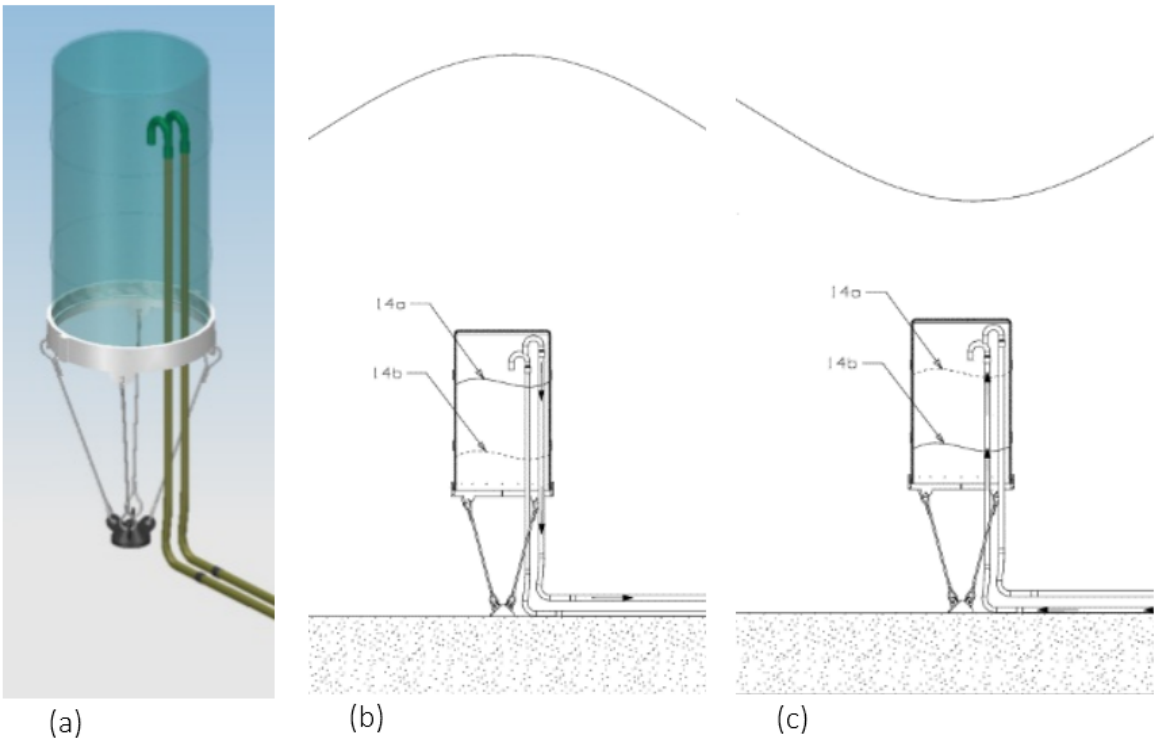

Figure 2.1: Air-Chamber Pumping Mechanism. (a) Air-chamber is basically an empty container; (b)Water level inside air-chamber rises until position 14a while wave crest is passing; (c) water level go downward inside air-chamber up to position 14b while wave trough is passing. Figures (b) and (c) [19].

devices components. Each air chamber has two flexible conduits, one to supply air to the turbine, and one to return air to the air-chamber. Both, supply-conduits and return-conduits, are coupled with check-valves which allow only either supply flow, or return flow respectively.

Supply-conduits, one from each air chamber, are merged together at the supply-manifold, and similarly the return-conduits are collected in the return-manifold. Supply-manifold is connected to the central conduit, where the central turbine is located, and the loop is completed by connecting the return manifold to the exit of the central conduit. It can be said, that all air-chambers are interconnected to each other.

The airflow direction and operation can be summarized with Figure 2.2 [19], air-

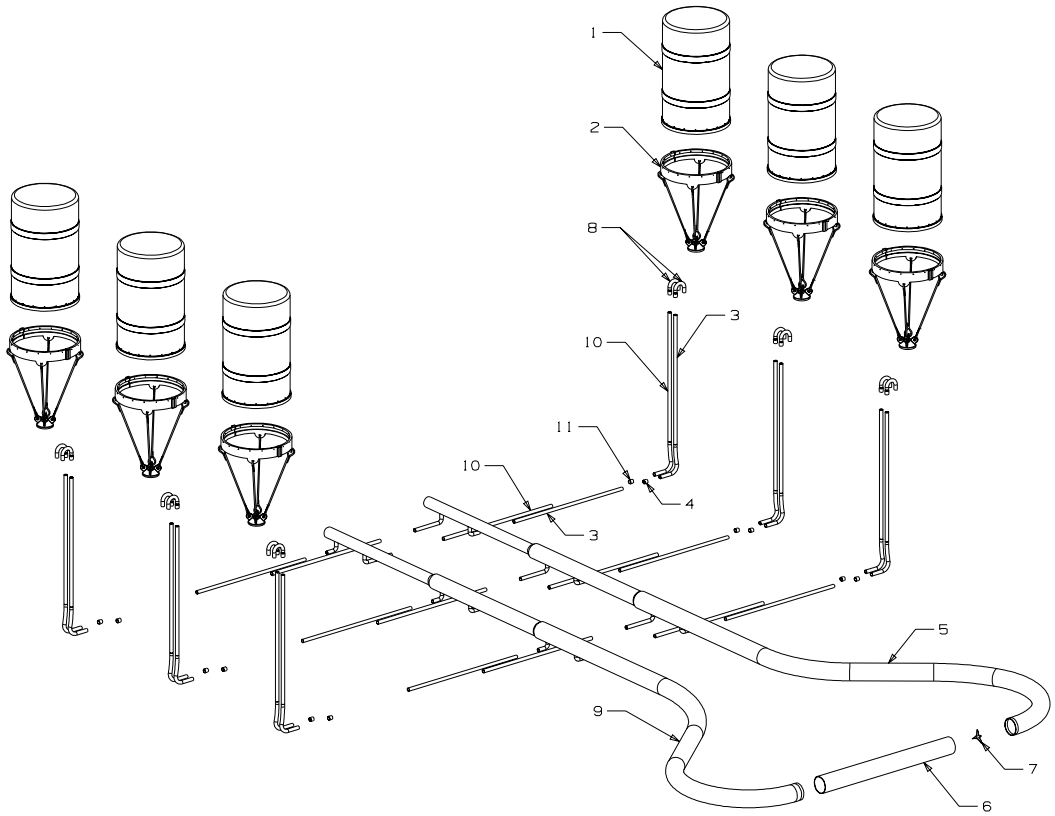

Figure 2.2: UFCAP Components; 1)air chamber, 2)mooring support, 3)supply conduit, 4)supply check valve, 5)supply manifold, 6)central conduit, 7)turbine, 8)floating valves, 9)return manifold, 10)return conduit, and 11)return check valve [19].

chambers pump air feeding the supply-manifold, not necessarily simultaneously, if the spacing between air-chambers is large compared to the wavelength, only those air-chambers surrounded by the wave crest would be pumping air towards the supply-manifold. Check-valves control the flow-direction, supply-conduits discharge flow into the supply-manifold and this direct all the collected flow towards the central-conduit where the turbine is located. The second half of the loop is completed when the flow which passed the turbine reach the return-manifold, and is distributed to the return-conduits back to the air-chambers. Air-chambers pressure, defined by the local surrounding wave, determines the amount of air each of the air-chambers takes

in. With such an array, the oscillating flow encountered normally in the OWC devices, is converted into a unidirectional flow which can be used to rotate a much simpler conventional turbine vs. a self-rectifying turbine. Conventional air turbines are more efficient, and considerably less expensive [34]. This topic will be covered in more detail in Chapter 3.

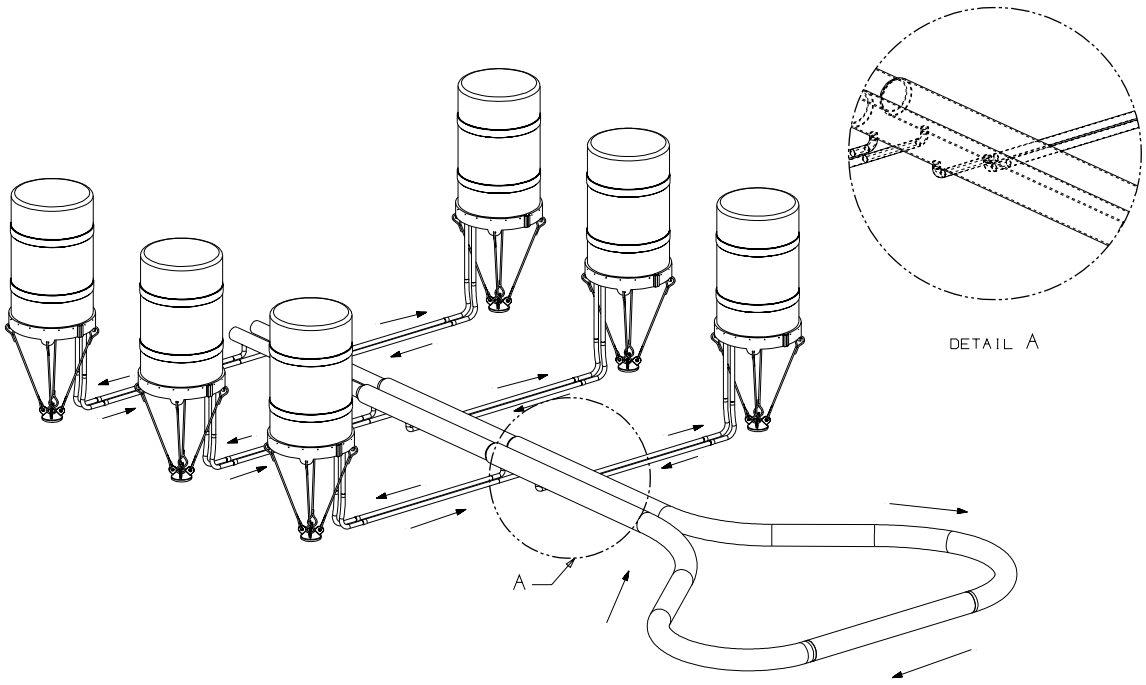

Figure 2.3: UFCAP Components; Creating the Unidirectional Flow. Arrows indicate the flow direction for a given conduit. Supply-conduits are those which supply air toward the central-conduit. Return-conduits return air towards the air-chambers. The Turbine (not visible) is inside the Central Conduit (bottom right portion) [19].

As observed, there are no-moving components in contact with the water, the only movable parts in the system are the self-opening check-valves and the turbine.

Without departing from same concept, some variations are possible. Turbine

could be placed either floating nearby the air-chambers, or right at the ground if the device is close to the shore as shown in Figure 2.4 which illustrates a 10kW pilot plant. In this configuration the cable cost, which is really high [18] (underwater, cooper, different types of cables for signals, power, channels, sealed, protected, etc.), is replaced for less expensive conduits/piping, and some losses due to friction added, however, if the wall of the conduits is smooth and distances are not excessively far from shore, the theoretical computed losses are on the order of 0.1% - 5% due to the low kinematic viscosity of air. Placing the Turbine at the ground facilitates the access for maintenance and improve the survivability.

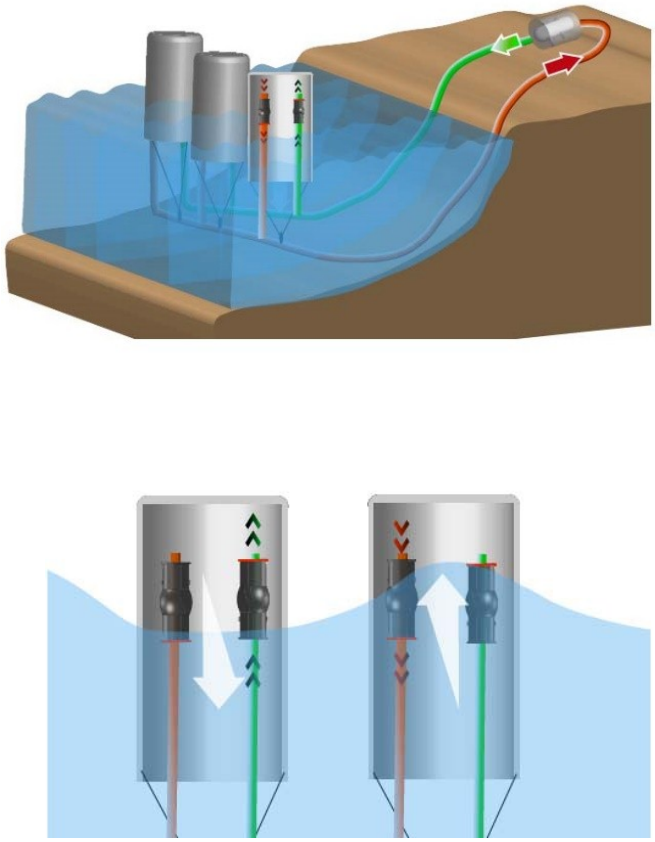

Figure 2.4: Artist representation of a UFCAP 10kW Pilot Plant with turbine at the ground *(top)*. Air-chambers section, supply-conduit in red, return conduit in green *(bottom)*.

Another configuration of the same UFCAP concept is the location of the air chamber which can be underwater or at the surface. Originally, it was proposed to place them underwater [19] with the advantages of not affecting the landscape and the obvious drawback of accessing to a lower available energy in the wave. After the ocean tests to be described in Chapter 6, the water-surface location is preferred since a perfect sealing is very difficult to achieve, and it is not required in such configuration. An additional variation is the use of upper holes (at the top of the air-chamber) and send the conduits to that area (See Figure 6.2), vs. having the conduits passing through the bottom opening as in Figure 2.4. A detailed description about the operating principle is given in [39].

2.3 Advantages

The UFCAP device has all the strengths from the OWC concept described earlier such as simplicity (no complex parts), long experience (information from several pilot plants connected to the grid since many years), natural force conversion (from low frequency large force waves, into high frequency low torque turbines), reliability (reduced number of failure modes), and additionally has the potential, with a proper development, to overcome the difficulties such as handling, manufacturing, operation, rapid tuning-up, impact to marine life, cost, and efficiency incremented by the expected better turbine performance due to its conduit-check valves configuration which converts the oscillating flow into unidirectional flow. Recalling the research line of this Dissertation is very practical and aim to contribute to proof a technology which can be used in a real pilot plant at a developing country, the simplicity, manufacturability, and the cost are also key items to be considered when selecting a technology. Being very economic device which can use off-the-shelf components

and local standard manufacturing facilities, the UFCAP is a perfect match for the project. Off-the-shelf components for conduits, air-chambers of a pilot plant would reduce the manufacturing time and reduce the cost. In the present work, three prototypes were created (two for lab test, and one for ocean test). A clear knowledge and certainty of the costs at this scale is already available since several models have been constructed. Nevertheless, prototype cost is still insufficient to compare technologies, cost projections of a scaled-up models are included in Appendix A. They are estimates made by sizing a UFCAP device with the analytical model, adjusting for available commercial sizes (e.g. conduit sizes), creating a bill of materials (BOM) from the main components and estimating a gross cost from all the smaller things as fasteners. Real suppliers and materials were quoted with prices as of 2010.

Due to its intrinsic characteristics and mode of operation, the UFCAP device is simple, less expensive than other devices reported in the literature reviewed in Chapter 1, and has the potential to reduce the current wave energy cost.

More specifically, the reasons to select the UFCAP technology can be summarized in the following technologys advantages:

- It has no-moving parts in contact with the water, which makes it safer for the marine life, reduce wear, reduce stresses which allow the use of plastic off-the-shelf air-chambers which are less expensive and readily available;
- It is made of relatively smaller parts which are later assembled, which facilitates its overall handling during manufacturing and installation;
- Lesser number of turbines (several air-chambers might use one turbine);
- Unidirectional flow allows it to use a simpler, more efficient, less expensive turbine, compared to self-rectifying turbines used in practically all OWC devices [34]. Unidirectional flow allows having non-symmetrical blades which are more

efficient, and twist the blades, not possible with the standard Wells turbine. More details about this topic in the Turbine Design Chapter;

- It is tunable. Tuning-up on OWC devices is normally made by adjusting the blade's pitch, and/or handling pressure with releasing valves. Without discussing at this point the control mechanism on OWCs, a specific advantage from the UFCAP device is that it may use several air-chambers rather than only one, placed at different locations, with distinct wave-phases, and then, the produced airflow is generated with the "sum" of those different waves. Summing waves at distinct phases, produces an addition/cancellation of waves with an interesting "smoothing" effect with respect to an equivalent variation that would have a single larger air-chamber. Details and figures on this topic may be found in [19]. The "smoothed" variation at the central conduit requires a slower tuning-up which is easier to achieve.

- *Rapid tuning-up*, which is the physical ability from a device to rapidly adjust for any incoming wave and performs at maximum efficiency. It is different than tunability, for example, picture the well known Pelamis WEC [88], with an imaginary capability of modifying its elements' length for adjusting to the different incoming waves (for the moment ignore other forms of control strategies such as adjusting oil pressure). *Tunability* would be the capacity of adjusting the length of its elements to improve efficiency for different waves, and *rapid-tunability* the capacity of doing so rapidly enough. Tunability would be limited by the lengths range. Rapid tunability by the inertia and actuators available to modify such a length, as well as having the elements' motion in the desired direction (e.g. if the element inertia is going down, and the incoming wave is not phase aligned to use that movement the energy is not harvested). Tuning-up, and rapid tuning-up abilities, they both may be improved with phase-control

[89], but its maximum is limited by the physics of the device (geometry, inertia and actuators), meaning some WECs can reach higher overall efficiencies than others, no matter a proper phase-control strategy is applied to each of them. In the case of UFCAP device, the rapid tunability is ruled by the blades inertia (assuming pitch control), gates inertia (assuming releasing valves), and water column inertia. While several phase control strategies are available, such as trying to achieve resonance or extracting the most of energy at the current wave and dropping the excess of energy when present, control-strategy is out of the scope of this work.

Rapid-tunability feature has not been widely discussed, or underestimated, nevertheless, it is fundamental to achieve an overall superior performance over the year.

- It is a simple system with most of its components passive. This, decreases the maintenance and the overall cost per kW-hr. This is key to get the project materialized in a real WEC.

An additional and important motivation of choosing this technology, is the real possibility of implementing a UFCAP full size device in Mexico. This device has been discussed and R&D will be continued after this work at the national Center for Ocean Energies (CEMIE-O). The former is possible due to very high targets set up by the government of Mexico on supplying its electricity demand with renewable energies which creates the need to look for alternatives and opens the possibility to get future support for this project. There are new regulations and programs to guide and govern this process, like the Law of sustainable use of energy [90], the Law to promote and Development of bioenergetics [91], and the Law for financing the energetic transition towards renewable energy [92]. One of the most notable examples is the approval

of the Energetic Transition Law which force the industry to use 25% and 35% of its energy from clean energy sources by 2018 and 2024 respectively [93].

2.4 State of development

The first records of the device are the patent [39] and the Master Thesis [19]. In the Patents, the device and mode of operation are clearly described as well as the form of the preferred embodiment. The Thesis is the only record of R&D. In that work, the UFCAP device was evaluated firstly numerically consisting of a single 2D air-chamber, which is the component where the two-phases (air and water) interact and the one where the pumping takes place, and with only hydrostatic sinusoidal boundary condition as input at the bottom of the air chamber. This analysis was conducted basically to observe if the expected pumping activity really occurred and test if the Volume of Fluid model to include the two phases could handle this kind of phenomenon.

Even though OWC devices were currently proved at that time, this device requires an additional proof of concept because different from other OWC of the time, the original preferred embodiment was an underwater array of air-chambers which was never proved before.

Being the pressure from the ocean waves the driving mechanism, the average pressure at the entrance conduit is expected to exhibit a sinusoidal form like the observed in Figure 2.5. Departure or variation from a perfect sinusoidal corresponds to inertial effects from water column. The vertical lines are numerical singularities due to the opening and closing of the check valve and its numerical effect over the equations. Additional details about numerical analysis assumptions and boundary conditions are presented in [19].

There are also records from some preliminary experiments using two air-chambers,

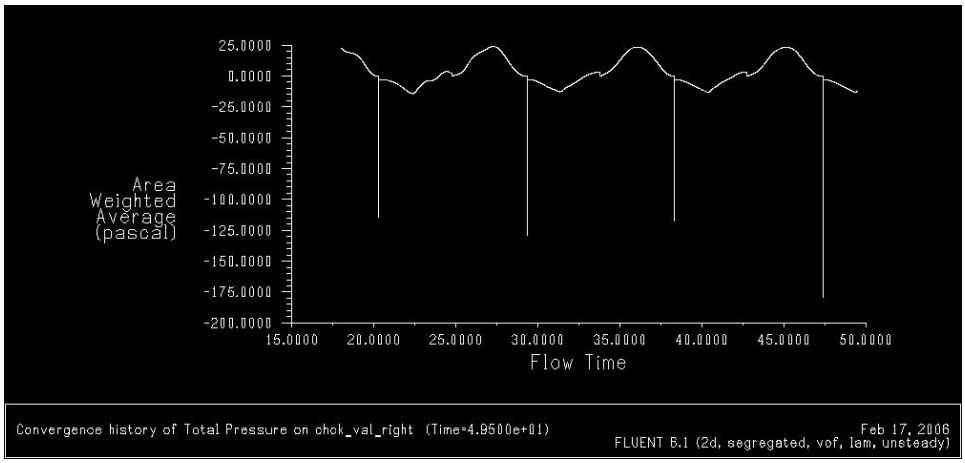

Figure 2.5: Quasi-sinusoidal behavior from average pressure on supply conduit from a 2D VOF numerical simulation [19].

a flowmeter and a device specially designed for this experiment which varies the water height. Such kind of water-height-maker has large limitations when compared to a wave flume, the water level could vary, but no wave dynamics was included, nor different wave phase could be examined, e.g. the water level increment in one air-chamber equals the water level reduction in the second air-chamber, and vice versa. Despite the ideal situation simulated included only the hydrostatic effects, the experiment was able to create the desired airflow, details in [19].

An additional analysis which was included in the same work from Rodriguez [19], was a numerical model to predict available power of a given device size. It receives the wave information as an input (wave height, and period), and compute the pressure-difference $P_{w1} - P_{w2}$ as

$$P_{w2} - P_{w1} = \rho_{water} g(2a_w) \tag{2.1}$$

where ρ_{water} is the salted water density, g, is the gravity, and a_w is the wave amplitude. The amplitude inside the air-chamber a_{ch} is unknown, and smaller than the wave amplitude a_w. a_{ch} is associated to a different pressure-difference which

occurs inside the air chamber $(P_{w2} - P_R) - (P_{w1} - P_S)$ which is proportional to a_{ch} given by

$$(P_{w2} - P_R) - (P_{w1} - P_S) = \rho_{water} g(2a_w) \tag{2.2}$$

Where P_R is the pressure at the end of the return conduit ant P_S the pressure at the end of the supply conduit. Figure 2.6 depicts the equivalence between the a_{ch} amplitude and the wave amplitude a_w.

The total volumetric flow depends basically on the number of air chambers, the a_{ch} amplitude, the rate of pumping given by the period, and size of the air-chamber. *Volumentric flow* is then given by

$$\Phi = N A_{ch} \frac{4a_{ch}}{T} \tag{2.3}$$

where Φ is the volumetric flow, N the number of air-chambers, A_{ch} the area of the cross section of the air-chamber, and T the period. For full details about the assumptions, losses, volumetric flow on pipes, and iterative process, refer to [19]. Knowing the volumetric flow and the diameter of the central conduit it is possible to compute the airflow power P_w with

$$P_w = \frac{1}{2} \rho_{air} (\pi R_{cent}^2) V_{air}^3 \tag{2.4}$$

The model is able even to predict the non-physically possible combinations. Once the central- conduit area got smaller than needed, the analytical model reports a zero meaning the results are not possible. The model does not include the kinetic energy term from the ocean waves, uses only the hydrostatic pressure, but it includes losses or pressure drop due to friction in the conduits, check valves, and turbine.

The model was coded to solve a set of equations through an iterative process. With

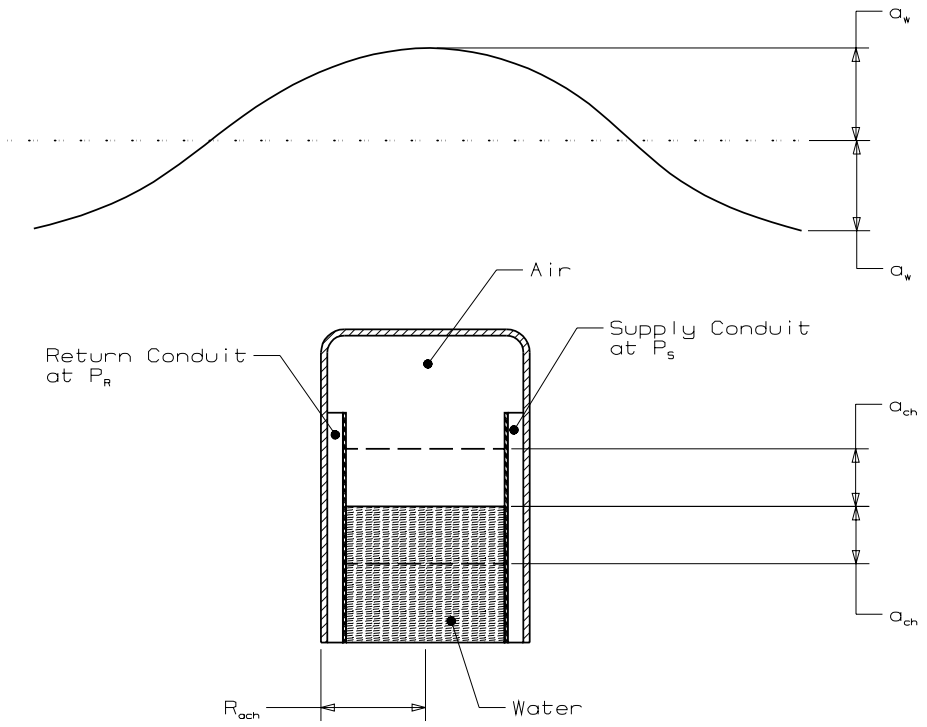

Figure 2.6: Amplitude inside air-chamber as a function of the wave parameters [19].

this basic model it is possible to size a device, preliminary predict the available power, and the minimum conduit diameters and results with combination of air chamber size and number of air chambers.

2.5 UFCAP complexity

UFCAP device is a promising approach due to its remarkable low cost and simplicity, however before the present work, it has not been completely proved.

While OWC mode of operation have already been widely proved, it is not possible to extend such a proof to the UFCAP, because the UFCAP device has additional complexities such as the ability of being underwater or above, the interactions between different air-chambers, which affect fluid dynamics, and mechanical stresses due to the inter-connected conduits which may behave as springs when air-chambers are

displaced by the waves, and then, the present work is necessary to proof the device may operate. Floating OWC devices are dynamically more complex than fixed OWC, they have 6 degrees of freedom. Dynamics due to inter-connected OWCs has been studied by Correia da Fonseca [71]. In the case of the UFCAP WEC, not only the conduits affect the motion, but also the mooring's tethers constrain its motion with a spring-like tension linkage [57].

Sizing a UFCAP device is more complex than sizing a standard OWC, since the same installed capacity might be achieved by different combinations of number of air-chambers (array size), and air-chamber size. Fluid dynamics, manufacturing equipment available, handling equipment during installation, transportation, distance to shore, and cost considerations should be included during the design stage along with the resource variables (wave height, period, shape of the waves and the other device parameters such as central conduit diameter, distance between air chambers, conduit diameter and installed capacity needed to mention the most important). For example, large diameter conduits necessary for a large array, might result unpractical and expensive, and then might be preferable to split the array into two devices.

After a literature review and having into consideration the objective of creating a real non-expensive-practical WEC which can be implemented in developing countries, the UFCAP device was selected to work with. Nevertheless, while the UFCAP concept offered significant and promising advantages, and seemed like a perfect match for developing countries due to its low cost, its feasibility had not been fully demonstrated and then, proving its feasibility became a basic objective of the current work which can justify further investment and development of this concept.

Most of the previous UFCAP work was numerical. To fully prove feasibility, experiments were needed due to the discussed many unknowns and uncertainties. The present work centered in solving all the obstacles, designing the necessary components,

such as low crack pressure check-valves, needed to perform such experiments and ultimately make the device operable in real conditions.

Facing a very complex device, two approaches were possible for a single person: 1) working with a part of it, and optimize it, or 2) working with the device as a system without optimizing it, but solving the issues which prevented it from operation, devising the needed components to make it work. The second approach is thought to be primary, and bring a greater contribution by generating knowledge which will reduce risk and R&D timeframe in future stages of development of a UFCAP WEC and building upon a more competitive wave energy.

Chapter 3

Low Crack-Pressure Check-Valve

This chapter describes the development of two novel check-valves to be used in an Oscillating Water Column (OWC) device to convert an oscillating airflow into a uni-directional airflow. While the airflow generated by the OWC device is large, the pressure-differences are only a few tens of kPa. This type of flow regime is not typical within the industry applications, and therefore practically none of the commercial check-valves are suited for the present OWC application. Two novel check-valve models are studied using computational fluid dynamics and their performance is compared with commercial check-valves. Subsequently, the check-valves have been validated and evaluated experimentally in wind tunnel and in-situ ocean tests. The proposed check-valves feature angled-gates, counter-weights, ultra-low crack-pressure and low pressure-drop with minimum losses. An improvement of two orders of magnitude in crack-pressure and five-fold in pressure-drop was achieved thus enabling operation of OWC WECs with waves as small as 0.1m in height.

3.1 Introduction

Wave Energy Converters (WECs) and OWCs have been properly introduced in Chapter 1. Recalling, OWC devices may be located either near-shore, or off-shore [9]. They utilize an air-chamber normally placed at the surface of the ocean and having typically two openings: one placed at the bottom and contacting the ocean surface and the second typically at the top where an air-turbine is placed. The change in height of the water level inside the air-chamber creates airflow, traditionally an oscillating airflow which turns a special turbine able to accept oscillating flow and generate electricity [35, 36, 37].

There are several types of turbines able to accept the reciprocating airflow (backward and forward airflow) and then which can be used in OWC devices. The most commonly used are the impulse turbine [43, 41], and the Wells turbine [42]. They both exhibit overall good characteristics, and performance. An alternative to reciprocating-turbines is rectifying the airflow with check-valves and conduits, and use a traditional turbine. For example, the UFCAP 10kW plant in Figure 2.4, shows two conduits per each air chamber, and the air flows-out through one conduit and flows-in through the other. The flow at the turbine is unidirectional no matter the oscillating nature from the ocean waves.

Check-valves are a type of valves also known as non-return valves. They are installed in pipelines to allow flow in only one direction. Almost all the check-valves rely on a certain amount of pressure called the crack-pressure to open the valve. When the pressure is lower than the crack-pressure, or back pressure over the pipeline is present, the check-valve will close preventing backflow. There are a plurality of check-valves which are used for a wide number of applications such as equipment/process-protection, which may be affected by reverse flow, such as flow-meters, strainers and control valves; minimizing water hammer from hydraulic forces [94]; flooding

prevention; reverse flow prevention on system shutdown; prevention of flow under gravity; vacuum relief, over-pressure prevention [95], among others. Examples of check valve types include lift, swing, wafer, disc, wafer-swing, ball, diaphragm, and tilting types. A full review of valve types, applications, materials, maintenance and repair can be found in [96].

In the present work, a novel check-valve design for application in small OCW devices is proposed. The performance from the two proposed check-valves will be compared to commercial check-valves (swing, and dual-disc models) which were chosen due to its good performance at low-pressures, and large flows which is the flow regime of interest present at OWC devices. A further explanation about these two commercial valves and most common failure modes with real data after years of usage might be found in [97].

Although a wide variety of check-valves is available, most of them are either for liquid at any pressure, or for gases at medium or high-pressure. OWC devices do not produce medium or high-pressure-difference, they only can produce large airflows at low pressures. One of the very few examples of check-valves suitable for this flow regime is presented in [98]. Other than this, none of the available commercial check-valves match for full size OWCs, and no commercial check-valve is appropriate for a scaled wave flume model. In a scaled physical model, the pressures become so tiny, that it is not possible to find a commercial check-valve operable with that flow regime. Check-valves for very low-pressure-difference applications are limited, examples of it is the one described by Ou & Chiao [99] which is able to open with very tiny pressures by the use of microspheres, or the one described by Tu for micro in-channel applications [100]. Nevertheless, while they are able to work fine with ultra-low-crack-pressure, or high-crack-pressure with low-pressure-drop [101], they are not suitable for large flowrates. This is the reason it was necessary to devise a novel check-valve which

could operate with a scaled prototype.

OWC devices generate a huge airflow with only a few kPa of pressure-difference. Therefore, they need a check-valve with minimal pressure-drop across it, and crack-pressure. Otherwise, an important percentage from the available energy is wasted. With a larger crack-pressure, the valve delays more in opening, and closes earlier. Qualitatively, the delayed opening has not a large negative effect, since the airflow will initiate faster due to buffering pressure. But the early closing, has indeed undesired losses. Also, a higher crack-pressure from valves with springs, have partial openings which also detriments performance. Pressure-drop, and crack-pressure, are then two of the main criteria when selecting an appropriated check-valve to be used in those few OWC devices which use a rectified airflow.

There are in the literature several examples of either investigating behavior of components such as check-valves [102] , characterize the check-valve [103], or designing new valves due to special requirements not satisfied with current technology, Valdes et al. describe a valve numerica development validated experimentally [104], Veenstra et al. constructed and measure a new check valve for cryogenic applications with very special requirements [105], Rao et al. develop a check valve for marine nuclear power using steady-state calculations and transient calculations which were compared with experimental data [106], Hansen et al. developed a check-valve able to switch with minimal pressure-difference [107, 108], and Al-Faqheri et al. developed check-valves for microfluidic [109].

3.2 Proposed Designs

The present development comprised 6 stages, a 1) state of the art review looking for commercial and available technology and research and identify the fine requirements

for the present application; followed by a 2) design proposal 1, called RDZ1, and a reviewed/improved version proposal called RDZ2, 3) CFD numerical analysis, a 4) prototype construction, 5) wind tunnel tests, and 6) ocean tests. Based on a literature review on check-valves with low crack-pressure and low pressure-drop, Dual-Disc and Surgebuster valves were selected to be analyzed numerically and compared to the proposed designs RDZ1 and RDZ2. Specification of these two commercial valves can be found in Table 3.1 [110, 111].

Table 3.1: Technical specs from two commercial check-valves best suitable for OWC application (large airflow at low pressure).

Model	Dual Disc	Surgebuster
Sizes (in)	2-12	2-42
Max Pressure (psig)	250	250; 150 (30-42 in)
Valve Type	Dual disc, wafer style	Disc Swing
Closure	Spring induced	counter pressure, disc accelerator
Cracking Pressure (psig)	0.25	0.30
Body Materials	Ductile Iron	Ductile Iron
Disc Material	Cast Bronze	Buna-N. ASTM D2000

3.2.1 Novel Check-Valve RDZ1

Dual-Disc, and Surgebuster, were the starting point to improve check-valve performance. They both have a large cross-section, and minimum change in flow-direction, characteristics which make them the two commercial check valves which better meet the crack-pressure, and pressure-drop requirements for this application. Other valves have a lot of elbows or cross-section reduction [96]. Check-valve RDZ1, aimed to reduce the gates shadow which is the portion of the gate which obstruct the flow when the gates are opened, in order to maximize the free-flow cross-section, leave flow direction invariant as possible in order to be able to reduce the current crack-pressure and the pressure-drop from commercial valves. One of the essential characteristic from the RDZ1 design are is angled-gates (or angle-discs) (Figure 3.1). This valve is similar to

dual-disc check-valve with a variation converting the flat gates to angled-gates which allowed a reduction on the gates shadow supporting pressure-drop reduction, and at the same reducing the angular displacement (gate stroke from the fully closed position to the fully open position) by 20-30% compared to dual-discs valve. Reducing the stroke, reduces also the opening-closing time.

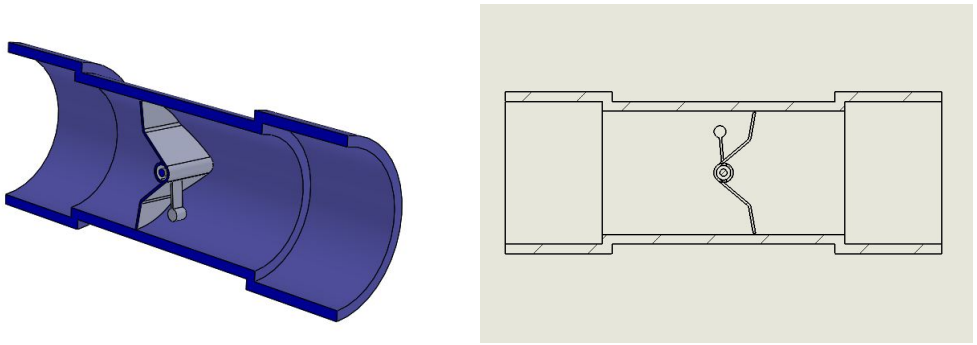

(a) 3D section (b) Section-view

Figure 3.1: RDZ1 valve in a closed position (both angled-gates have counterweight, but only one is visible due to the section) (a) 3D section ; (b) Drawing section-view.

Besides reducing the gates shadow, the second important variable from RDZ 1 (angular discs design) is the angle γ (see Figure 3.2) which creates a wedge. Whenever backflow is present, such a wedge rotates the angled-gates closing the valve. RDZ1 valve was able to improve both pressure-drop, and crack-pressure. Its performance is described in section 3.3.

Another significant feature from RDZ1 check-valve is the inclusion of counterweights, see Figures 3.1, and 3.2. The Counterweights function reduces the necessary torque to rotate the gates. Counterweights is the main reason to succeed achieving extremely low-crack- pressure on this design proposal. When gates and counterweights are perfectly balanced with the respect its axis, friction is the only force to overcome, and gates can be easily opened and closed. A method to compute the crack-pressure analytically is included in [112], the effect of the counterweights can

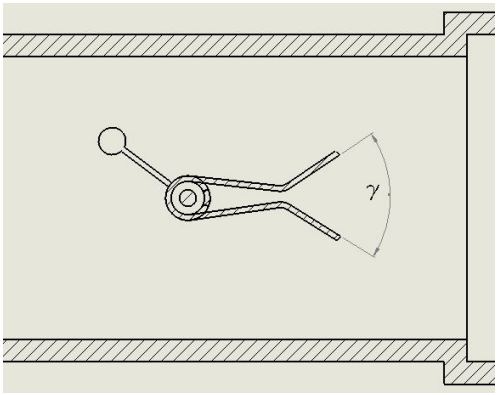

Figure 3.2: RDZ1 valve in a opened position. γ angle is an important angled-gates' parameter for good performance (both angled-gates have counterweight, but only one is visible due to the section).

be seen there. Due to an actual prototype was manufactured and available in this study it an experimental approach to measure the crack-pressure was preferred rather than an analytical method. Experimental approach can be more accurate for this application since it includes real friction, weights, and rattle effects from each of the components, which are difficult to determine or otherwise need to be approximated or assumed when working the analytical approach.

Another distinctive in RDZ1 is the performance at different orientations. Normally check-valves performance varies with respect to the mounting orientation. Imagine the Dual Disc mounted in a vertical pipeline, the Discs weight will act favorable to open the Disc when fluid flow moves downward, and will act contrary when trying to close the check-valve. Using counterweights, the orientation and weight is no longer an issue. Being independent of the mounting orientation is an additional advantage from the RDZ1 valve. In other words, crack-pressure is independent from the mounting orientation, differently from most of commercial check-valves.

In the present application, being independent from the mounting orientation is an important feature since check-valves might be mounted in opposite direction while being installed on the supply-conduit and return-conduit respectively, and the valves

orientation might be changing due to the devices dynamics at the ocean.

When the instant available pressure-difference at the conduit is lower than the crack pressure, and do not achieve to open the valve, the valve's gates may rattle attempting to open-close without achieving it causing additional wearing and failure modes. The larger crack-pressure the larger the probability to encounter below such a pressure within the system.

The use of counter-weights greatly reduce the crack-pressure of a check-valve, and therefore decreases the probability of encounter the system below such pressures. Hence, an additional advantage of using counterweights is the reduction of valve wear over the gates, axis, and involved components [112].

3.2.2 Novel Check-Valve RDZ2

From RDZ1 check-valve numerical simulations, a couple of areas of improvement were identified such as zones where the flow was largely accelerated and pressure incremented. By reducing these peak values, it is possible to reduce the pressure-drop across the valve. RDZ2 valve is therefore a modification from RDZ1. While RDZ1 has a constant circular section, RDZ2 has a variable section incremented at the center. The wider section allows a homogeneous pressure distribution which ultimately reduces the pressure-drop across the valve, enhancing the overall performance of the valve.

RDZ2 design utilizes also angled-gates. RDZ2s angled-gates also incorporate counterweights which allow opening and closing the valve with very low torque, or equivalently with very low-pressure-difference across the flow. Figure 3.3 illustrates the RDZ2 model opened. The small connected spheres are the representation of the counterweights which balance the gates weight with respect the axis of rotation.

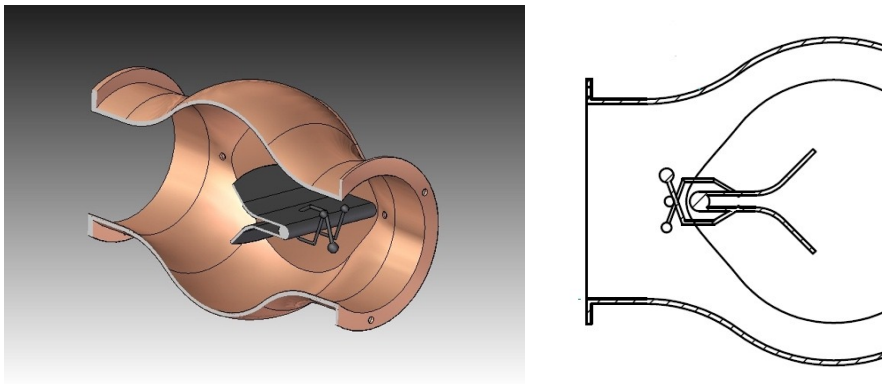

(a) 3D section (b) Section-view

Figure 3.3: RDZ2 valve in a closed position (a) 3D section ; (b) Drawing section-view.

3.2.3 Computational Evaluation

UFCAPS check-valves control the flow from the air-chamber towards the turbine, and backwards. Imagine the simplest configuration for explanation purposes with only one air-chamber connected with conduits to a turbine, where one check-valve is located at the supply conduit (to supply flow to the turbine), and a second check valve on the return-conduit (to return air to the chamber). The fluid which passes through the check-valves is air. Even though the pressure-difference is small, the flow rate is large. When the air-chamber is supplying air to the turbine, the check-valve at the supply conduit is open, and the check-valve at the return conduit is automatically closed due to the pressure-difference. For details about the UFCAP mode of operation, check-valves, manifold, and the ocean waves interaction with the whole device please refer to [19]. Nevertheless, some leakage might be present at the return-conduit. A small amount of leakage is not critical for this application. Conversely, having a high pressure drop, or a high crack-pressure could reduce dramatically the efficiency or even left it completely inoperable. Therefore, a design decision was made to improve the crack-pressure at the expense of losing tightness.

A steady-state analysis using CFD was conducted using the maximum flow for

an array of 4 air-chambers of diameter 3 m with a significant wave height of 3m which corresponds to a prototype size for a specific location where the device is to be deployed. This Chapter focus on the development of check valves, computations about sizing of the UFCAP WEC are not included here. With the interest of computing the pressure-drop from the maximum flow in such conditions (prototype size and local climate), the valve is assumed to be fully open. No transient effects nor instabilities are of interest in the present study. It is not easy to calculate the crack-pressure computationally since transient effects with moving meshes would be necessary, and several assumptions such as friction among axis, gates, bushings and other unknowns would have been needed to validate the model experimentally. Crack-pressure was measured experimentally to compare different check-valve models.

Four check-valve models were analyzed numerically: the dual disc (commercial), Surgebuster (commercial), and the two proposed solutions RDZ1 and RDZ2. A steady, isothermal analysis, with turbulence model k-ε was realized. The continuity and momentum equations were solved using Ansys-CFX. A tetrahedral mesh of 400k elements was used for each valve, mesh independence verified. A pipe diameter of 288 mm, computed with the numerical tool described in Chapter 1 corresponding to a 10kW pilot plant, and valve length of 396 mm were defined. Opening and closing effects from the gates were not included in this steady state analysis. Being this a preliminary CFD analysis, a simple high turbulence intensity of 10% was assumed in the analysis with Reynolds number of 4 x 10^6 and the additional turbulence expected from transient effects in real operation.

At the inlet boundary condition, a subsonic flow regime was used, with a static-relative pressure of 1,981 Pa, and a zero-gradient in the flow direction. In all four cases, a mass flow rate of 0.678 kg/s was assumed at the outlet which corresponds to an air-velocity of 21 m/s. Given that no high-pressures, high velocities, nor thermal

effects are present, it is assumed that no heat-exchange takes place.

3.2.4 Experimental Evaluation

The RDZ1 check-valve prototype was built for evaluation. This prototype was designed to be manufacturable with standard tools. Figure 3.4 depicts its components. The housing was built with a nipple, and two bended discs are the gates which already incorporate the counterweights. They are intercalated so there is no interference between the left and right disc-counterweights. As discussed before, counterweights help in reducing the necessary torque to open and close the valve.

The present design was focus on the manufacturability, crack-pressure, pressure-drop, and not on a perfect sealing when it is closed. Actually, it was necessary to reduce the sealing performance in order to maximize the opening-closing performance. The valves work is examined in section 3.3.

Table 3.2 list the main components of the RDZ1 check-valve. The assembly is simple and does not require the use of a spring to assist the valve opening or closing. As the check-valve is a component of a scaled UFCAP WEC prototype, the size was an important aspect in the prototype design.

Table 3.2: Bill of Materials (BOM) RDZ1 check-valve prototype.

Item	Component	Material	Quantity
1	Housing	Galvanized	1
2	Nut	Steel	2
3	O-rings	Rubber	2
4	Safety nut	Steel	1
5	Shaft	Steel	1
6	Angled Gate	Galvanized	2

The RDZ1 check-valve prototype was tested in the wind tunnel Armfield C15-10 in order to measure the crack-pressure. The wind tunnel has an integrated sensor that measures pressure, and air-velocity. Figure 3.5 show the wind tunnel and valve

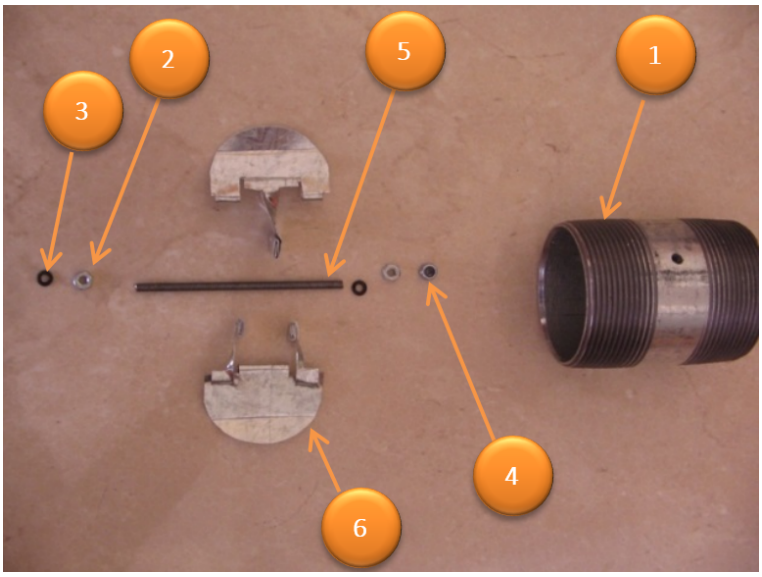

Figure 3.4: RDZ1 check-valve prototype (exploded view).

Table 3.3: RDZ1 Technical Description.

Characteristic	Description/value
Valve Type	Counterweighted angled disc
Closure	Back flow
Cracking Pressure	0.0016 psig (experimental)
Body Materials	Ductile Iron
Disc Material	Galvanized Steel
Sealing	Not seal used

fixation.

Tests were performed in Queretaro, a city elevated 1,800 m over sea level, then, atmospheric pressure and local air-density is estimated with

$$\rho_{air} = \frac{P_{atm}}{R * T} \tag{3.1}$$

where P_{atm} is the atmospheric Pressure, R the Universal Gas Constant and T the atmospheric Temperature. According to the tests series, the minimum air speed that opens the valve is 4.7 m/s at the start of the tunnel. By using *Bernoullis equation* and stagnation conditions it is found the crack-pressure

(a) 3D section (b) Section-view

Figure 3.5: RDZ1 pressure-crack measurement set-up in wind tunnel.

$$\Delta P = \frac{\rho_{air} V_1^2}{2} \tag{3.2}$$

with ΔP being the crack-pressure, ρ_{air} the local density V_1 the air velocity at wind tunnel inlet.

RDZ1 check-valve performance was also tested at the ocean. The tests are described in detail in Chapter 5. Two air-chamber sizes were tested, 200lt and 40lt with diameters 0.58 m and 0.28 m respectively with two RDZ1 valves per each air-chamber size, one check-valve to discharge air, and the other to bring air inside the air-chamber. The intention was to observe if small waves (10-50 cm), could produce enough air-flow to open and close the valves.

3.3 Results

3.3.1 CFD Results

Figures 3.6 and 3.7 show the pressure contours and velocity vectors of the four valves at a fully opened position. From the Dual-Discs model, it is possible to observe that the flow is accelerated at the disc zone due to a reduction of the available cross-

section. A decrement on the pressure, and increment on the velocity is evident right after the discs (flow from right to left). Although the valve has a wider section with the intention to improve such a reduction in cross-section area, it is currently located upstream from needed. This same idea was incorporated in RDZ2 valve, where it is possible to observe that the increment in cross-section area occurs right where it is needed (flow from left to right RDZ1, RDZ2, Surgebuster). With the Surgebuster model it is possible to observe that a wide cross-sectional area is available, and changes on the flow direction occurs smoothly. Both characteristics are good for achieving a valve with low pressure-drop. Nevertheless, the cross-section is reduced by the stop tab (bottom of the valve), and the stroke of the gate opening. These two concepts were incorporated in RDZ1 and RDZ2. In RDZ1 the gates were designed to fully open trying to have the largest cross-section possible. RDZ1 and RDZ2 both have large cross-section areas all along the valve, and soft changes of direction which allow them to have better pressure-drop and crack-pressure values.

Overall results are compared in Table 3.4. Two of the most important parameters for this OWC application are the pressure-drop and the crack-pressure. The pressure-drop is the difference between the average pressure at the inlet and outlet. The pressure-difference is the difference between the pressure max and the pressure min. Comparing pressure-drop results, there is no a large difference between the first three valves (dual-disc, Surgebuster and RDZ1), but there is clearly a large difference comparing RDZ2 with only 28 Pa of pressure-drop vs. 132, 135 and 205 Pa from the other valves.

Given the small pressure difference available in the OWCs, as explained in the introductory section, a valve with a reduced pressure-drop is highly desirable. There is a correlation with the velocity gradient across the valve. It is observed that the RDZ2 valve has the minimum velocity gradient or equivalently, their velocities are more

Table 3.4: Comparative Chart CFD and Experimental Results

Variable	Dual Disc	Surgebuster	RDZ1	RDZ2
Pressure-drop *(Pa)*	132	205	135	28
Crack-pressure* *(Psig)*	0.25	0.30	0.0016	**
Pressure Max *(Pa)*	2,000	2,050	2,300	2,060
Pressure Min *(Pa)*	1,675	1,380	1,400	1,880
Velocity Max *(m/s)*	25	35	37	17
Velocity Min *(m/s)*	3	2	6	1
Pressure difference *(Pa)*	325	670	900	180
Vel. gradient *(m/s)*	22	33	31	16

* Computed from wind tunnel measurements (RDZ1), and datasheets (Dual Disc, Surgebuster)

** not measured, but observed to be of similar order of magnitude than RDZ1 model.

homogeneous across the whole body of the valve. The pressure drop was computed

$$P_{drop} = P_{inlet} - P_{outlet} \tag{3.3}$$

where P_{inlet} is the average pressure from all the nodes at the inlet boundary, and P_{outlet} is the average pressure at the outlet boundary. Similarly, the velocity gradient was computed by

$$\Delta V = V_{max} - V_{min} \tag{3.4}$$

where V_{max} is the maximum value in all the domain, and V_{min} the minimum value.

The pressure drop was improved considerably, making it about five-fold better than the dual disc, and seven times better than the Surgebuster. RDZ1 and RDZ2 are better options than the dual-disc and Surgebuster valves with respect to the pressure-drop and crack-pressure. While RDZ1 valve is easier to manufacture, RDZ2 valve exhibits better pressure-drop performance. Figure 3.6 shows a qualitative comparison between RDZ1 and RDZ2.

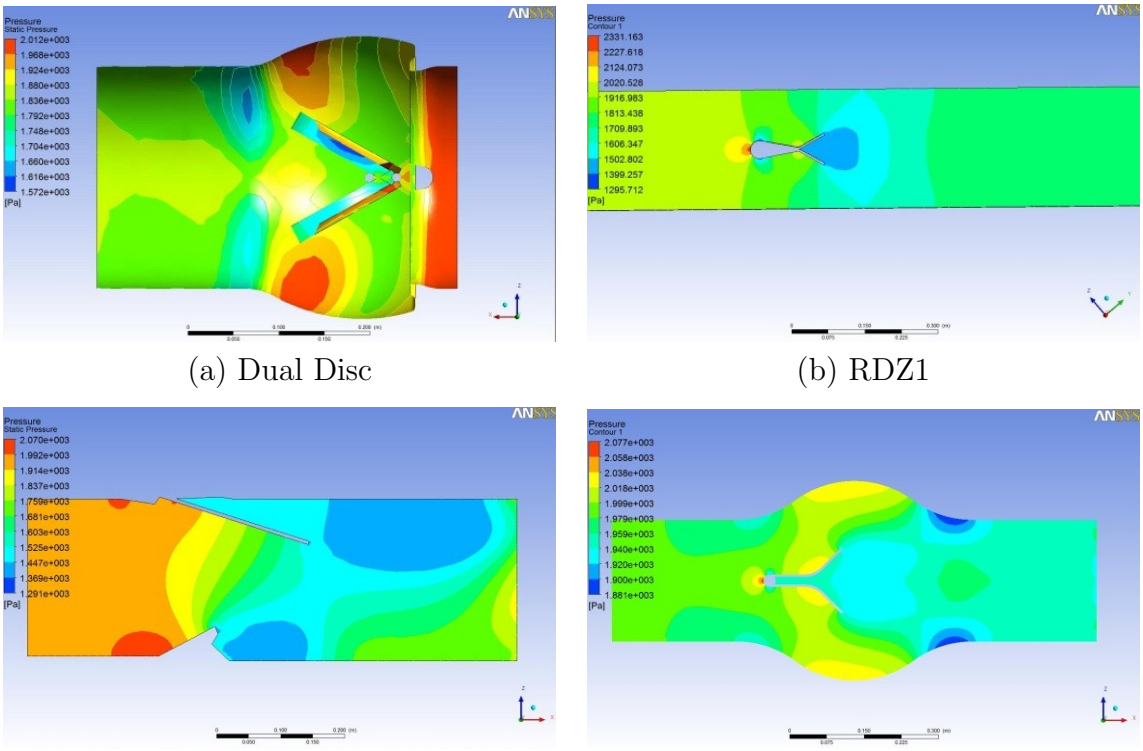

(a) Dual Disc (b) RDZ1

(c) Surgebuster (d) RDZ2

Figure 3.6: Check-Valves Pressure Contours (a). Dual Disc; (b) RDZ1; (c) Surgebuster; and (d) RDZ2.

3.3.2 Experimental Results

The characteristic crack-pressure for RDZ1 wind tunnel tests is 10.7 Pa $\equiv$ 0.0016 psig which is 150 times smaller than Dual-Discs crack-pressure and 180 times smaller than Surgebusters. It is important to note that the prototype used was already rusted due to ocean water. Even though the measured crack-pressure appear to be very small when compared with the others models, check-valves behavior at the ocean provide some insights about the order of magnitude of the crack-pressure. The available max pressure from a wave 0.11 m which was observed during the ocean tests, is 0.16 psig. From that value, losses due to efficiency, and friction must be subtracted. For a check valve to be operating the major part of the time as it was observed during the experiments, the crack-pressure should then be considerable smaller than this value.

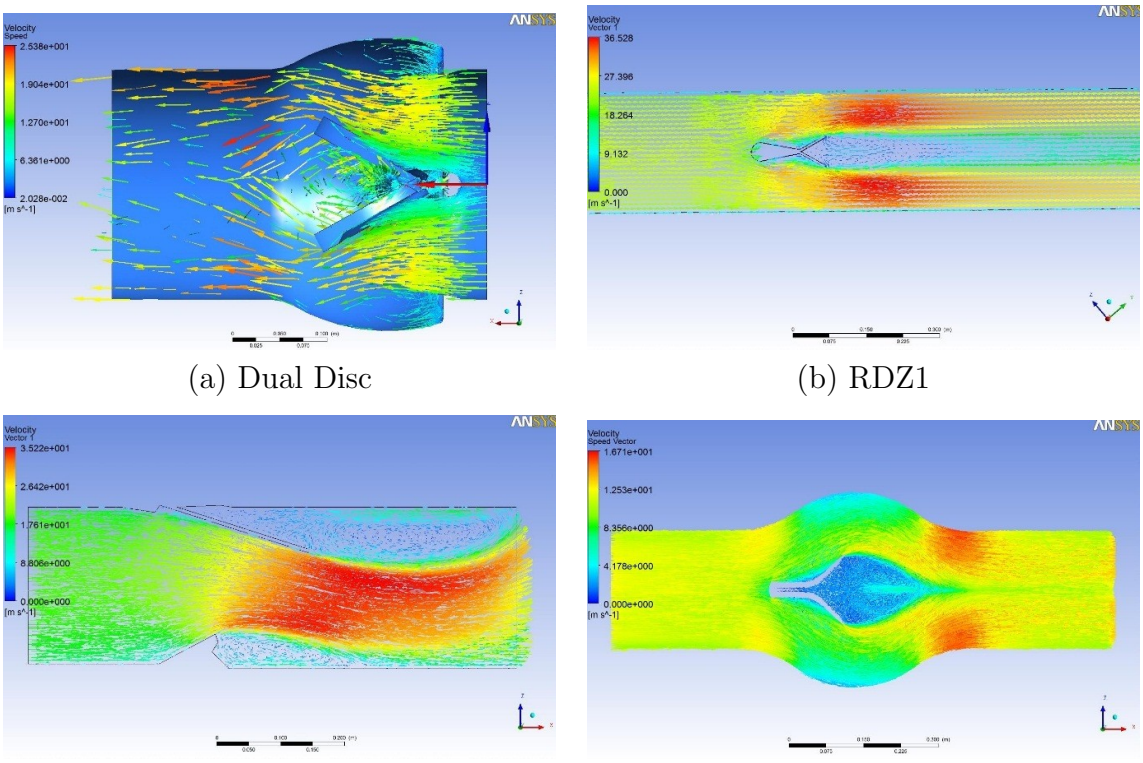

(a) Dual Disc (b) RDZ1

(c) Surgebuster (d) RDZ2

Figure 3.7: Velocity vectors of 4 check valves (a). Dual Disc; (b) RDZ1; (c) Surgebuster; and (d) RDZ2.

Surgebuster and Dual-Disc valves were chosen as those commercial valves models with the lowest crack-pressure. According to the manufacturer datasheets [110, 111], they are 0.3 psig and 0.25 psig respectively. RDZ1 valve crack-pressure is only 0.0016 psig, which is 0.5% the crack-pressure from the commercial models. That is an enormous difference which greatly impact on the performance of the OWC WEC. Such a great improvement is due mainly to the counterweight features added to the RDZ1 and RDZ2 designs.

Additionally, RDZ1 valve's performance was tested at the ocean. First, it was coupled to a 200lt air chamber, when the pressure was positive inside the air-chamber, one of the valves got fully opened and the second valve closed. When the wave passed, the two valves inverted their opened/closed configuration as should happen. They

were able to open and close very rapidly. Due to the angle-gates, the RDZ1 check valve has a smaller stroke to open/close, smaller strokes might faster the open-closing of the valves [97]. The time to move the full stroke ranged 0.4-0.8 seconds. They were able to open and close with all wave sizes. It can be said that operated better than expected.

RDZ1 check-valves were tested also with a smaller 40 lt air-chamber. The amount of displaced air is 4 times less (section area from 200lt air chamber is compared with section area of 40lt air-chamber), and then it was of interest evaluate valve performance at this condition. The 40lt air-chamber is seen in Figure 3.8. RDZ1 were still able to operate with this smaller air-chamber. They were able to open and close even with waves as small as 0.1 m of wave-height.

(a) Opened (left Valve) (b) Closed (left valve)

Figure 3.8: RDZ1 Check-Valve tested at the ocean in a 40lt air-chamber (a) Left valve being open while wave crest is passing (water level higher). Right valve is closed; (b) Left valve being closed while wave trough is around (water level lower). Right valve is opened.

Since the tests were at the ocean, there were no control over the wave-height sizes. Wave-heights ranged from 0.11 m to 0.55 m. Check-valves opened and closed with every wave, even with the smallest ones. Given the complications of bringing expensive equipment to the ocean, this test is only a go/ no-go, test. From the test, it is known that the valve opened with waves as small as 0.11 m, and that the pressure

difference generated for a 0.1 m wave is 1,007.5 Pa assuming a density of 1027 kg/m^3 for salted water. Commercial check-valves with these flow-rates cannot open or close with these small pressure-differences. It can be said then that the performance of the RDZ1 valve during the test was better than expected.

Table 3.5: RDZ1 check-valve results from ocean test.

Air-Chamber (lt)	Wave-height (m)	Air-speed (m/s)	Pressure (Pa)	Open/close?
200	0.1	0.38	1000	Yes
40	0.1	0.056	1000	Yes
200	0.5	3	5037	Yes
40	0.5	0.5	5037	Yes

RDZ1 valve has a very low crack-pressure and pressure drop, and then, it is able to open and close even with the smallest waves, but offers a poor sealing allowing back-flow pass through. This result is not a surprise, it was decided from design to sacrifice sealing to improve crack/pressure. Even though, most check-valves require a good sealing [97], for the present application having a poor sealing or back-flow presence is not relevant since it does not have a large impact on performance. Conversely, crack-pressure is a much more important characteristic with a quantitative large impact on performance.

In order to be able to select the best check-valve for the UFCAP WEC application, the CFD and experimental results along with other identified important criteria were incorporated into a decision matrix, so the selection process is clear and systematic. Each criterion is weighted.

Criteria for the proposed OWC WEC are: pressure-drop, crack-pressure, use of spring, mounting orientation effect, cost, and availability/or manufacturability. All values are measured in percentage such that a score of 100% from each column represents the best and a score of 0% represents the least desirable attribute. The largest score in the last column corresponds to the valve with the best performance for the

present UFCAP application.

The best valve per each of the concepts (rows) is assigned with 100%. The other 3 valves, are computed as follows:

- Pressure drop = Best Valve P_{drop} / Actual Valve P_{drop}
- Crack Pressure= Best Valve P_{crack} / Actual Valve P_{crack}
- Use of spring: if valve uses spring = 0% (larger crack-pressure); if valve does not use spring = 100%. Valves which use spring tend to close the gate, and it will be semi-closed during a range of values around crack pressure in detriment of performance.
- Orientation independence: Subjective value based on experience. If the crack pressure is not affected by gravity (mounting orientation) = 100%. If crack-pressure is largely impacted by gravity = 0%.
- Cost: Based on manufacturing cost, and/or the price in the market.
- Manufacturability-availability: From the prototype-experiment perspective, if valves are readily available for the experiment = 100%.

Cost is an important criterion while evaluating the valves. Commercial valves are readily available, which is an advantage, but the prices are quite high. Surgebuster can be found at about $200 USD, and Dual Disc at $80 USD. One of the reason they are more expensive is that they are designed to stand for not only low-pressures, but also for higher pressures. For this reason, Surgebuster got the lowest cost score in the decision matrix. The other reason is that they are built with very accurate tooling to guarantee a perfect sealing, which is needed in most of the applications. The present WECs application does not require neither a good sealing, nor high- pressures, and

Table 3.6: Decision Matrix to select best check-valve

Valve	Pressure drop (%)	Crack-Pressure (%)	Spring used (%)	Orientation (%)	Cost (%)	Manuf./ Avail. (%)	Score (%)
Dual Discs	21.2	0.6	0	40	8.8	100	
RDZ1	20.7	100	100	100	100	80	
Surgebuster	13.7	0.5	100	60	3.5	100	
RDZ2	100	100	100	100	100	19.5	
Weighted Values (% above * Weight/100)							
Weight	10	10	2	8	6	4	
Dual Discs	2.1	0.1	0	3.2	0.5	4.0	**0.25**
RDZ1	2.1	10.0	2.0	8.0	6.0	3.2	**0.78**
Surgebuster	1.4	0.1	2.0	4.8	0.2	4.0	**0.31**
RDZ2	10.0	10.0	2.0	8.0	1.2	1.2	**0.81**

then, it was possible to find the way to build lower-cost solutions, which are the two RDZ valves. RDZ1 has the lowest cost because it uses off-the-shelf components for its construction plus routed sheet metal. RDZ2 has a higher cost than RDZ1 because of its relatively more complex shape requires a customized mold or machining.

According to the decision matrix, RDZ2 and RDZ1 are the best solutions with a weighted score of 0.81 and 0.78, respectively. They are followed by the Surgebuster check-valve with a score of 0.31 and the Dual disc with 0.25. The RDZ1 and RDZ2 valves are better suited for application in OWC WEC.

3.4 Concluding Remarks

Oscillating Water Columns require specialized check-valves for operation in low wave height conditions. The proposed designs, RDZ1 & RDZ2, have good performance and demonstrated to be overall a feasible solution. Since the available pressure-difference in a OWC device is so small, crack-pressure and pressure drop are of essential importance to the proper operation of the device. The most important criteria for a check-valve to be used in the UFCAP device are in order of importance, crack-

pressure, pressure-drop, mounting orientation-independence, cost, availability, and use of spring. RDZ1 and RDZ2 valves demonstrated and outstanding performance in these two criteria overcoming by far, any other large-flowrates check-valve.

Counterweights resulted also to be a valuable feature, they are the reason to reach the ultra-low-crack-pressure achieved by RDZ valves, and also enable the valves orientation-independence (gates weight independent) meaning the valves might be directed upward, downward or horizontally while keeping the same crack-pressure value. When slight changes in pressure may deeply affect the whole performance of the WEC, the orientation-independence attribute becomes an important advantage.

While wind-tunnel tests allowed to measure the crack-pressure, ocean tests presented an opportunity to test for the first time the performance of an ultra-low-crack-pressure check-valve, and observe the valve operation (opening-closing) with very small ocean waves (0.11 m).

While most of the check-valve applications require a good sealing for backflow, the present application presents no adverse effects when small backflow is present. Nevertheless, it is possible to improve the current sealing by using a rubber material or increase the tolerance during manufacturing. Currently, improving the sealing was assumed to be of secondary importance and it was decided to focus on improving the crack-pressure. Additionally, it is still possible to reduce the wall thickness in order to improve cost since no medium or large pressures are present.

RDZ1 and RDZ2 offer different advantages. For example, RDZ1 is superior in manufacturability and cost, due to its constant section and ability to use off-the-shelf housing, while RDZ2 is about five times better in terms of pressure-drop losses due to its streamlined geometry which might be more important in the long term if the device is used in real electricity production.

With the results obtained using CFD analysis, and the experimental validation

and evaluation, it is concluded that the RDZ1 and RDZ2 valve functionality performed better compared to commercial solutions available in the marked. The crack-pressure presented the most notable advantage with an improvement by a factor of 150 over commercial valves.

For future work, it is possible to convert RDZ2 into a fully spherical valve (eliminate current flat areas) and expect to observe an improvement in the pressure-drop. Originally, it was decided to include the flat walls in the RDZ2's housing due to manufacturability. Another feature that can be improved are the angled-discs. It is also possible to streamline them in both positions, opened and closed, and reduce the pressure-drop. Finally, an optimization of the angle-discs geometry is desirable including angle, length, and location inside the housing.

Chapter 4

UFCAP Turbine Design

A fundamental part of WECs is power-take-off (PTO). In the case of oscillating water column (OWC) devices, the PTO mechanism comprises the turbine - generator coupling. Even though there has been an intense R&D on self-rectifying turbines for OWC devices, there is almost nothing on unidirectional turbines for OWC applications. Being scaled prototype, and the available energy from the wave-flume's waves so tiny, an efficient turbine designed specially for this application was required. Development of a unidirectional air-turbine for scaled OWC application is described in the present Chapter.

There are different types of turbines designed for a wide range of applications. It is important to identify which is the type of turbine which best fit the application. Turbines, such as Francis, Kaplan, Pelton, radial, ship-propeller are intended for high head liquids and are not operable at the available pressure-difference on OWCs [113, 114]. OWC devices have a reduced pressure-difference available, especially in the case of the scaled prototypes, where pressure-difference are of only hundreds of Pascals which reduces the alternatives since most of the industry applications use either medium or high pressure-difference.

Nonetheless, there are similar applications which lead to identify turbines for OWCs. Chapter 1 includes a literature review on turbines used in OWC, and introduces the two most used, the Wells turbine and the impulse turbine which are axial turbines [115]. In addition to them, wind-turbines are also suitable for the present UFCAP application, wind-turbines can be divided for the direction of their axis in Vertical Axis Wind Turbines (VAWT) like Savonious or Darrius, and Horizontal Axis Wind Turbines like the 3 blades Danish model widely known. Typically VAWT are recommended for lower wind-speeds than Danish type turbine with normally a maximum velocity toped for 20-25 m/s winds [116] which is still low compared to the UFCAP airflow velocities which may reach up to 60 m/s in a large device.

There are two design approaches to perform the development of the desired turbine: Wind-turbine design theory such as "Blade Element Momentum (BEM) Theory" [116], and "Compressor/gas-turbine Design Theory" [117]. Both are very well developed being Compressor/gas-turbine Theory the more mature from the two. Both methods could produce in theory a suitable turbine design appropriate for the small pressure-difference available. In this study, the Compressor/gas-turbine design approach was chosen. Wind-turbine design approach is more suitable for open wind, it focusses in long blades, low RPMs, large torques, gear reduction. For the present application wind-turbines-theory recommends 1-3 blades for rapid wind-speed, compressor/gas-turbine-theory recommends 7-20 blades. Compressor/gas-turbine design approach, pointed conversely toward higher RPMs, shorter blade length. It was evaluated that Compressor/gas-turbine design approach could lead to better results, and then, the chosen methodology was based on compressor/gas-turbine approach.

4.1 Airfoil

While it is possible to start from scratch and numerically design a customized airfoil to operate with the current flow regime with CFD numerical solutions or tools such as Xfoil6.9, or Qblade, the chosen approach consisted in using an existing airfoil, selected for its performance at the current flow conditions as base airfoil, and modify it. A large list of suitable good performance airfoils is available in the literature, for example the Applied Dynamics group from the University of Illinois have published a wide airfoil list [118], including the very well know NACA airfoils and others.

Several families were considered for the selection of the airfoil with regards to its application in the industry, those with similar use (e.g. wind-turbines, helicopters, etc.). The full list is found in Appendix B. From these list, it was arbitrarily decided to evaluate only the NACA family which has information readily available. Thickness is a parameter that must be also considered since small values constrain manufacturing and max stresses, and large thickness values may create large drag forces which are contrary to performance.

With Equation 4.1 Reynolds number is computed and lift coefficient C_l, and drag coefficient C_d are obtained from experimental graphs for the closest Reynolds number available. The top 10% with less C_d was nominated. From this smaller group, 3 profiles with the highest C_l/C_d relation are selected. From these three, C_l and C_d are computed numerically for their exact Reynolds number with Xfoil 6.96 software. Finally, the airfoil with best relation between lift-coefficient and drag-coefficient for the desired angle of attack is selected.

$$Re = \rho_{air} C_{amod} \frac{c}{\mu_{air}} \tag{4.1}$$

Note that most of OWC devices do not supply a unidirectional flow and cannot

Table 4.1: Finalist NACA Airfoils

NACA	$\alpha()$	C_l/C_d
63209	7	4.96
63618	8	0.935
64618	8	0.932

use non-symmetrical airfoils from Table 4.1.

4.2 Blade Design

In this section the number of blades, size, comb, entry angle, and exit angle are computed. The methodology followed comprises three main steps, i) computing the pressure-difference available for a given wave range and prototype size without turbine; ii) turbine design based in the available airflow power, and finally iii) iteratively re-calculate the axial velocity and mass flow rate with the turbine in place.

Following the methodology from [19], the volumetric flow is computed for a given UFCAP prototype size and wave regime. Actual sizes from the scaled prototype and waves are used. Prototype size will be described in Chapter 6. The flow is assummed incompressible, steady, and uniform. With conduit diameter, and volumetric airflow known, the axial velocity C_a, and mass flow $\dot{m}$ are computed with

$$C_a = \frac{\dot{Q}}{A_{cond}} \tag{4.2}$$

$$\dot{m} = \rho_{air}\dot{Q} \tag{4.3}$$

where $\dot{Q}$ is the volumetric flow, A_{cond} is the conduit cross section area, and ρ_{air} is the air density.

To compute the available pressure ΔP_{avail} and power $\dot{W}$, the system is idealized as

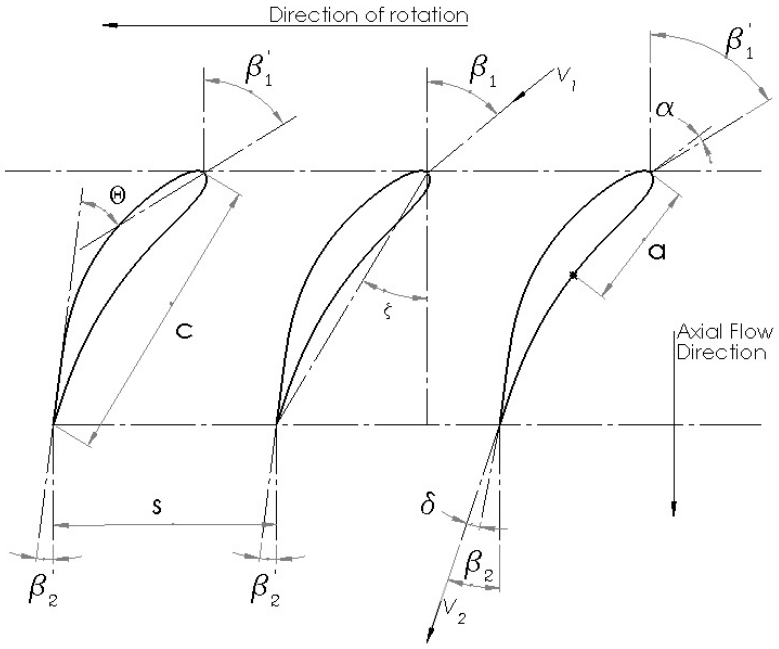

Figure 4.1: Blade nomenclature β_1' = blade entry angle; β_2' = blade exit angle; $\Theta = \beta_1' - \beta_2'$ = comb angle; ζ = rotation angle; s = space between blades; β_1 = air entry angle; β_2 = air exit angle; V_1 = air entry velocity; V_2 = air exit velocity; $\alpha = \beta_1' - \beta_1$ = angle of attack; $\delta = \beta_2 - \beta_2'$ = deviation angle; c = cord; a distance to max comb. (Figure created new by the author extracted from [117]).

a closed container with a conduit closed for the moment, containing air at P_1. When the container is opened, the air is released and arrive to the conduit at pressure P_2 and velocity v_2. With this instantaneous assumptions and Bernoulli the following equations are included

$$\Delta P_{avail} = P_1 - P_2 = \frac{1}{2}\rho_{air} C_{a2}^{\,2} \tag{4.4}$$

$$\dot{W} = \frac{1}{2}\dot{m} C_{a2}^{\,2} \tag{4.5}$$

According to the methodology from Cohen et. al [117] for turbine design, the

modified axial velocity must be computed by removing the generator area from the conduit area. Assuming target RPMs by generator and grid needs, and using the velocity triangles described in deep by Cohen et. al, the entry and exit angles β_1, and β_2 respectively are computed with equations

$$\tan \beta_1 = \frac{U_{tan}}{C_{amod}} \tag{4.6}$$

$$\tan \beta_2 = \frac{\dot{W}}{U_{tan} C_{amod} \dot{m}} \tag{4.7}$$

where U_{tan} is the tangent or radial velocity.

With the entry angle β_1 and exit angle β_2 defined, the parameter "optimum s/c" can be obtained from the *"optimum s/c"* table, which relates β_1, and β_2 with s/c where s is the space between blades, and c is the cord. The aspect ratio x is defined by equation

$$x = H/c \tag{4.8}$$

which determines the blade's aspect ratio between the height, and cord, H and c respectively which normally is $3 \leq x \leq 4$ and not recommendable ≤ 1 for most gas turbines. However, the present application must not follow gas turbines conventions due to its size, RPMs, and flow velocity, and then, it is possible to have values of x close to 1.

The number of blades is calculated with

$$n = 2\pi \frac{r_m}{s} \tag{4.9}$$

where r_m is the median radius of the turbine.

With these parameters determined and the airfoil selected, the distance of max comb a and the proportionality constant m are computed with equations 4.10, and 4.11

$$a = c\,(\%c) \tag{4.10}$$

$$m = 0.23\left(\frac{2a}{c}\right)^2 + 0.1\left(\frac{\beta_2}{50}\right) \tag{4.11}$$

The comb angle δ, deviation angle Θ and rotation angle ζ are computed with Equations 4.12, 4.13, and 4.14

$$\delta = m\Theta\sqrt{\frac{s}{c}} \tag{4.12}$$

$$\Theta = \beta_1 + \beta_2 + \delta \tag{4.13}$$

$$\zeta = \beta_1 - \left(\frac{\Theta}{2}\right) \tag{4.14}$$

With the above angles computed, the selected airfoil is "bended" to adapt to bended middle comb line. The procedure to bend the middle comb line with auxiliaries lines and the airfoil adaption to the bended middle comb line is described in detail in Cohen et. al. [117].

The blade design is complete if a constant cord, and no pitch along the blade are desired. As a first attempt, the blade design is stopped here though, including a reduction of cord length and pitch is desired in future designs.

It is possible to calculate iteratively what will be the fluid velocity and the mass flow after the designed turbine is in place within the conduit. That is, the turbine was

designed for an expected airflow, once the turbine is designed, it is possible to add the resistance it imposes to the fluid, and recalculate the efficiency and power extracted by the turbine. Only the axial velocity C_{a2}^2 is updated when the turbine is added to the system, angles β_1 and β_2 are kept constant. If H_t is defined as the pressure losses due to the air passing the turbine, the new pressure-difference available is

$$\Delta P_{avail} = P_1 - P_2 = \frac{1}{2}\rho_{air} C_{a2}^{\ 2} + H_t \tag{4.15}$$

with H_t equal to

$$H_t = \frac{1}{2}\rho_{air} C_{a2}^{\ 2} n C D_T \tag{4.16}$$

where n is the number of blades, and CD_T are the total losses given by

$$CD_T = C_{DP} + CD_S + CD_A \tag{4.17}$$

with C_{DP} being the losses due to the airfoil geometry (obtained from the airfoil graphs and corresponding Re), CD_S are secondary losses, and CD_A are the losses due to conduits walls and rotor nose.

$$CD_S = 0.018 C_L^2 \tag{4.18}$$

$$CD_A = 0.020 \frac{s}{H} \tag{4.19}$$

being s the spacing between blades and H the height of the blade.

Since C_a is a function of CD_T and CD_T is a function of C_a, the equations are solved iteratively updating the values of Re and C_{DP} at every iteration.

4.3 Case Study Results

Two different turbines were designed. First generation J1-1 with 11 blades and designed for low 450 RPMs and second generation J1-2 designed for 1500 RPMs. Main parameters from both turbines are included in Tables 4.4 and 4.5, and full details from the last generation J1-2. The first part of the analysis consisted in computing axial velocity, mass flow-rate, pressure-difference and max power available from input parameters summarized in Table 4.2. Results for airflow characteristics and angles for bending and orienting the airfoil are shown in Tables 4.3, and 4.4 respectively.

Table 4.2: Turbine design parameters

Conduit diameter (mm)	50.4
Generator diameter (mm)	25.4
Volumetric Flow lt/s	12
Target RPMs* (J1-1 turbine)	450
Target RPMs* (J1-2 turbine)	1500
Air density (kg/s)	1.225
Air viscosity ($Pa\,s$)	$1.8x10^{-5}$

* Defined from local experiments with similar turbines and literature review specs of the like turbines.

Table 4.3: Airflow Characteristics

Axial velocity (m/s)	6
Mass flowrate (g/s)	14.9
Pressure-difference Pa	65
Max airflow power (W)	1.34

Table 4.4: Angles results

Angle	J1-1 Turbine	J1-2 Turbine
Entry angle $\beta_1(^\circ)$	6	20
Exit angle $\beta_1(^\circ)$	85	47
Comb angle $\Theta(^\circ)$	96	39
Rotation angle $\zeta(^\circ)$	57	40

The large difference between the entry and exit angle from J1-1 to J1-2 relay mainly in the target RPMs defined by design which of course impact the relative velocities between the blade and air, affecting then the tangent velocity.

With the entry and exit angles β_1 and β_2 defined, the dimensional parameters in Table 4.5 are then computed. There is also a large difference between the two turbines which is also due to the target design RPMs from 450 for J1-1 to 1500 for J1-2. Experiments measuring the RPMs on turbine-generator suggest incrementing the target RPMs.

J1-2 is designed for faster RPMs, that is the tangent component becomes larger and the blade needs to adjust accordingly. This is the reason the rotation angle in Table 4.4 goes from 57 to 40; likewise, the entry and exit angles are shifted also towards the rotation plane and the comb angle reduces significantly from 96° to 39°.

The relation s/c changes also considerable (see Table 4.5), meaning a lesser number of airfoils is required, which agrees with the theory. The faster the turbine rotates, the lesser number of required blades. H is the blade length. According to gas turbine theory, the value H/c should remain between 3 and 4. The meaning of this parameter is how long the blade is with respect to the cord, in other words, the blade's aspect ratio. Given the large velocities in gas turbines, high flow rates, high RPMs, and normal sizes, those guidelines make sense. In the present case, as mentioned earlier, reducing the aspect relation close to the unity is allowed.

Table 4.5: Blade geometric parameters

Parameter	J1-1 Turbine	J1-2 Turbine
Relation s/c	0.46	0.85
Aspect relation H/c	1	0.91
Cord $c(mm)$	12.4	13.7
Number of blades n	11	7

The two airfoils J1-1 and J1-2 both designed for the ocean prototype with turbine

diameter 2" are displayed in Figure 4.2 in turbine orientation. Figure 4.3 shows the complete model from J1-1 turbine with all the blades. Figure 4.4 illustrate the turbine J1-1 rapid prototype in ABS material. Figure 4.5 include the model of J1-2 turbine, observe the lesser number of blades due to it was designed for faster RPMs. Figure 4.6 show turbine J1-2 rapid prototype which was redesigned in several parts to facilitate assemblability within the whole assembly e.g. central conduit, supports, and generator. Airfoil coordinates can be found in the Appendix B.

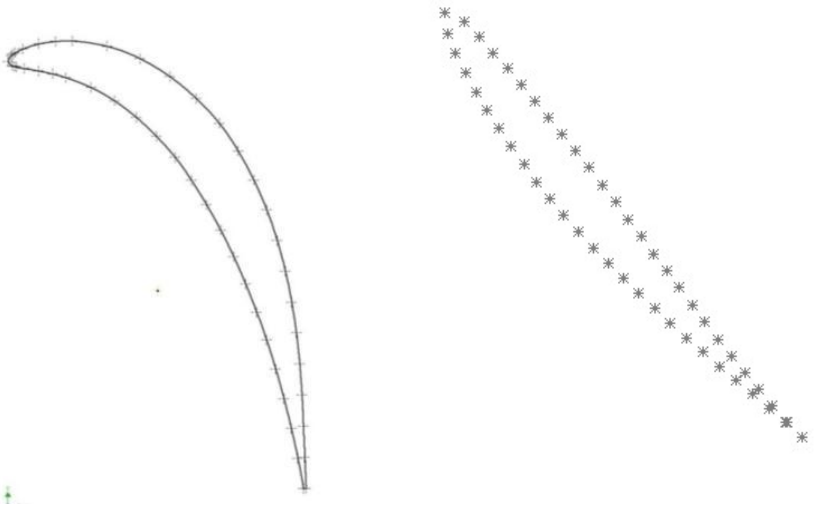

(a) J1-1 Turbine (b) J1-2 Turbine

Figure 4.2: Final shape of airfoils with entry and exit angles in turbine orientation (a) J1-1 ; (b) J1-2.

Figures 4.7, 4.8, and 4.9 illustrate in red the J1-2 airfoil in orientation with respect the horizontal at 6° , 8.5°, and 10° *angle of attack* respectively. Pressure Coefficient is calculated and plotted for each angle of attack. Lift C_l, and drag C_d coefficients are also included as well as the lift-drag ratio C_l/C_d.

All other angle of attack were computed, and not included here. The maximum C_l/C_d for airfoil J1-2 occurred at $\alpha = 8.5°$ angle of attack. At this angle of attack $\alpha = 8.5°$ lift $C_l = 0.994$, and $C_l/C_d = 15.39$. Comparing this numbers with an

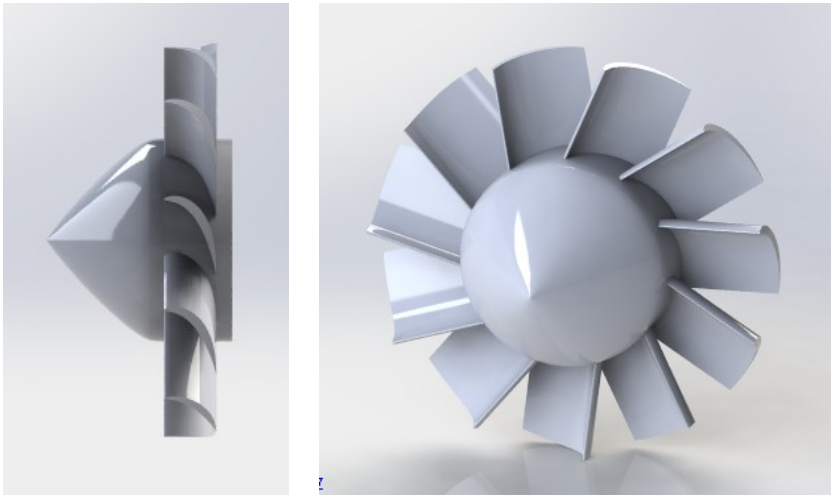

(a) Left view (b) Front view

Figure 4.3: J1-1 turbine model for ocean prototype (a) J1-1 left view ; (b) J1-1 front view.

standard well known airfoil NACA 0015, commonly used in small wind-turbines and even in Wells turbines, at angle of attack 7.5, when the C_l/C_d relation is maximum for NACA 0015, the $C_l = 0.59$; and $C_l/C_d = 8.23$. It can be seen the designed J1-2 airfoil may reach considerable larger C_l/C_d than NACA 0015 proving the effectiveness of the present methodology.

Figure 4.10 depicts the polars from J1-2 compared to NACA0015 airfoil for reference. While maximum ratio C_l/C_d is much larger for J1-2, it occurs for a limited narrow range of angle of attack, it drops rapidly. While NACA0015 C_l/C_d does not reach those height values, is more stable. Regarding drag-coefficient C_d, J1-2 airfoil has better performance for all angles of attack, recalling drag force should be minimized.

Numerical simulations of the turbine with the software Qblade and the parameters already mentioned are performed to predict power, and torque. Figure 4.11 shows the predicted power for J1-2 turbine at different airflow-speeds, and also at its effect when running at a variety of RPMs. The maximum power which can be generated

(a) Mounted in central-conduit

(b) only turbine

Figure 4.4: J1-1 turbine rapid prototype in ABS material (a) mounted in UFCAP prototype ; (b) only turbine.

by the turbine is around 0.6 W occurring at 3,000 RPM and with airflow speeds of 20 m/s, which is in agreement with the expected for a scaled prototype since power is scaled largely (Froude scale to be discussed in next chapter).

It is standard in the wind-turbine R&D to represent results as a function of tip speed ratio (TSR) which is the ratio between the wind-speed and the blade tip speed. Figure 4.12 includes results for turbine J1-2 power vs.TSR, and generated torque vs. TSR both at different air-speeds. It is not surprisingly that TSR values achieved < 1 contrast with those observed in most of the wind-turbines where the optimum occurs at around $TSR = 6$. The reason is that most of wind-turbines use a gearbox which habilitate to run the rotor at low RPMs compared to RPMs in the current application. Therefore, while RPMs are high for J1-2 turbine, TSR values decrease.

4.4 Experimental Tests

Turbine test is accomplished by coupling it with a generator and an array of LEDs.

Generators from the same type may still be very different regarding RPMs, start-up torque, resistivity, size and shape, output voltage, k_e, and current. The generator selection is also crucial for the good performance of OWCs [86, 82] and usually disre-

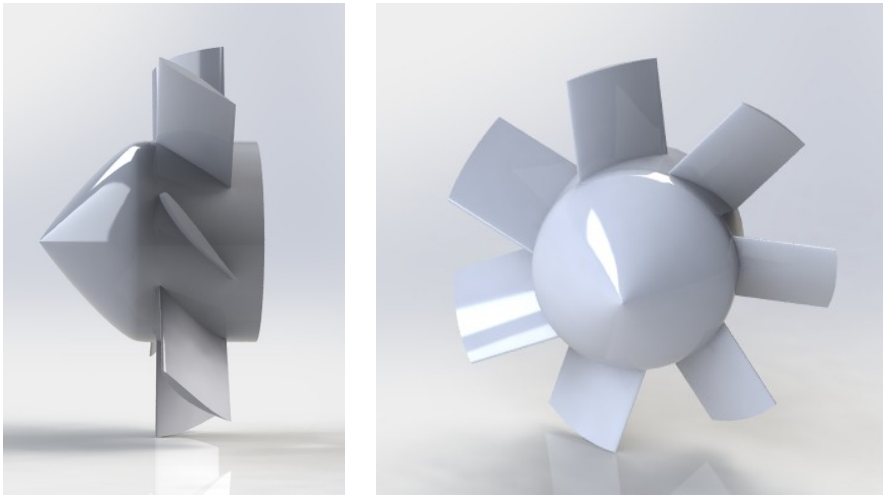

(a) Left view (b) Front view

Figure 4.5: J1-2 turbine model for ocean prototype (a) J1-2 left view ; (b) J1-2 front view.

garded. A total of 11 generators were investigated theoretically via data sheet, and other 5 available motors experimentally.

With the generator already selected, the relative performance of the two turbines is compared. The test consisted in coupling the turbine to a generator, measuring RPMs, and output voltage, with and without electrical load given by an array of LEDs. They are tested at three different air-speeds. The two turbines are compared. All conditions were the same for both turbines. Results can be found in Table 4.4

K_e is the generator's electric constant in $volts/1000RPMs$, it indicates the required voltage per revolution, when operated as a motor. It is computed with equation

$$K_e = \frac{\mathcal{V}}{1000RPM} \tag{4.20}$$

where $\mathcal{V}$ is the voltage, RPMs are the rotor's revolutions per minute. K_e is an important parameter to select the appropriated generator. A generator with a low K_e requires high RPMs in order to generate the desired voltage. Conversely a generator with an elevated K_e requires high torque to rotate it, it will not rotate unless the

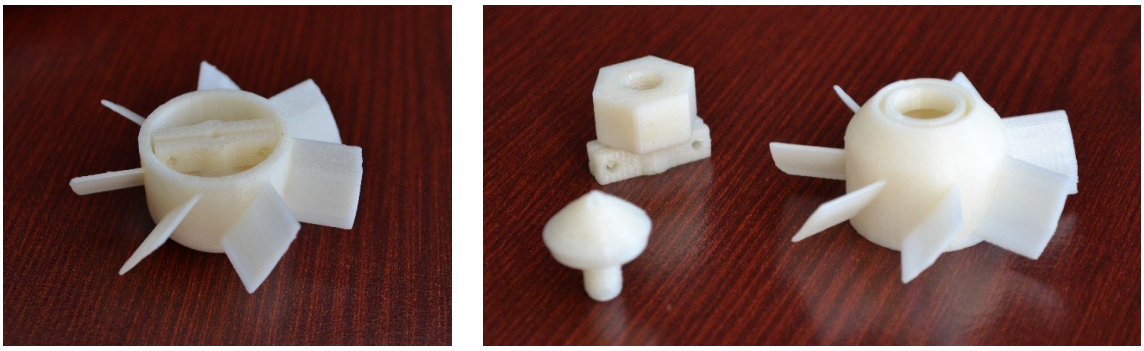

(a) Mounted in conduit (b) only turbine

Figure 4.6: J1-2 turbine rapid prototype in ABS material. (a) assembled ; (b) exploded.

imposed torque by the airflow-turbine is also high, leaving it static for most of the air-speeds.

Table 4.6: Turbine performance comparison

		without LED load			with LED load		
Air-speed	Turbine	RPM	Volts	K_e	RPM	Volts	K_e
low	J1-1	640	0.4	0.625	766	0.56	0.7311
airflow	J1-2	440	0.06	0.136	545	0.3	0.5505
medium	J1-1	1440	1.25	0.8681	1325	1.1	0.8302
airflow	J1-2	1040	0.82	0.7885	1508	1.3	0.8621
high	J1-1	3800	3.9	1.0263	3320	2.9	0.8735
airflow	J1-2	4215	4.42	1.0486	3530	3	0.8499

4.5 Concluding Remarks

In the methodology used for the development of the turbine airfoils, the selection criteria for the blade seeks to maximize the relation C_l/C_d. The performance is good for the design range of angles of attack as seen in the polar plots. However, the UFCAP flow-rate is changing in time, and with that, turbine RPMs are also changing in time, and equivalently, angle of attach is changing in time. The selected airfoil performs well when operating close to the design angle of attack, but falls rapidly

Figure 4.7: J1-2 Pressure coefficient plot and other parameters at $\alpha = 6°$.

when departing from the target, dropping the overall performance of the turbine when operating in real conditions and a plurality of airflow speeds. A different airfoil with a lower peak C_l/C_d relation, but still high in a wider range of angle of attack is desirable for this kind of applications.

For the scaled prototypes, it is recommended to lower the design RPMs to a value of 1000 rpm which falls between the currently used design rotational speed of 450 rpm for J1-1 and 1500 rpm for J1-2. the proposed value of 1000 RPMs keeps the rotational speed sufficiently high for the good operation of the generator, and sufficiently low for a low cut in speed and low flow-rates available which are observed for an extended time. For the case of full size prototypes, higher rotational speeds would be required, and flow rates will be faster than in the scaled model.

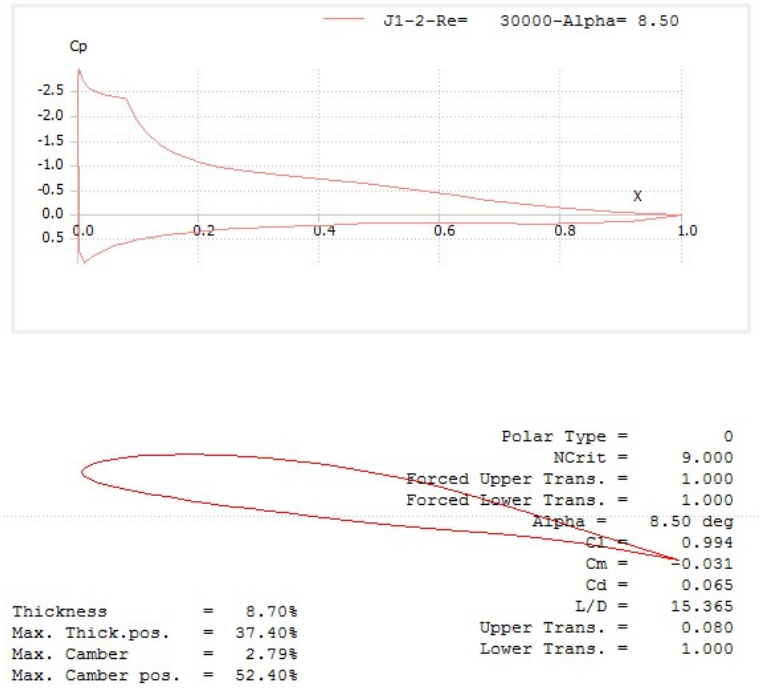

Figure 4.8: J1-2 Pressure coefficient plot and other parameters at $\alpha = 8.5°$.

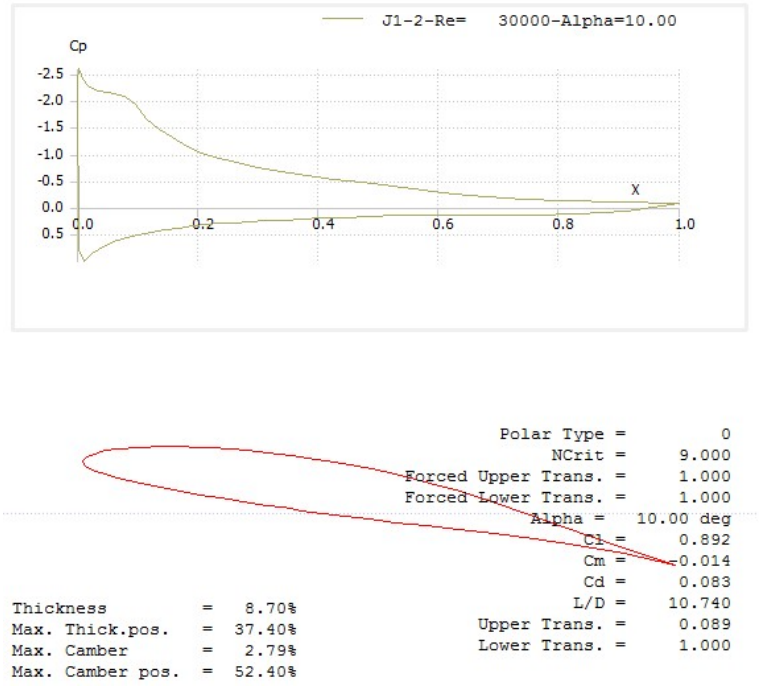

Figure 4.9: J1-2 Pressure coefficient plot and other parameters at $\alpha = 10°$.

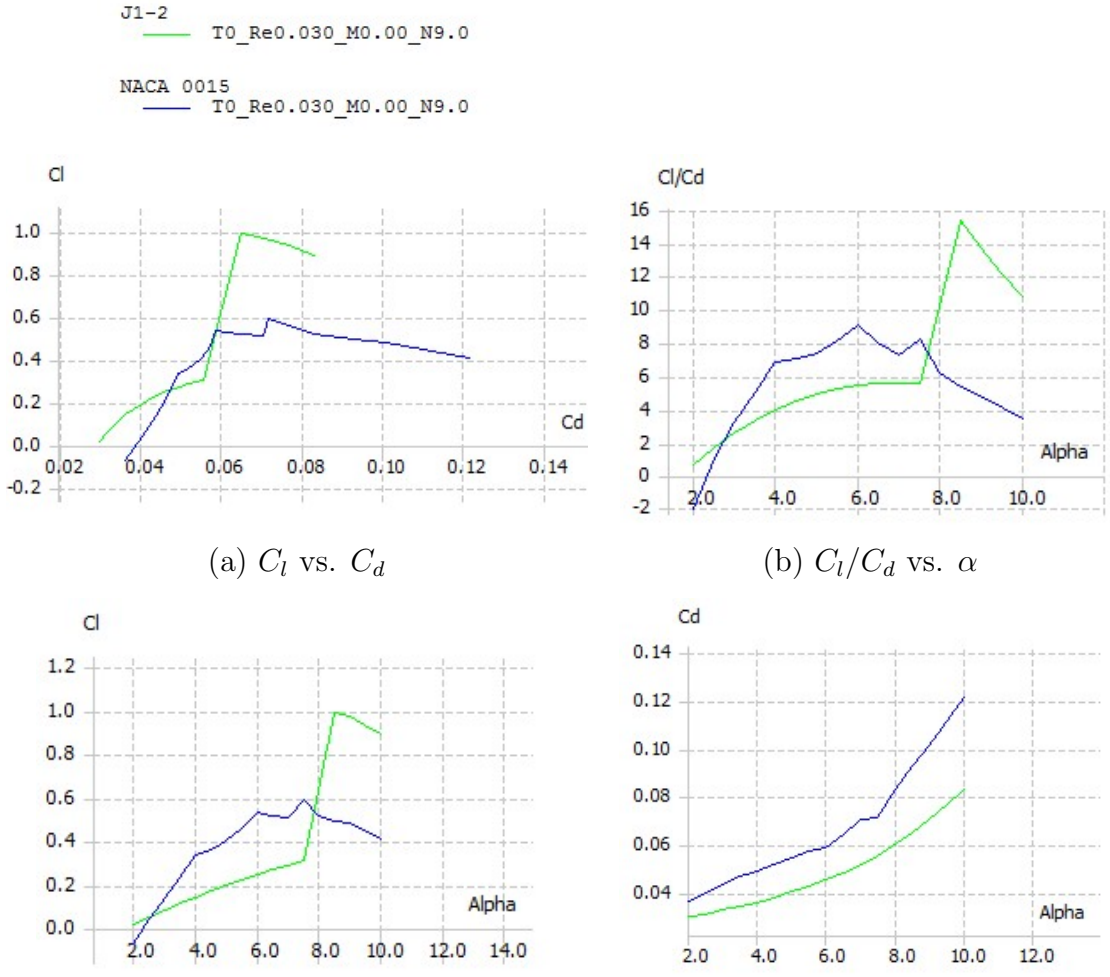

(a) C_l vs. C_d

(b) C_l/C_d vs. α

(c) C_l vs. α

(d) C_d vs. α

Figure 4.10: Polars for J1-2 & NACA0015

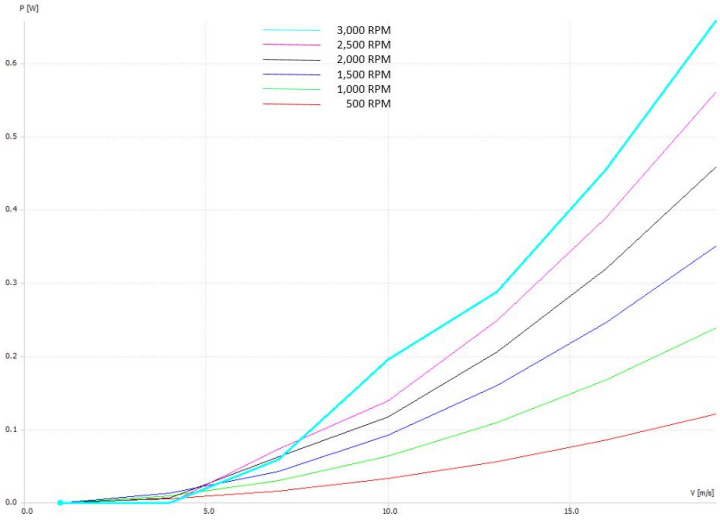

Figure 4.11: Predicted power for J1-2 turbine vs. air-speed.

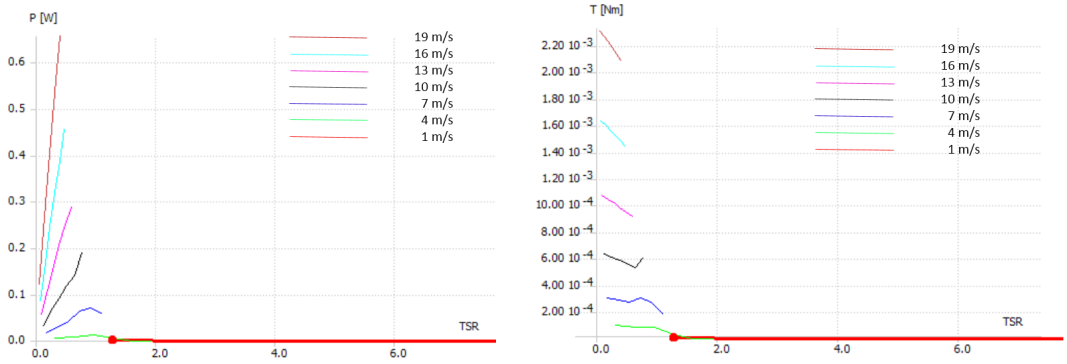

(a) P vs. TSR (b) $Torque$ vs. TSR

Figure 4.12: J1-2 turbine power and torque vs. tip speed ratio

Chapter 5

Ocean Tests

When workability from a novel WEC is unclear, the first step is proving technology feasibility. The fact that UFCAP WEC's performance is highly sensible to any pressure's losses, and interactions among its constituents (air flowing from one air-chamber into another at different wave phases, damping/resonance interaction among air chambers), makes not evident assuming the device will work as intended. Before investing a large amount of effort on deeper development to understand behavior details, creating a full model, or optimizing the device, a proof is required.

Numerical models can normally be used to prove workability. However, proving UFCAP's feasibility required both, component-level and complete system-level numerical models which were not achievable within the available time frame. Due to the high interaction of its components, a component-level is not sufficient, and then a system-level numerical simulation is necessary to prove device feasibility. Nonetheless, due to its numerous unknowns and performance impact of them (check-valve friction, pressure-drop due to check valve, variable pressure-drop due to conduit-variable-bending, compression effects, air-chambers motion with 6 degrees of freedom affecting water column dynamics, among others), a simplified system-level numerical

simulation would have been inaccurate and then, still not a full proof of feasibility without its respective experimental validation.

Conversely, experiments let observe if the device is operable, which is a fundamental query to make decisions over future steps such as investing a large amount of resources trying to develop detailed numerical and experimental models to accurately simulate its behavior.

WECs development stages, numerical models, and experiments, are described in section 1.2.3. Experiments with WECs are much less common than numerical studies because they require larger amount of resources not only to build a WEC model but also to use the wave-flume facility [119]. Typically, WECs experiments are performed first in a wave-flume and later at the ocean. There is high added value operating in this order, since wave-flume's tests allow better control over the variables and risk management since normally requires less resources. Due to UFCAP's simplicity, cost of materials, and incorporation from off-the-shelf components, marine maneuvers' support, the cost of the ocean's tests was one tenth of the cost of using a wave flume facility. Having not access to a wave flume by the time these experiments were conducted, it was decided to prove UFCAP feasibility at the ocean.

5.1 WEC Model

The physical model and its features were designed to support the main objective of proving feasibility. Different from a WEC pilot-plant, which is intended to operate for long time, the present model needs to work only briefly. A pilot-plant should consider wave conditions as one of their top criterion for site selection, among other criteria [120]. Conversely, while the wave weather is also fundamental for a proof-of-concept test run, since it determines the device's size and shape, it does not determine

the experimentation site. In a proof-of-concept experiment, test location must be determined basically for the ease of access to the site, distance to base camp, and availability of handling resources in the area.

Manzanillo, Mexico was selected to perform the ocean tests mainly because of CFE's *(Electricity Federal Commission)* local support for the marine maneuvers (specialized team and resources). Choosing the site based on the desired waves, would have required moving equipment and people to such a site (typically far) making the proof-of-concept test not cost-feasible. After a preliminary evaluation across the zone close to the CFE team, three potential specific locations nearby were evaluated, called Tepalcates, Ventanas, and Enamorados. They were identified based on *availability, distant from people, out of marine routes, and safety.* Wave-height, wavelength, depth, accessibility, and permissions were investigated to select the final test location.

Ventanas-beach was closer to the harbor, with easier access for equipment, and appropriated wave sizes for the intended evaluation test. Even though wave data (date, depth, speed, dir, Hs, Tp, Tz, T, Sprd, Ep, Ev, Energy) was available from a CFE's buoy 9 km away since 1994, no wave history data was available for the exact location. Nevertheless, a long wave history is not required for a proof-of-concept short test. Water depth, wave height and wavelength absolute measurements on Ventanas beach are tabulated in Table 5.1.

Table 5.1: Local Measurements at Ventanas beach

Characteristic	Value
Wave-height m	0.2-0.6
Wave-length m	80-130
Period s	9-14
Water depth	4-17
(@ closer -farther air-chamber)	
Distance to shore	100

Base design is illustrated in Figure 5.1. It shows and array of several 200 *lt* air-chambers interconnected with two conduits each, and compares them with the approximate size of a person. A configuration with 4 air-chambers was devised to have the ability to operate with either one (independent air-chamber), two, or four air-chambers. Figure 5.2 outlines a four air-chamber model and the position of ball valves labeled "A" those at mid location, and "B" at the turbine region which serve for different purposes. Closing valves "A" changes the model from a 4 to a 2 air-chambers configuration, valve "B" can impose a regulated pressure-drop to simulate a larger generator load, or may close the central conduit completely when needed e.g. during the control board assembly, a failure, maintenance, or danger.

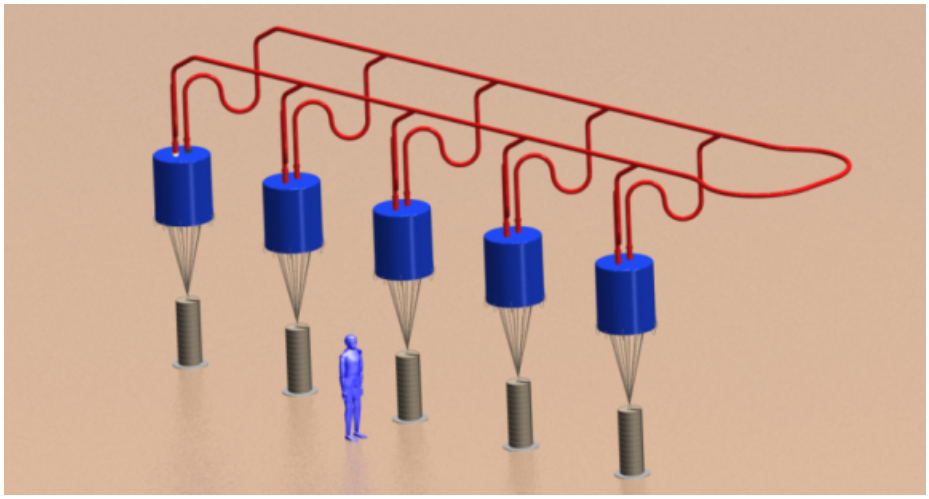

Figure 5.1: UFCAP ocean model/prototype.

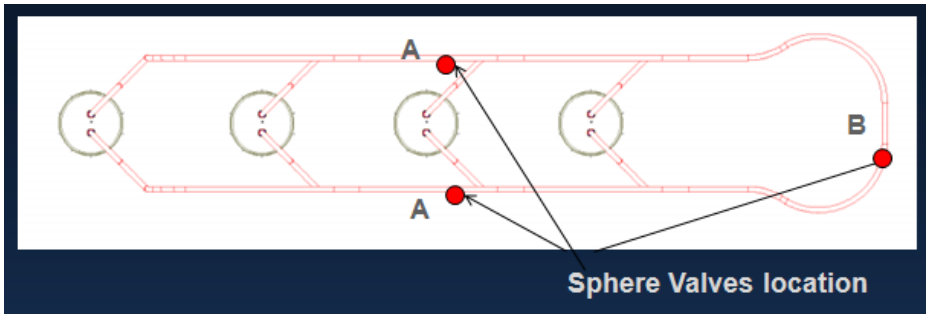

Figure 5.2: UFCAP ocean model configurations.

Figure 5.3 depicts an exploded view from the actual model assembly. For simplicity only 1 air-chamber is shown and full conduits are not included. The air chamber is a plastic 200 *lt* container, with couples, check-valves, conduits, which are directed towards the supply and return manifolds, PVC "Y" fits with rapid connectors, mooring included the yellow adjustable cable with a representative load (1 out of 12) at the center, and the control board at the center-right which incorporates all the electronics, sensors, turbine, and LEDs.

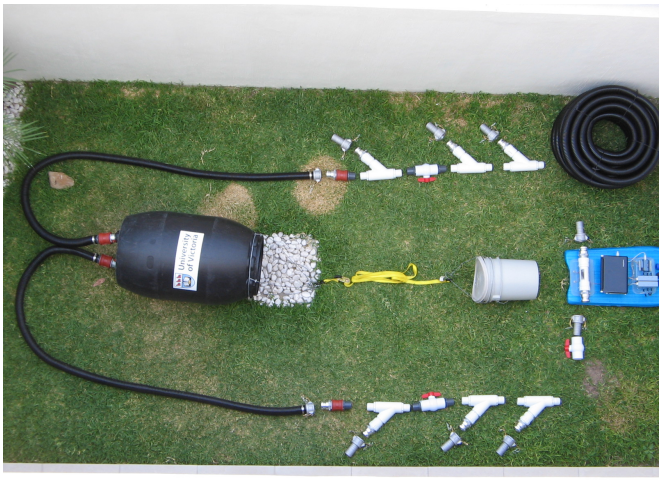

Figure 5.3: UFCAP ocean model explosion (only 1 air chamber shown).

While the complete UFCAP model includes many components, they can be grouped into 4 subsystems:

1. **Control board**, which includes all the electronics (the generator, LEDs, turbine, DAQ, laptop, sensors).

2. **Mooring**, which includes all the means to fix-anchor the model.

3. **Air-chambers**, which includes the containers, bracket, chamber fits, check-valves, floating valves.

4. **Conduits**, including all the conduits-array with connections and means to keep them floating during installation).

Figure 5.4a shows conduit-fits with floaters and sensors' hoses, and Figure 5.4b illustrate the check-valve scaled models.

Although all of them require development and design considerations, AIR-CHAMBERS, and CONDUITS subsystems need only conventional work and will not be discussed. The CONTROL-BOARD subsystem on the other hand, requires specialized development, it contains all the electronics and measuring equipment (Figure 5.5). It includes a turbine-generator, a computer, 6 pressure sensors, data acquisition card (DAQ), a laptop, floating board, and flashlights. Pressure sensors are able to measure wave height, water level inside air-chambers, and air-speed. The LEDs are incorporated with switches to light either 3, 5 or 8 LEDs.

The control board is able to float right at the test site while keeping all the electronics dry and ventilated to prevent both electric shorting, and overheating damages. The pressure is communicated through the pressure hoses from the measuring point inside the water, towards the dry pressure sensors (blue hoses in Figure 5.4 a).

The pressure sensors are MPXV5050GP case 1369-01 differential-pressure-sensors which convert pressure-variations from the waves into voltage. They are protected by a plastic housing.

Communication between laptop-DAQ-pressure-sensors is achieved through a customized software coded in Labview which recognizes measures from pressure sensors, and induced voltage from the generator, for instantaneously plotting the information and writing log files.

The split mooring concept is a clear example of such innovative transformations. Large boats and lifters are extremely expensive and inaccessible for the current project. Each of the four chambers requires 250-300 kg dead weight to get them fixed. In order to be able to handle them without any fork or lift, the mooring was split into small packages so it could be performed with small boats and without fork.

(a) (b)

Figure 5.4: (a) Actual conduits assembly with floaters; (b) check valves.

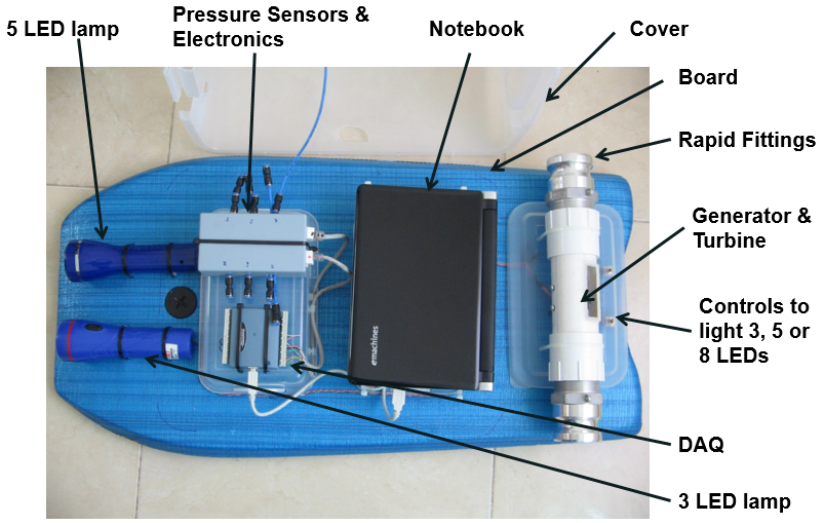

Figure 5.5: UFCAP ocean's model control board.

Each of the four air-chambers counted 12 mooring elements incrementing the tether length from approximately 60 m if a single weight per chamber were used, into 700 m if the weight per air chamber is split, but eliminating the need of heavy equipment (see Figure 5.6). This mooring concept evolved into a simpler one shown in Appendix C.

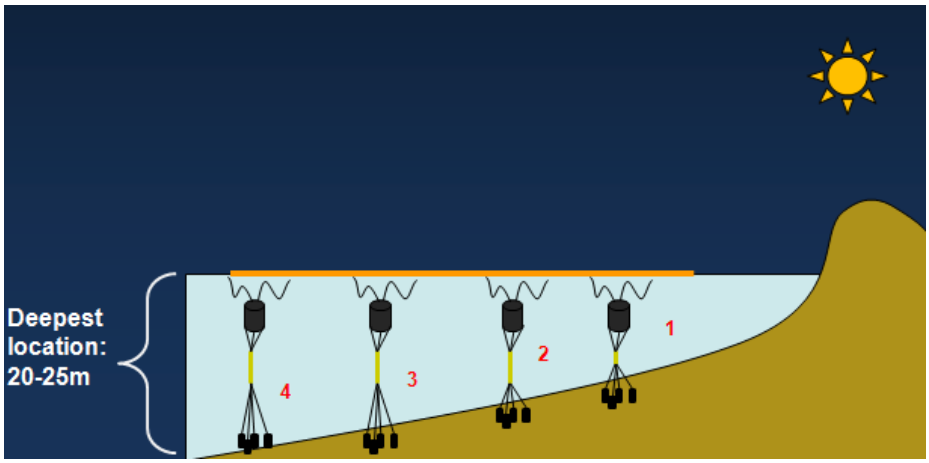

Figure 5.6: Split mooring concept.

5.1.1 Model sizing

Sizing the model is a key activity to successfully generate electricity with the local ocean waves. Air-chamber's size and conduit's size are computed using wave measurements from Table 5.1 as an input for the analytical iterative method described by Rodriguez in [19] and summarized in section 2.4, and Appendix D) to determine air-chamber, and conduit. Detailed fluid behavior is not used in this step, only overall flow.

The results from the previous methodology are coupled with the additional method described in section 4.2 to include turbine's pressure-drop effect iteratively. The method assumes regular waves, neglects losses due to friction, steady flow, flat velocity profile across conduits, constant pressure drop at check valve, and turbine. This method can be used to compute air speed, power, and size the device.

A parametric analysis is made for a variety of air-chamber and conduits sizes in combination with different wave-height and wave-periods. The model size with best results for the local weather is selected. Air-chamber and conduit sizes are defined by commercial available products. Other manufacturing and installation constrains such as equipment, rough material, and transportation are also included in the design

process.

Figures 5.7, 5.8, 5.9, and 5.10 show a sample of the results for a given model size that were used in the parametric analysis.

Figure 5.7 depicts the airflow velocity without turbine which can be reachable with different sizes of a single air-chamber; diameters 400 mm, 495 mm, and 580 mm which correspond to 60lt, 120lt, and 200lt containers which are commercial sizes readily available and no need to build special tooling for prototype them. As expected the larger the wave-height, the larger the airflow produced, and the larger the air-chamber diameter, the larger the airflow as well.

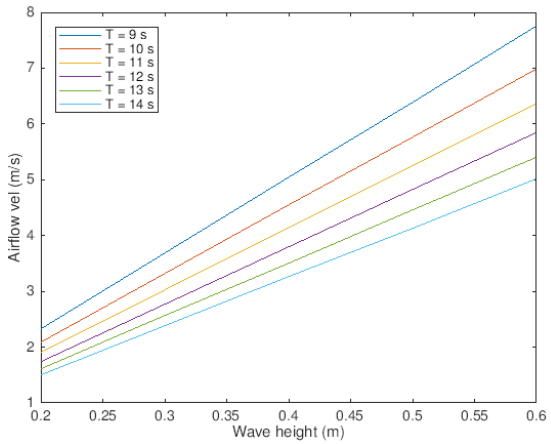

(a) N=1 Diam 400 mm

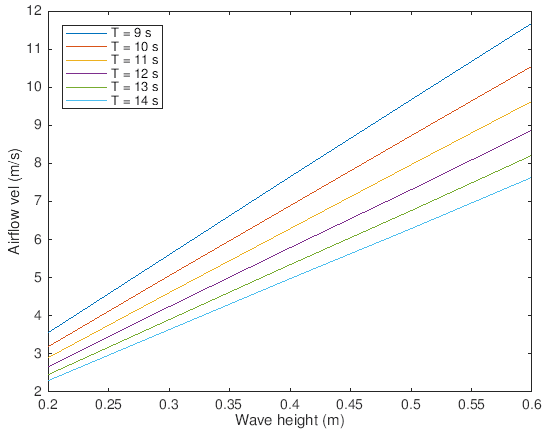

(b) N=1 Diam 495 mm

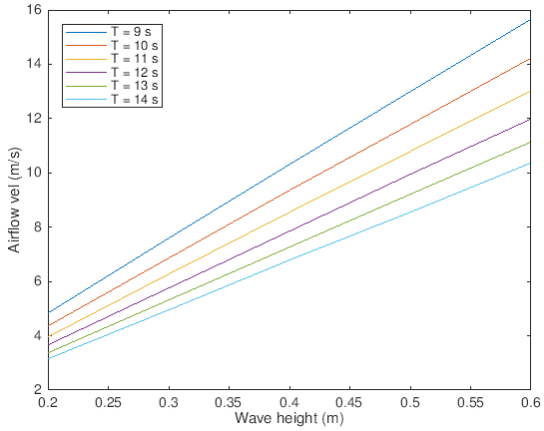

(c) N=1 Diam 580 mm

Figure 5.7: 1 air-chamber airflow velocities for different air-chamber sizes.

Figure 5.8, includes the same information with two air-chambers operating together. Only the wave heights of interests, those present in the Ventanas beach, are included in the figures. For the 400 mm (Figure 5.8 a) results are almost perfectly summed to twice as much when comparing 1 air-chamber with two air-chambers. But for some results of 495 mm air-chamber and 580 mm air-chamber (Figure 5.8 b and c), results are not longer mere summations. The larger the air-speed, the more difficult to discharge all of it through the same conduit size. At Figure 5.8 c the results are more clearly curved.

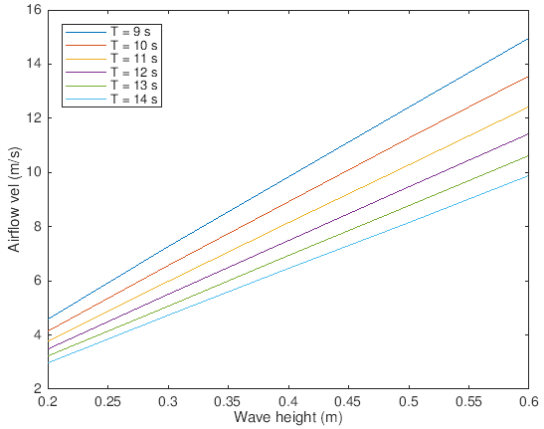

(a) N=2 Diam 400 mm

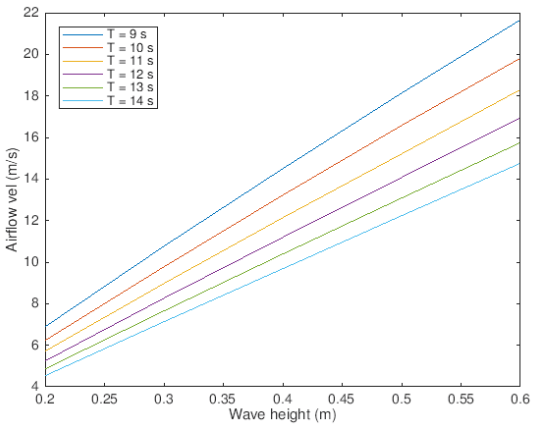

(b) N=2 Diam 495 mm

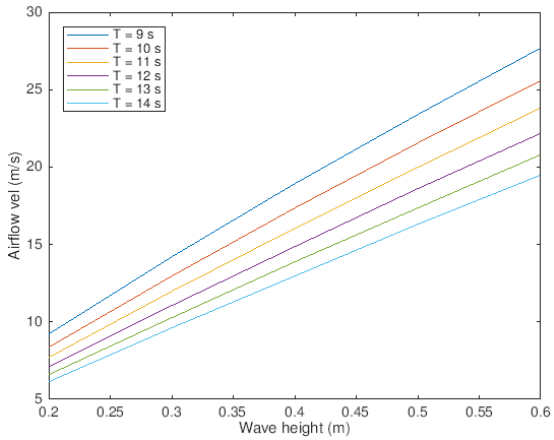

(c) N=2 Diam 580 mm

Figure 5.8: 2 air-chamber airflow velocities for different air-chamber sizes.

Computed airflow-power is visualized in Figures 5.9, and 5.10. Figure 5.9 displays

the results for 1 air-chambers of 3 different sizes. Pinpointing a frequent wave of 0.4 m height and period 11s, the average expected airflow power for the 580 mm diameter air-chamber will be 0.6 W without turbine (see Figure 5.9). With turbine included it will be reduced up to 70%-85% (depending on the turbine and generator selected, see turbine results in chapter 4) to review the iterative method to compute turbine inclusion.

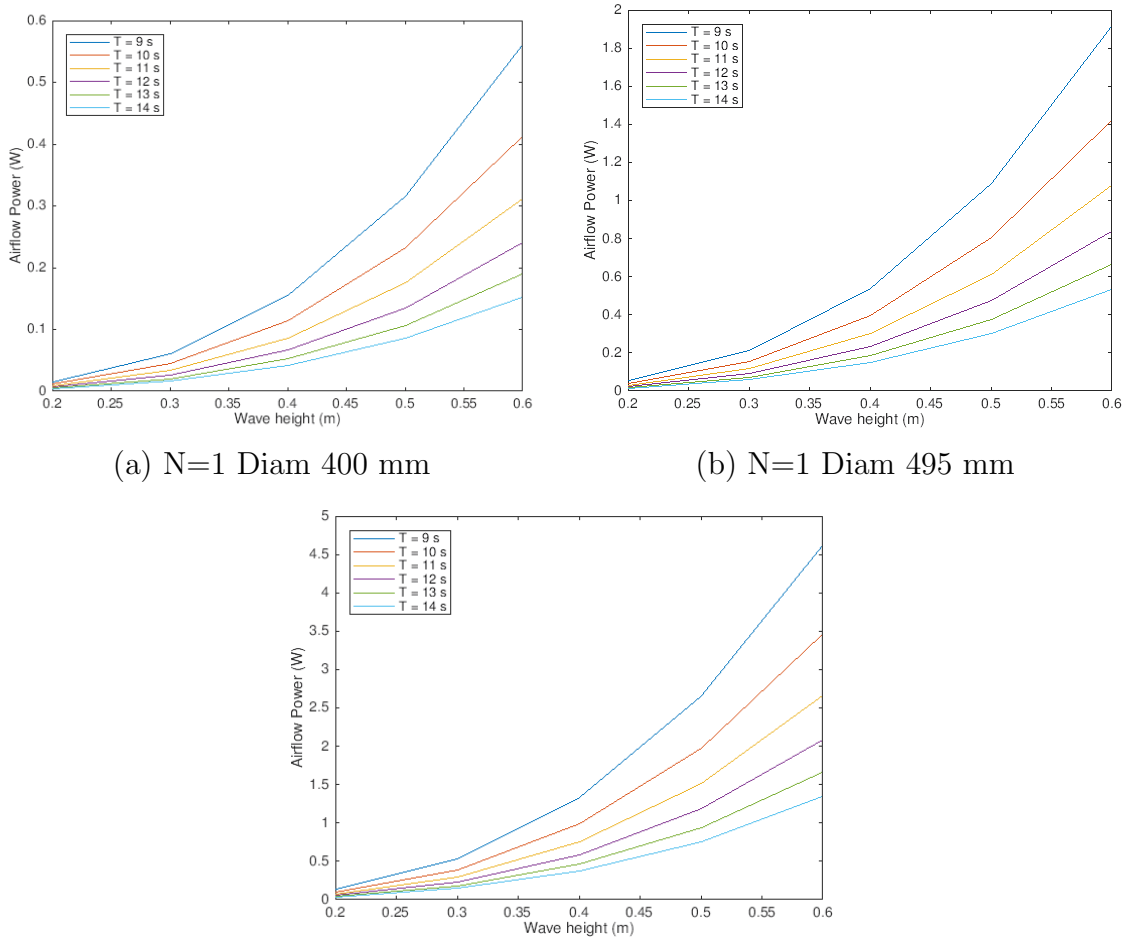

(a) N=1 Diam 400 mm

(b) N=1 Diam 495 mm

(c) N=1 Diam 580 mm

Figure 5.9: 1 air-chamber airflow power for different air-chamber sizes.

Airflow-power with two air chambers (N=2) increases significantly. While the air-velocity increases almost lineally from one air chamber to two air chambers, the airflow power increases with the cube of the velocity and the average computed power

for the same wave increases to almost 5 W (see Figure 5.10 c).

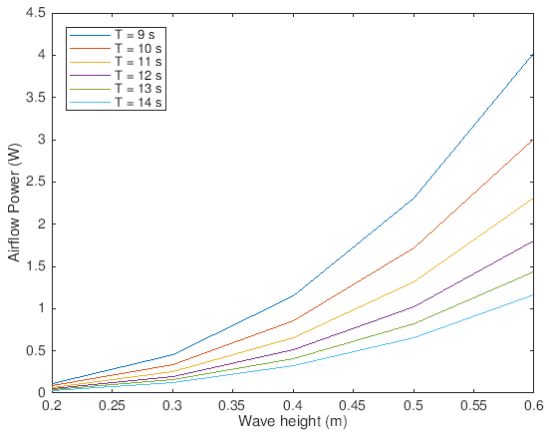

(a) N=2 Diam 400 mm

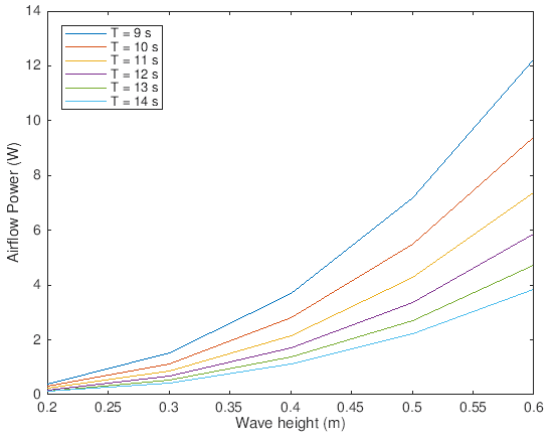

(b) N=2 Diam 495 mm

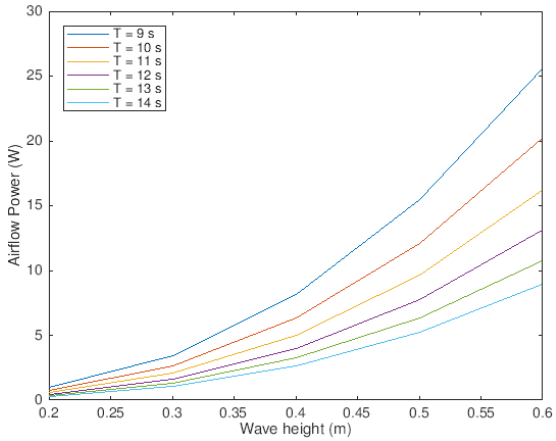

(c) N=2 Diam 580 mm

Figure 5.10: 2 air-chamber airflow power for different air-chamber sizes.

The model was sized using the discussed parametric analysis, plus a safety factor to oversize the device. Due to the many variables which are not in control at the ocean, e.g. the exact wave-height occurring the day of testing; the novelty of the test (proof-of-concept at the ocean in this scale with no previous history, conducted over a novel device); and the large amount of unknowns e.g. uncertainties due to friction losses (wall roughness, conduit bending, check valves), components performance (generator and turbine efficiency, valves torque, air-chambers motion, leakage, etc.), among others; and the impossibility of repeating the test (due to resources availabil-

ity) it was decided to use a safety approach where the device is over-sized to ensure LEDs will be lighted with ocean waves, disregarding device efficiency. Proving the mode of operation works as devised is the main interest of this test and not high performance.

OWC's wave flume models can be scaled with Froude criterion or a improved method as described in section 6.1 which accounts wave-height and wave-length simultaneously. Nevertheless, the present proof-of-concept test presents an additional complication since surrounding rocks at the test site made possible to reduced ocean wave-heights considerable (a desirable situation to be able to use a smaller model), but do not have an equivalent effect over the wave-lengths (see table 5.1 for local wave sizes). The physical separation of the air chambers should be on the same physical scale as the wavelengths observed at the site so it may face different wave-phases. Although having this length is not needed to operate, it is a desirable feature (see tunability in section 2.3). Two approaches were used, moving the device closer to the beach, where shallow water wavelength are smaller, and increase model spacing, or equivalently increasing conduits length while keeping the rest of the device sizes as obtained from the parametric analysis previously described.

Model size results and specs are summarized in Table 5.2.

5.2 Execution

Ocean deployments were executed in different times, with the opportunity to redesign the model between them to face the observed problems and be able to meet the tests objectives which were to generate sufficient energy to light a LED flashlight, to quantify the airflow generation, and to identify the design issues and operational challenges.

Table 5.2: Ocean model specifications

Characteristic	Value
Overall model length (m)	90
Max height ** (m)	15
Min height ** (m)	5
Air chambers	1, 2, or 4
Conduit diameter (in)	2
Total conduit length (m)	200
Contained air (lt)	1,200*
Total weight (kg)	1,200**
Rated wave-height (m)	0.6
Rated wave period (s)	9
Rated power *** (W)	0.72
Turbine diam (in)	2
Number of LEDs	3, 5, or 8
Pressure sensors	6
Computer	1
Software code	Labview
Air-speed at turbine*** (m/s)	3.2
Generator type	DC 9 ($\mathcal{V}$)

* 800 lt air-chambers, 400 lt conduits

** Mooring included.

*** With 1 air-chamber.

During the incremental testing of the UFCAP WEC, the first deployment used the model with the original design already described, a few modifications, detailed in Appendix C, were made and tested, and also a stand-alone test was carried out to test the components independently.

Project planning is of core importance in ocean testing, including resources, equipment, climate, sequence, transportation, among many things. Installation has its own complexity, requires plan with specific tasks and sequence of tasks that will not be included within the scope.

Ocean deployments were performed by experienced divers and under the environmental monitoring of the regulatory government body. Figure 5.11 illustrates a few moments during the installation. Only the mooring required a full day to be installed.

The rest of the model was connected the next day. In Figure 5.11a, two persons are dropping by hand air-chamber showing how light it is. In Figure 5.11b, the sensor hoses are visible in blue along with the supply and return conduits (larger conduits in black). Figure 5.11c shows underwater maneuvers to the air-chamber fixed and aligned in height.

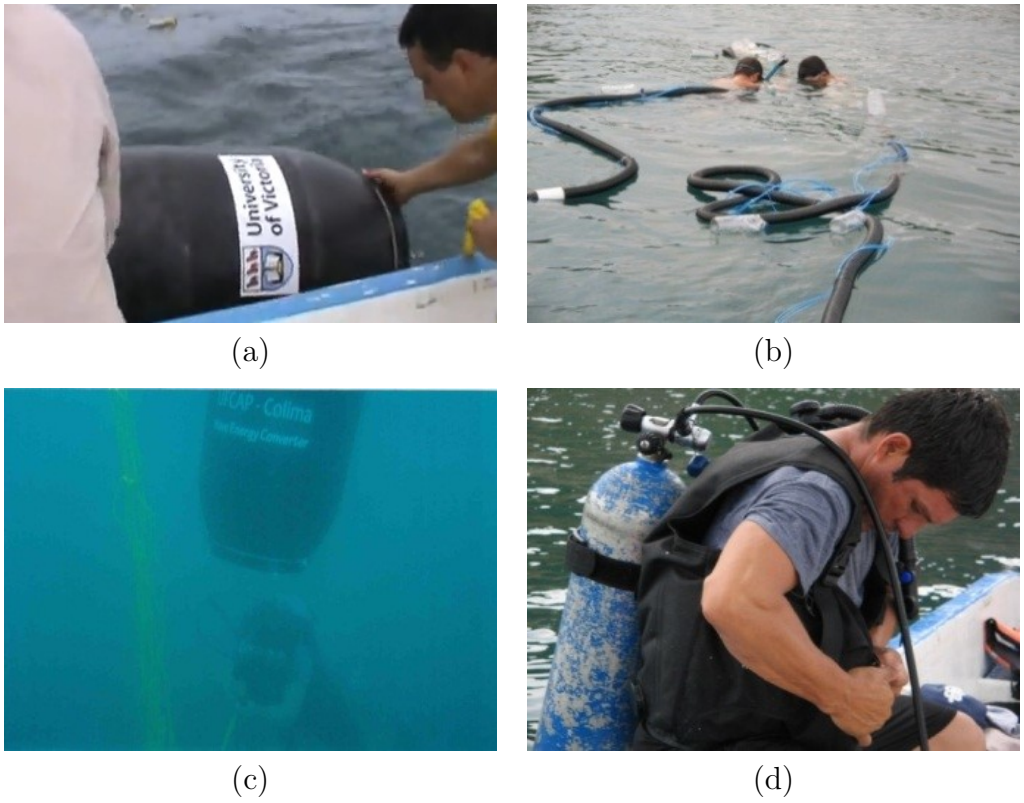

Figure 5.11: UFCAP ocean model deployment (a) air-chamber deployment; (b) sensor hoses connection; (c) under water mooring handling for air-chamber 1; (d) diver readiness.

Figure 5.12a, displays the control-board in operation, it keeps all the electronics inside, such as computer, sensors, or DAQ, dry and ventilated while floating at the ocean. The electronics was elevated 5cm, and covered with an outer housing. The outer housing has elongated slots 2.54 cm high. Salted water did pass through the slots inside the outer housing, but it was in contact only with the bases, and never with the electronics which were elevated. In Figure 5.12b, the model is shown in its

full length during the first deployment (with the air-chambers underwater connected to the supply and return manifolds).

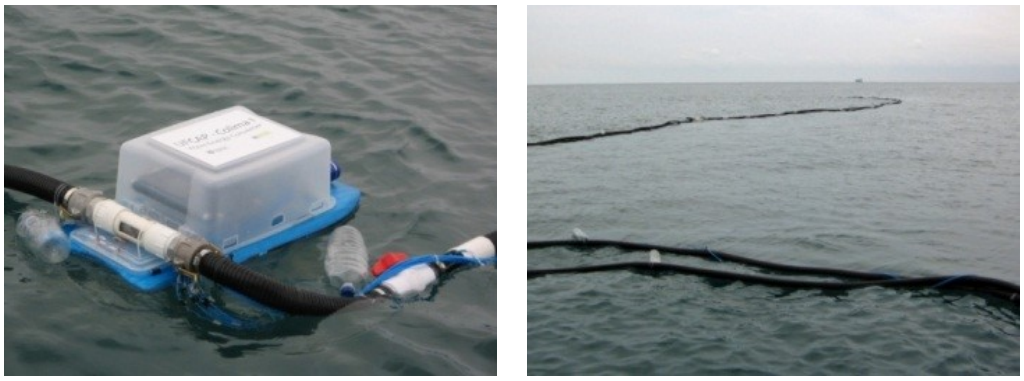

(a) (b)

Figure 5.12: UFCAP ocean model installed (a) floating control board (electronics, turbine, generator sensors, computer, LEDs); (b) installed UFCAP WEC.

After installation, and previous the operation, it was necessary to set-up to ensure WEC readiness. A summary of such operations is presented in Table 5.3. Several components were tested independently to observe proper work. Even though they are not core of the research, two examples will be mentioned to provide a wider overview of what happen during ocean tests. For example, check-valve's operation was reviewed under border line situations (small 40 lt air-chamber combined with small waves). Air-chamber was prepared with floaters around them (see Figure 3.8), to keep them floating, while at the same time was fixed to the ocean floor (no heave allowed). Generator was also tried-out stand-alone (with only one air-chamber) with a similar floating 200 lt air-chamber.

5.3 Results and Discussion

Valuable lessons learned and device behavior experience was gained during the tests that might serve for future models construction and redesigns.

Table 5.3: Set-up operations

Operation	Observe
Test 200lt air-chamber without hoses	Performance of check-valves opening and closing
Connect Supply hose	Hose friction effect
Connect Control Board	Turbine performance
Connect supply hose with Venturi	Turbine performance and Venturi sensors
Repeat all test with a 40lt air-chamber	Check-valves; hose friction effect; turbine performance; Venturi sensors; wave sensors

The turbine and generator couple is one of the most important device components. During operation it was observed they operated, could capture a wide range of wave sizes, or equivalently, wide range of airspeeds. When not connected to the LEDs (open circuit), it could produce a maximum peak of 7 $\mathcal{V}$ with the larger waves.

Figure 5.13 illustrates the recorded ocean waves, and the generated voltage, both being measured right at the ocean site through the DAQ. During the stand-alone test (single air-chamber), the turbine-generator was connected only to the supply conduit (vs. the supply-return loop), and only half of the wave (while rising) was used to harness energy and generate electricity. Therefore, the generated voltage is present only at the "rising" portion, and appears flat otherwise.

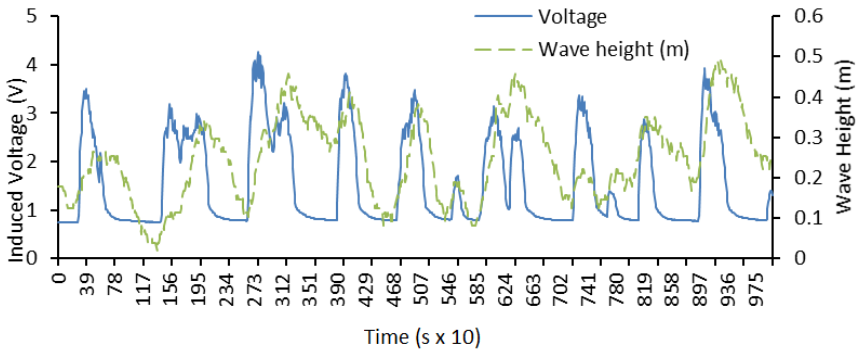

Figure 5.13: Generated voltage with a single air-chamber and ocean waves rising only.

When the generator was connected to the LEDs, electricity generation was achieved

and LEDs lighted. Though it was not a large WEC generating a significant amount of energy, it is remarkable the UFCAP was fully operating, and the first time any WEC have successfully lighted LEDs out of ocean wave energy in the country.

Figure 5.14: Eight LEDs lighted by the UFCAP WEC. Control-board over the boat.

The equivalent electrical resistance from the LEDs-turbine system is difficult to compute theoretically. It was measured in the lab after the tests and shown in Figure 5.15. This is useful to make future computations if needed.

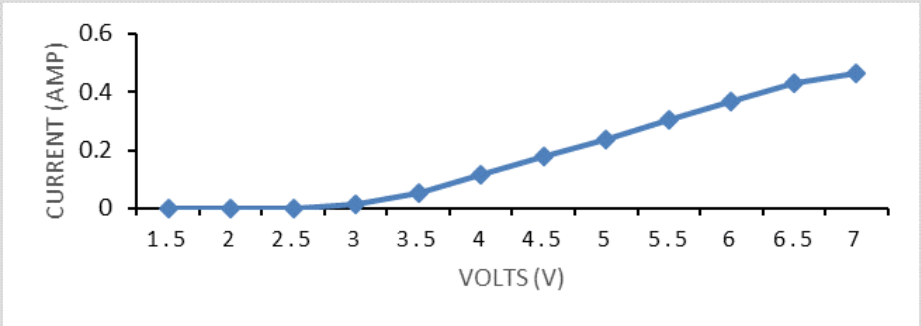

Figure 5.15: Generator-LED currents at different voltages.

Figure 5.16 shows two different cases of wave-height measurements recorded with a pressure sensor MPXV5050GP - case 1369-01, and the power generated with by the UFCAP with the rising portion of the wave (on UFCAP standard application, power

is generated not only during the rising but also when the water level decreases). It is observable that the larger the wave-height, the larger the generated power, and also the steeper (faster rate change) the larger the recorded power. Figure 5.16a illustrates a case with more homogeneous waves with wave-heights around average size. Figure 5.16b shows a group of waves with shorter average wave-height which deeply affects power generation reducing performance or even not generating power at all.

Figure 5.17a shows an case where reduced power is generated due to waves with larger period which reduce the rate of change of the water level (steepness). Conversely a large peak of power is observed due to a high-rate of change in the water level.

An additional case including a large wave is shown in Figure 5.17b. A large wave-height suggests a large amount of produced power, nonetheless, a small power is observed due to a reduced steepness. The "flat" portion of such large wave also does not produce large amount of power.

Distance to shore is a variable that must be studied in the future to determine UFCAP's test location and model size. Distance to shore changes the wave shape. Off-shore waves are wider, when approaching to the shore, wave spectra and wave shape change, wave-heights, frequency, and steepness become higher. Such waves create a different UFCAP pumping (air velocity), are more intense, but spaced (period). It was learned that *wave spectra and shape* must be considered when dimensioning the UFCAP. These resource differences need to be taken into account when designing the prototype. In the present work, the design was made before these learnings, it assumed off-shore wave shapes because initially was intended to be placed off-shore, but later was placed on-shore due to practical reasons.

Check-valves were able to open and close very rapidly and got activated even with the smallest available wave-heights of 0.11 m which were the smallest observed (see section 3.3.2).

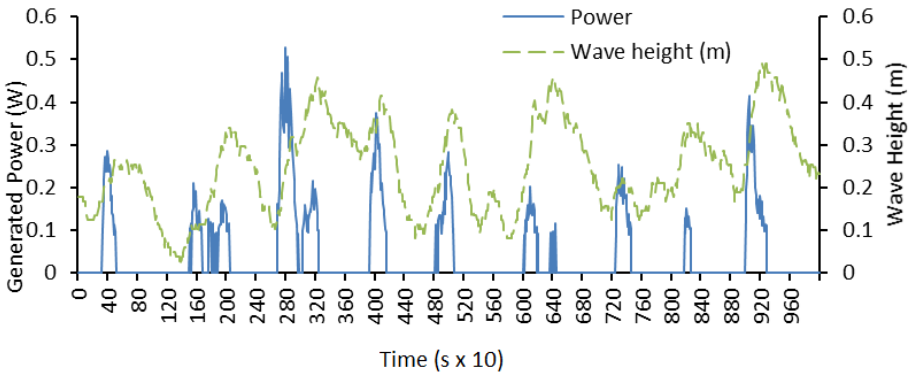

(a)

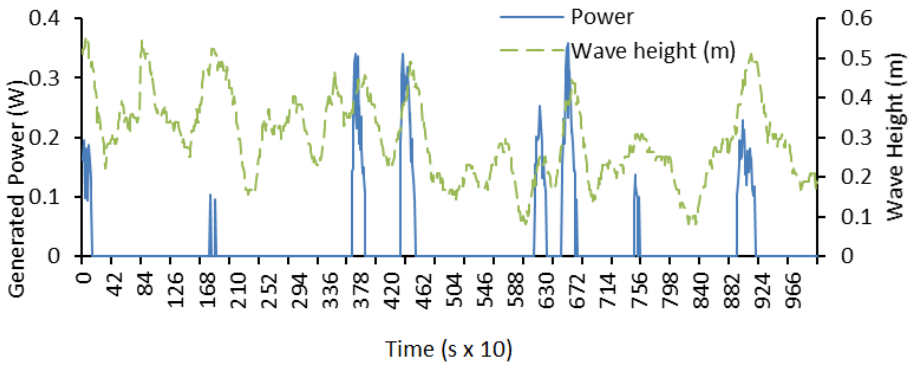

(b)

Figure 5.16: Generated power and wave-height with a single air chamber with waves at (a) record 1, (b) record 2.

The Venturi tube is an instrument used to measure the air-speed inside a turbine. It accelerates the air inside a conduit by reducing its cross section area. The air-speed is then calculated by measuring pressure in the two cross section areas. Supply and return conduit diameter is 50 mm. The used Venturi tube has diameter 23 mm in its reduced cross section. Recorded data demonstrated that the used Venturi tube imposes an extra pressure-drop which significantly reduced performance, or even prevented device operation. With the 200lt air-chamber size, the performance losses ranged between 15-35% while for the 40lt air-chamber it ranged between 70-100%. It was decided to remove the Venturi tube due to the large impact it has over the UFCAP performance.

Ocean experimentation is difficult to perform and repeat. Therefore, the following

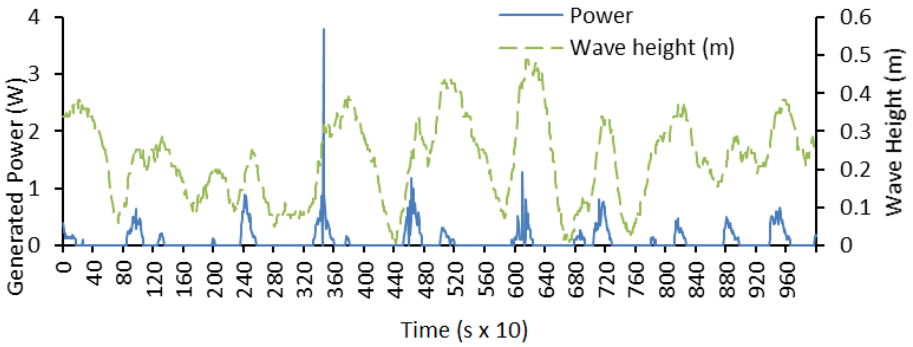

(a)

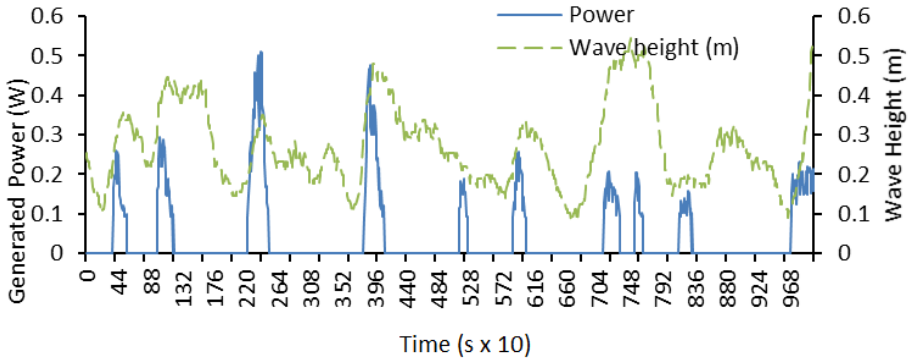

(b)

Figure 5.17: Generated power and wave-height with a single air chamber with waves at (a) record 3, (b) record 4.

lessons learned are included as material that will be valuable in future testing.

Lessons Learned

1. Tightness: a few leakages were observed in different unions. PVC-PVC elements, hose-PVC. Venturi Tube union is very weak due to constant deformation of hoses.

2. Blue glue used for PVC elements react with hot silicon eliminating adhesion.

3. Mooring with metal gaskets is a much better alternative.

4. Underwater conduits could eliminate water filled regions within the conduits avoiding a lot of problems; however, mooring of the whole conduits would be

necessary.

5. Opening and fitting to fill up air next to the control board is needed addition. At least for prototypes with floating conduits.

6. Air chambers may sink and could get lost.

7. Generator does not get damage with salted water, even when totally sunk.

8. LEDs switches get rust rapidly, and tend to fail because of it.

9. Everything rusts very fast and need to be oiled to prevent it.

10. Forecast need to be studied carefully. Extreme waves may appear (higher or smaller) than computed.

11. Water inside manifolds may sink the control-board.

12. Water inside manifold can sink air-chambers.

13. Shorter central conduit is desirable to minimize water intrusion opportunity within this region.

14. Aligning air chambers height is complicated. An alternative method need to be created. So far, the best alternative was to measure the floating portion of the conected conduits rather than the sunken portion.

15. Mooring the floating conduits is desired to avoid large stressed against air-chambers.

16. Fixation of pneumatic hoses (sensors) was broken. Need to be improved.

17. Few sensors did not behave appropriately, still by unknown causes. Further research need to be done.

5.4 Concluding Remarks

The objective of the present test has been proving feasibility of a WEC concept which can be used for cost-effective applications or projects where costs could be a large barrier. A scaled model has been tested with small ocean waves (irregular waves), electricity has been generated, and important lessons learned from model scaling, construction, components-performance, device-performance, and project management has been produced.

Experimental results suggests that wave shape and not only wave-height has a deep impact on UFCAP's performance. Waves with the same wave-height and period but with larger steepness can produce more energy. Waves with similar wave-height but with low steepness may even not generate electricity at all. Consequently, it can be inferred that wave steepness must be included in further research to determine more accurately the amount of energy that the system is able to generate. Data suggests that low steepness' waves even with large wave-heights will not produce the desired results. Since on-shore waves have normally higher steepness, it is suggested that on-shore locations may be an option for the UFCAP device.

Experimental runs also allowed to observe behavior at both, component level and system level. Check-valves' crack-pressure, and pressure-drop across them are small enough to be triggered even with the smallest waves. Experiments made possible to understand components and redesign them with improvements e.g. mooring, conduits, or floating valve which have been already modified. More importantly, the present ocean tests have absolutely proved *the device can generate electricity with ocean waves* from a system level perspective which was very difficult to achieve numerically, and then, the R&D program may continue towards further research.

Additionally, it has been demonstrated the prototype can be constructed relatively easily, non-expensively, and then it is a good alternative for such applications where

manufacturing and costs restrictions are important. Modularity within the concept, manifested being an advantage which facilitates manufacturing and handling. Deployments provided relevant experience and information on how the device must be built, handled and implemented which will be key for the success of future deployment-tests. Several new *modes of failures* which are difficult to predict in advance were observed during the tests. As a case study, water intrusion due to leakage was the most important mode of failure at a system level, the water flooded the conduits preventing operation in the whole device. Failure modes identification is important to re-design the device to prevent such situations making the new version more reliable. The generated experience also provide guidelines to improve performance.

Chapter 6

Wave Flume Tests

6.1 Model Design

In ocean tests it is difficult to have control over the variables, and it is necessary to test the model under the true operational and environmental conditions present during the trial period. Conversely, wave-flume tests allow examining a device in a controlled environment where it is possible to measure, or vary conditions easily [62].

Experimentation allows to prove numerical models, performance of a device or a structure. When they are large in size, such as harbor structure, ship, or WEC, testing a scaled model is a necessary step in the development process, because it is tremendously less expensive than the full size, and it is easy to manipulate and study.

Scaling is then an important and necessary step in model testing. Improper scaling may result in accidents or major losses. Thought perfect scalability of all physics of a phenomenon is possible in theory, in practice sometimes it is not. Scalability of length for example, is straightforward, but that is not the case for gravity, which requires a centrifugal equipment and then only small experiments can be performed in such equipments, or for viscosity which requires a different fluid. In a wave-flume, where

thousands of litters are needed, it is not practical to replace water by another fluid.

The perfect similarity between a model and full size device is known as *mechanical similarity*. It requires three conditions, i) *geometric similarity*, which is similarity in shape, meaning all dimensions are scaled by a scale factor sf, ii) *kinematic similarity*, which is similarity in shape and in motion, and iii) *dynamic similarity* which requires similarity in shape, motion, and force ratios.

When it is not possible to meet *mechanical similarity* between model and full size device, it is necessary to identify the predominant forces, and keep similarities of those only. The most relevant forces in fluid dynamics are gravitational, inertial, viscous, elastic, compression, and pressure forces. In the case of WECs, ships, and in general any open channel test, the most relevant forces are gravitational and inertial. When scaling is met keeping similarity between inertial and gravitational forces, it is known as *Froude scaling* since Froude number is kept constant between model and full size device [62, 67]. This scaling is normally used to scale experiments involving not only OWC but most of WECs wave flume experiments [60, 121, 71].

The Froude number is the ratio between the inertial force eq. (6.1) and gravitational force eq. (6.2) given by eq. (6.3)

$$F_i \propto \rho V^2 L^2 \tag{6.1}$$

$$F_g \propto \rho g L^3 \tag{6.2}$$

$$F_r = \frac{F_i}{F_g} = \frac{\rho V^2 L^2}{\rho g L^3} = \frac{V}{\sqrt{gL}} \tag{6.3}$$

where F_i is the inertial force, F_g is the gravitational force, ρ the fluid density, g the gravity, V the velocity, and L the length.

Keeping the Froude number constant between the model and the full size implies

$$\frac{V_M}{\sqrt{gL_M}} = \frac{V_F}{\sqrt{gL_F}} \Rightarrow V_F = V_M\sqrt{\frac{L_F}{L_M}} = V_M\sqrt{sf} \tag{6.4}$$

being the subscript $_M$ for the model, $_F$ for the full size device, and sf the scale factor equal to

$$sf = L_F/L_M \tag{6.5}$$

Froude multiplication factors are listed in Table 6.1.

Table 6.1: Froude scaling table

Parameter	Unit	Multiplication factor
Length	(m)	sf
Mass	(kg)	sf^3
Force	(N)	sf^3
Moment	(Nm)	sf^4
Acceleration	(m/s^2)	1
Time	(s)	$sf^{0.5}$
Velocity	(m/s)	$sf^{0.5}$
Pressure	(Pa)	sf
Volume Flow	(m^3/s)	$sf^{5/2}$
Power	(W)	$sf^{7/2}$

Nonetheless, scaling an OWC device is more complex than scaling other WECs since the predominant forces are different below and above the water surface. In the wetted part of the device, hydrodynamics rules the motion, the predominant forces are inertial, and gravitational [67, 122], while above the surface level, aerodynamics rule the air region, being the inertial and viscous forces the predominant.

Therefore, if the interest is the turbine, or any airflow phenomena in general, additional scaling assumptions are necessary to interpret the results correctly [62]. One example of the needed adaptions is the volume of the air chamber. According to Froude criterion, the volume of the air chamber m^3 must to be scaled by sf^3, however

several studies from different researches and methods suggest scaling the air-chamber volume by a factor of sf^2 due to compressibility effects [67].

The full size device was customized for the prevalent weather in Rosarito, Baja California which is the end location where the device will be used. Mexico is not characterized for a having a large wave result generally, but there are a few locations with relatively good wave resource such as Rosarito. The wave data was provided by CFE from a private buoy with records from more than 15 years [123]. To size the device, it was used the methodology from [19] described in Chapter 2, as well as manufacturing and installation criteria to avoid large devices difficult to transport and / or install. Then, it was scaled down utilizing Froude criterion in order to meet the wave-flume capabilities and sizes. Table 6.2 condense this information.

Table 6.2: Full size and model size parameters with $sf = 0.555$ 1:18

Parameter	Full size	Model size
Wave-height max* (m)	2.7	0.15
Wave-height min* (m)	1.2	0.06
Period max (s)	12	2.8
Period min (s)	8	1.8
Air chamber** $\varnothing(m)$	7/ 4.85	0.39/ 0.27
Depth (m)	9	0.5
Power** (W)	30,000/ 6,200	1.2/ 0.25

* Wave-height min-max design values, these
are the most common max, min heights along the year.
** Two different sizes

Froude criterion is widely accepted and normally used to scale down devices, an example can be found in [76]. In the present study it was also used, however, after some details detected, the matter was additionally studied with interesting findings described in the results section 6.3. An example of a parameter which is not well scaled with Froude criterion is the amplitude of oscillation described Boccotti et. al [124]. There are other phenomena which results fit outside the limits of expected

performance such as 14 times larger efficiency described in [125] which make necessary to look for other causes to explain them.

To study the similarity issue, a **new criterion is proposed** in addition to Froude similarity in order to select the best scaling factor.

During the design stage, it is possible to determine both, the size of the device, and the scale factor. Normally the full size device would be determined by the predominant wave weather, but still with that, small variations in size are possible since the ocean provides waves from all sizes within the local range. In the case of the UFCAP WEC it is possible also to vary the air-chamber diameter for a given fixed nominal capacity while compensating with the number of air-chambers, then the allowed variation of air-chamber size (diameter) is even more flexible than with other WECs. In other words, an extra degree of freedom is present, and then, it is theoretically possible to use different air-chamber diameters (within a range) for a given scale factor.

If the ratio between the wavelength and the air-chamber diameter is defined by

$$r = \frac{\lambda_F}{\varnothing_F} \tag{6.6}$$

and use linear wave theory to define wavelength implicitly by eq. (6.7)

$$T = \left[\frac{g}{2\pi\lambda}\tanh\left(\frac{2\pi z}{\lambda}\right)\right]^{-1/2} \tag{6.7}$$

where λ is the wavelength, and z is the depth.

WECs must be sized for the predominant wave weather at the location of interest. Regarding wavelength, assume the range of interest is comprised within a range defined by $[\lambda_{min}, \lambda_{max}]$ then two new coefficients can be defined for the same WEC

$$r_{max,min} = \begin{cases} \frac{\lambda_{max}}{\varnothing} \\ \\ \frac{\lambda_{min}}{\varnothing} \end{cases} \tag{6.8}$$

which can be computed for both full size and model size. The desired condition is to approximate the two coefficients as much as possible to ensure similarity between model and full size.

$$\begin{cases} \frac{\lambda_{F_{max}}}{\varnothing_F} \approx \frac{\lambda_{M_{max}}}{\varnothing_M} \\ \frac{\lambda_{F_{min}}}{\varnothing_F} \approx \frac{\lambda_{M_{min}}}{\varnothing_M} \end{cases} \tag{6.9}$$

Such conditions can be written as a parameter in equation form by defining ξ as

$$\xi = \left(\frac{\lambda_{F_{max}}}{\varnothing_F} - \frac{\lambda_{M_{max}}}{\varnothing_M} \right) + \left(\frac{\lambda_{F_{min}}}{\varnothing_F} - \frac{\lambda_{M_{min}}}{\varnothing_M} \right) \tag{6.10}$$

with an objective defined as the minimum of the absolute value of ξ

$$min\,|\xi| \tag{6.11}$$

The ξ parameter provides an additional insight to define the air-chamber diameter and scale factor to improve the equivalence of results between model and full size. The scale factor sf which better represents similarity between model and full-size is that sf which minimizes the absolute value of ξ.

The scaled model needs to be designed not only for implementation, but also for manufacturing. The proposed model design is configurable (single air chamber, or multiple air chambers, floating, fixed, with/without turbine, etc.), non-expensive, easy to built. All conduits, fittings and connections, coupling, are commercial parts. 1" diameter for the small sections and 2" diameter for the large conduits. Air-chambers, check-valves, turbine, turbine mounting, shaft, are customized-designed

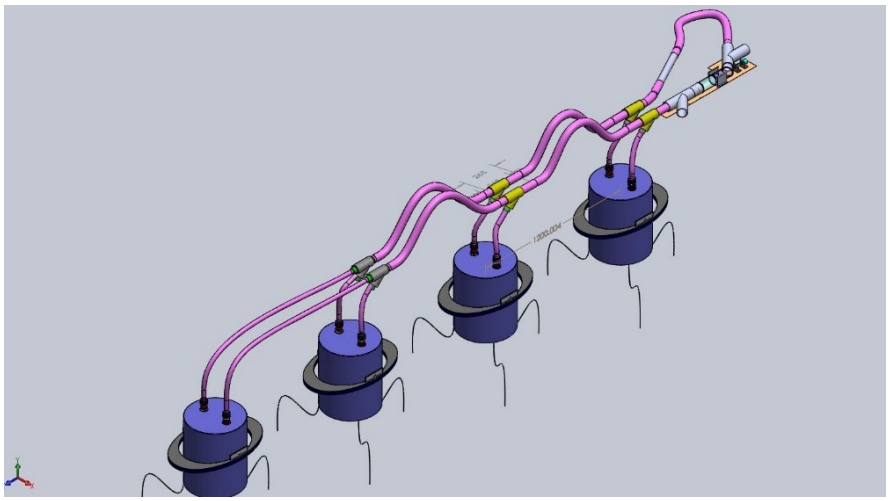

Figure 6.1: Four air-chamber UFCAP model scaled for wave-flume size.

components but still designed for easy manufacturing. Figure 6.1 illustrate the wave-flume model of up to four air-chambers in purple. Air-chambers are numerated from right to left being chamber 1 the one in the very right. Chamber 4, at the very left, has two conduits at its top, one to supply air to the manifold and ultimately to the turbine, and one to return air to the air-chamber. Between the conduits and the air-chamber, it is possible to observe the check-valves in black which control the flow direction, converting the oscillating flow from OWC into a unidirectional flow which is split into the two conduits. The next chamber to the right is chamber 3, which is equal to air-chamber 4. At the top of air-chamber 3 there are "Y" fittings which aim to collect the flow from both air chamber 4 and 3. Following, there are air-chamber 2, and 1 which look the same as the previous chambers. The conduits between them are curled to allow for relative motion between the chambers. Right to chamber 1 is the central conduit, where the flow from 1 or several air chambers arrive to the turbine. Two openings, one before and one after the turbine coupled with check valves, allow to drop excess energy when present reducing the compressibility inside the system, and avoiding phase resonance or cancellation.

The air-chambers were built in transparent polycarbonate for ease visualization,

with an aluminum ring to provide robust support for the intended mooring. Air-chamber model is visible in Figure 6.2. Floaters are made of polyurethane, and black polycarbonate. Top cover is made of black polycarbonate. In Figure 6.2 (b) a close-up of the installed check valves over the air-chamber is visible. All materials have good mechanical properties while in contact with water in the long term.

The central conduit model is visible in Figure 6.3 (a). A red point mark the region where the turbine is located. Shown turbine is rapid prototyped. Through the central conduit the unidirectional flow comming from either 1 or several chambers feeds the turbine. In Figure 6.3 (b) the turbine inside the central conduit is visible (conduit opened not in operation).

Figure 6.4 show a proposal of the design to support the shaft, bearing and generator for future tests. Figure 6.5 depicts the check-valve used in the model. Check valves housings are machined in black acetal polymer; angled gates, are rapid prototyped and axis and fasteners are galvanized. Conduits are flexible commercial 1" and 2" reinforced plastic hoses.

(a) Front view (b) check-valve close-up

Figure 6.2: Single air-chamber with check valves installed (a) front-view ; (b) check-valve view close-up.

Two mooring concepts were studied, the first one, with tethers S shaped connected to a metal load, and the second one with fixation bars from the top which fully fix the

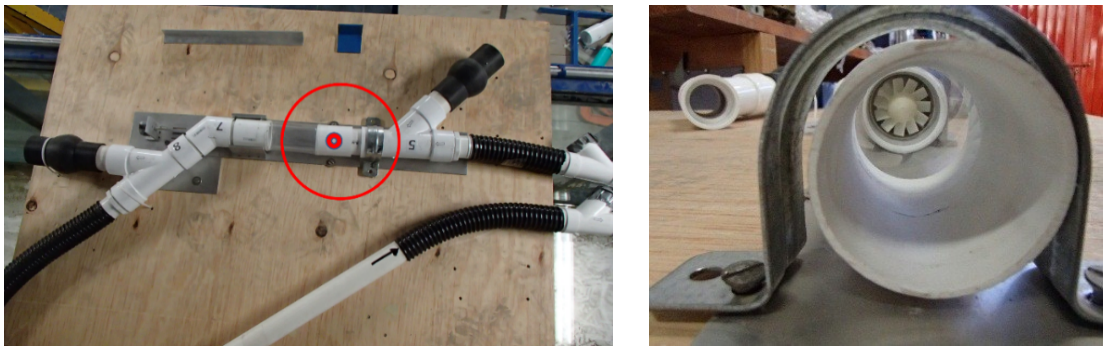

(a) Central conduit (b) Turbine inside central conduit

Figure 6.3: Central conduit assembly (a) central-conduit ; (b) turbine inside central conduit.

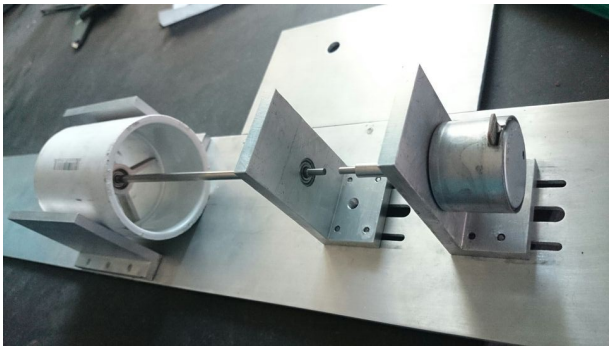

Figure 6.4: Torque transmission mechanism.

air-chamber and then a single DOF will be evaluated as studied by Bhinder [119]. The size of the loads from the first mooring concept created problems since they needed to be voluminous with respect to the wave flume size, affecting the test performance, and then, it was decided to use the second approach.

6.2 Experimental Set-up

Tests were conducted at the UNAM Institute of Engineering in a 37-m long wave-flume. It uses a HR Wallingford wave generator which can create either regular or irregular waves. Flap Paddle has 0.85 m stroke and max velocity of 0.81 m/s. Other wave-flume parameters are included in Table 6.2. A sand beach was added to

(a) Assembled check-valve (b) Check-valve in parts

Figure 6.5: Check valve model for wave-flume test (a) assembled ; (b) in parts.

Table 6.3: Two UFCAP model sizes

Characteristic	Large model	Small model
air-chamber diameter m	0.39	0.27
air-chamber height m	0.50	0.50
Conduit diameter (air-chamber)	1”	1”

minimize reflection. The wave-flume was provided with eight height sensors, 1 at the beginning of wave-flume, 3 before the model, 3 after the model and 1 near the beach. A hot-wire anemometer connected to a data logger was used to record the airflow speed at the central conduit in m/s at a rate of 5 Hz.

The test configurations are summarized in Table 6.5. Tests were conducted with both, regular waves and irregular waves. A *Jonswap spectrum* was used to generate the irregular waves. Two submersion configurations were tested, 30% and 50% submersion which means the same water depth, but different air chamber elevation with respect the mean water level.

Four variation of models were included, a 0.39 m in diameter un-modified, a 0.39 m with flaps, a 0.39 m with reinforced cap, and a reduced 0.27 m model. The model

Figure 6.6: Single air-chamber test in wave flume.

Table 6.4: Wave-flume specs

Characteristic	Min	Max
Period s	0.5	3
Wave height x depth	0.1	0.5
Depth m	0.15	0.5
Wave height m	0.05	0.25
Wave length m	0.39	6.28
Flume wide m	N/A	0.8
Flume height m	N/A	1.2

with lateral flaps was created to observe the effect of wave reflection over the test. The reinforced cap was created to observe the effect of the cap deformation occurred during air compression with a stronger cap, and the reduced/smaller 0.27 m model to reduce compression during the pumping. Both models have 1:18 scale. Model sizes can be found in Table 6.3.

Additionally, a test including 2 air-chambers simultaneously was conducted to be able to compare the performance while running with 1 or 2 air chambers.

Each *configuration* included 40 estates, a combination of 5 different wave-height and 8 periods; each test-run comprises 20k-30k data entries taken at a rate of 20 Hz.

Table 6.5: Test configurations

Model	Characteristic 1	Characteristic 2
0.39 m model	Regular waves	30% submerged
0.39 m model	Regular waves	50% submerged
0.39 m model	Irregular waves	30% submerged
0.39 m model	Irregular waves	50% submerged
2 0.39 m chambers	Irregular waves	50% submerged
2 0.39 m chambers reinforced cap	Irregular waves	50% submerged
0.39 m with flaps	Regular waves	50% submerged
0.39 m with flaps	Irregular waves	50% submerged
0.27 m model	Regular waves	50% submerged
0.27 m model	Irregular waves	50% submerged

A summary of the studied waves is found in Table 6.6.

No turbine was included during the tests, the air speed was measured without turbine. When testing scaled OWC models, usually the turbine is either replaced for a damping equivalent load such as hole or porous wall [56, 71], or completely eliminated [6] when testing with an scaled model scaled with Froude criterion, the power is scaled by a factor of $sf^{7/2}$ and then, generated power is very small to have reliable records not affected by friction.

Being preliminary tests over a novel device, it was decided to measure the airflow speed without any load, turbine-generator, porous wall or hole, to prevent adding variation or being affected by friction from the torque transmission mechanism (shaft, bearing, coupling) with no reference to compare with. The current objective is to observe if operation is possible, learn about it, and identify needed re-designs which will expedite development of a larger device in the long term, there is no need to include the turbine.

Table 6.6: Wave-flume test plan for periods and wave-height

Characteristic	Values
Wave height (m)	0.05 ; 0.075 ; 0.10 ; 0.125 ; 0.150
Wave period (s)	1.6 ; 1.8 ; 2.0 ; 2.2 ; 2.4 ; 2.6 ; 2.8 ; 3.0

6.3 Results and Discussion

After analyzing similarity between different model sizes and scales when Froude criterion is utilized, it was found theoretically that such a criterion can met similarity simultaneously for size, time and wavelength only for 1 scale factor, and may not scale arbitrarily to any scale factor. This is not relevant for point absorbers, but might be of particular importance to WECs which are susceptible to wavelenght scale, such as attenuators. Wavelength scale errors might grow as large as 18% in some cases affecting results interpretation.

A variation in ratio r values with respect to different air-chamber diameters $\varnothing$, and different sf is observed in Figure 6.7. This result implies that Froude criterion can not ensure geometrical similarity with wavelength λ because it depends on the period T which has a scale factor of $sf^{0.5}$, and the depth z which is scaled with sf, while the $\varnothing$ is scaled only with sf.

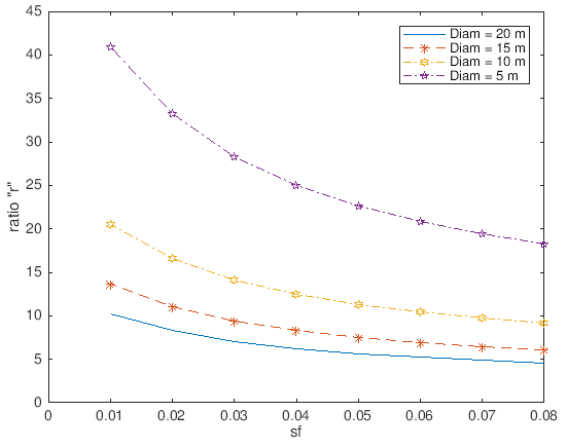

Figure 6.7: Wavelength-diameter ratio vs. sf for different air-chamber diameters.

Figure 6.8 shows the ξ parameter vs. sf for different air-chamber diameters. Recalling the objective is to minimize the absolute value of ξ in order to achieve a more complete similarity which includes also the wavelength similarity between model and full size device. The ξ parameter is given in that form equation (6.10) because

sometimes during the design process, it is not possible to adjust to use the optimum scale factor, and then, trying to reduce the value of the ξ parameter, reduces the similarity error.

A variation in the ξ parameter exists for different sf and diameter sizes which also implies that the wavelength-model similarity is not achieved for all sf but only for one sf, and then, some error is being carried out from model tests toward full size performance. In the case study, which is the model tested during these experiments, the sf which minimizes the absolute value of the ξ parameter is 0.285. Only this sf ensures similarity with wavelength as well as the other similarities (geometrical and dynamical) kept with Froude criterion.

Additionally, it is interesting to note that all air chambers diameters have the same minimum at 0.285, but not the same sensitivity to variations to the scale factor. It is important to note, that the minimum from ξ absolute value depends on the depth used in the study. The result would be different for other depths.

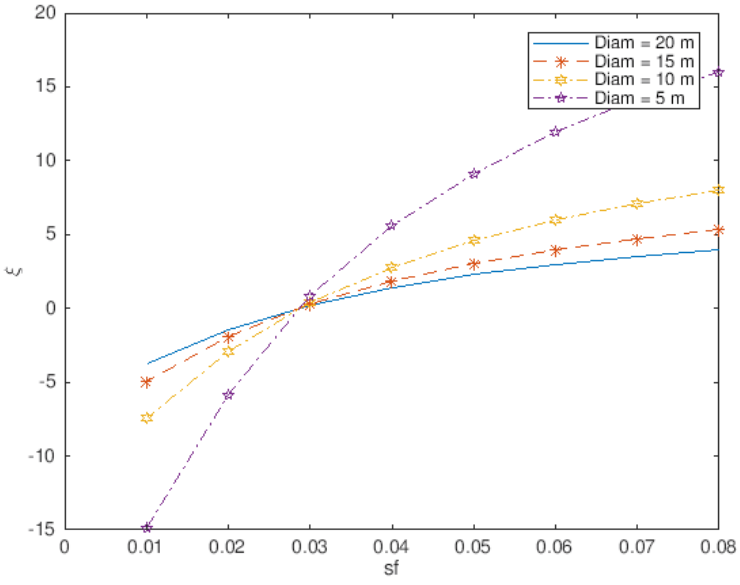

Figure 6.8: ξ parameter vs. sf for different air-chamber diameters.

Regarding the experimental runs in the wave-flume, the test consistency was eval-

uated by running several tests on different days and set-ups. The same test with irregular waves obtained similar records in different set-ups and days confirming the consistency.

A first set of test-runs studied the air-chamber submersion at 30% and 50% of its height. Differences were expected since the wave dynamics decreases exponentially with the depth, the compressibility is changed by changing the volume of air, and the wave transmission, and reflection is also affected. The results are shown in Figures 6.9 and 6.10.

Figure 6.9 (a) and (c) correspond to air-chamber 30% submerged, and Figure 6.9 (b) and (d) to 50% submersion. The performance is reported with air speed average velocity, and maximum velocity respectively. Figures (a) and (b) compare average velocities for the two submersion depths and 40 sea estates. Comparing each wave-height from Figure 6.9 (a) and Figure 6.9 (b), 30% and 50% submersion respectively, 30% submersion performs better in H=0.05m and H=0.075m. In the rest of the wave-heights they perform very similar. However, when comparing the max velocities (c) and (d) a peak higher value can be observed in the 50% depth.

In Figure 6.9 (c), it is clear that a negative trend at T = 2 s occurs with the highest three sea wave estates. This effect can be explained due to wave reflection and further phase partially canceled. Analyzing the reflection coefficients, it was found that they indeed increase with regular waves around this period.

Moving from 30% to 50% submersion reduced the airflow velocity for small periods, but improved it at larger periods in both, regular and irregular waves. In the case of wave-height 0.05 m, the effect was negative, reducing performance. Figure 6.10 shows the same information than Figure 6.9, but with irregular waves. The cancellation just mentioned due to reflection is disappeared with irregular waves, since no addition or subtraction is met periodically.

A further test run was performed to observe the produced airflow with 2 air chambers plotted in Figure 6.11. Airflow velocity with 1 air chamber (from the previous figure) was included for comparative purposes (H = 0.15 m) to observe differences between 1 and 2 air chambers. To observe difference between 1 and 2 air chambers for other values of H, Figure 6.11 may be compared with Figure 6.10 (d). It can be observed that an improvement on the performance from one air-chamber to two air-chambers. Though expected, it is a valuable finding since it demonstrates that in some cases may exists a detrimental performance due to interaction of the air-chambers. For example, in the ocean tests described in Chapter 5, it was necessary to incorporate check valves in the conduits to prevent some mal-functioning due to interaction between chambers. Conversely, the observed performance is considerably higher in all cases, and the difference increases for higher values of period. It has already been discussed why higher periods performed better.

An additional two air-chamber test was performed with a reinforced cover (the top cover from the air-chamber). Reinforced cover was intended to prevent the observed deformation on the top cover and attempt to assess the effect that this deformation has on the performance. Results pointed that cover deformation has not significant effects, thought sometimes is slightly improving the performance. The explanation is similar than above; it is acting as a spring that helps a larger mass of air to be directed through the conduits.

Studies by Gomes et al. prove that wave-flume walls may amplify the power capture up to 15% for regular waves and 10% for irregular waves [66]. In order to be able to observe the effects of reflection imposed by the wave-flume walls and beach, a modification to the model was made adding lateral flaps.

An additional series of test runs were conducted to observe the effect of the reflected waves due to potentially large air-chamber size. Figure 6.12 shows the mea-

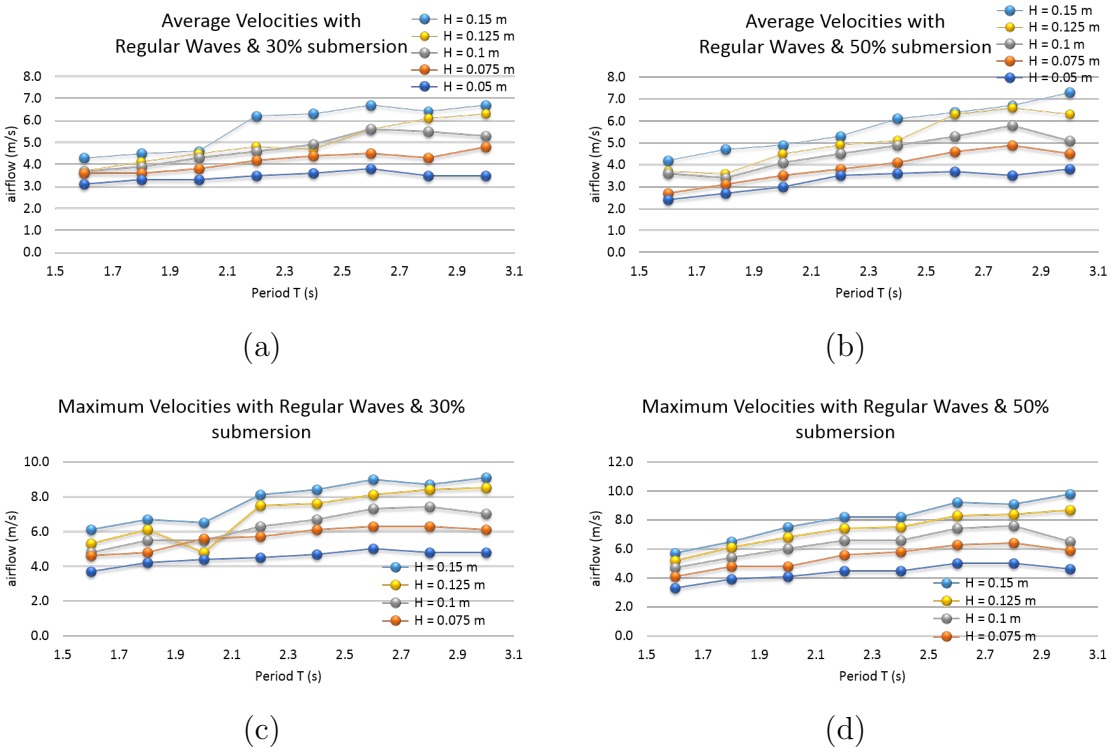

Figure 6.9: Wave flume test with regular waves. Comparative of average and maximum velocities of two submersion estates and different regular sea estates.

sured air-flow, with a standard 0.39 m diameter air-chamber, a second similar air chamber with lateral flaps (which help to eliminate the effect of reflected waves over the air chamber), and a third air-chamber with reduced diameter 0.27 m. At this point, the hypothesis of increasing the conduit size has been formulated (or equivalently reduce the air-chamber diameter). Testing with a reduced air-chamber was the initial step to observe the validity of the hypothesis. Comparing the air-flow at base size 0.39m and reduced size 0.27 m seems the performance decreased. Nevertheless, a correct comparison would require to normalize the airflow velocities. Being a reduced air-chamber diameter, it is natural to expect a reduction on the airflow. The performance on the reduced air-chamber was normalized by multiplying by base size section area, and dividing by the reduced air-chamber section area. With such a normalization, it is possible to compare the two performances, and it was found

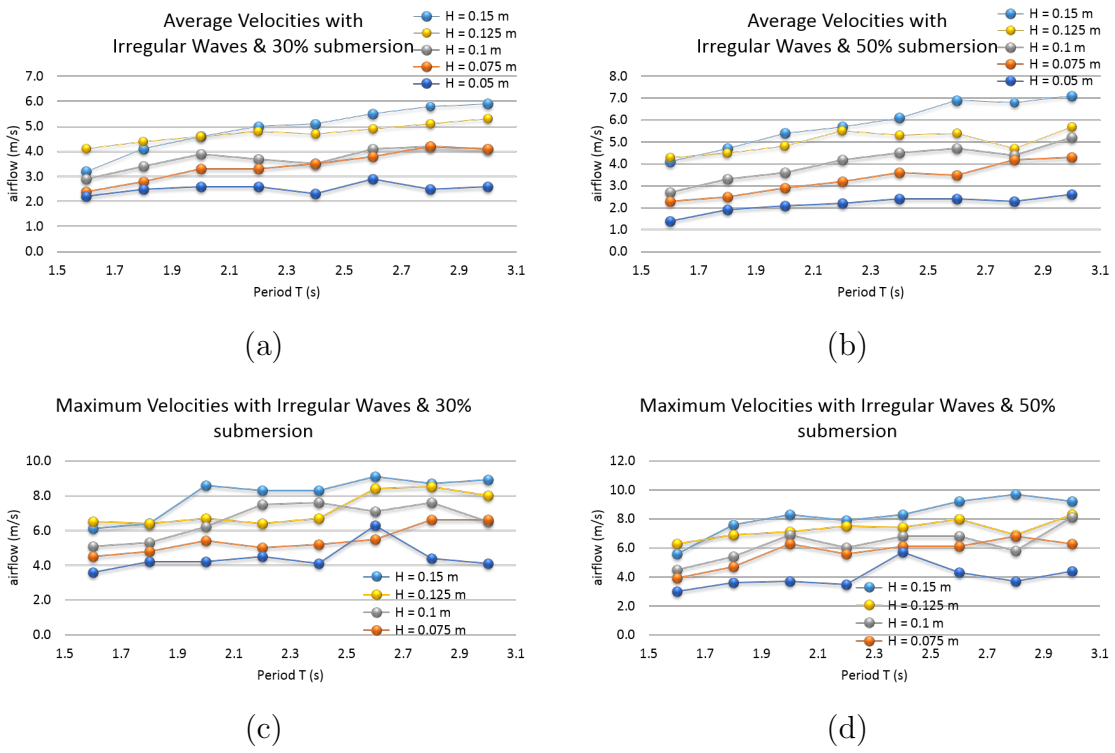

Figure 6.10: Wave flume test with irregular waves. Comparative of average and maximum velocities of two submersion states and different irregular sea estates.

that the reduced (normalized) air-chamber offers better performance in the majority of the evaluated sea estates.

6.4 Concluding Remarks

An additional scaling criterion has been proposed. It complements Froude criterion and improve similarity accuracy between model and full size devices/structures. The scaling error identified might be relevant or not in the interpretation of results depending if the device or structure is affected by wavelength span. For example, point absorbers might not be impacted much. Nevertheless, the proposed criterion provides a more robust scaling method which ensures similarity in all spans reflecting the physics of the full size device more reliable while supports sizing of the device

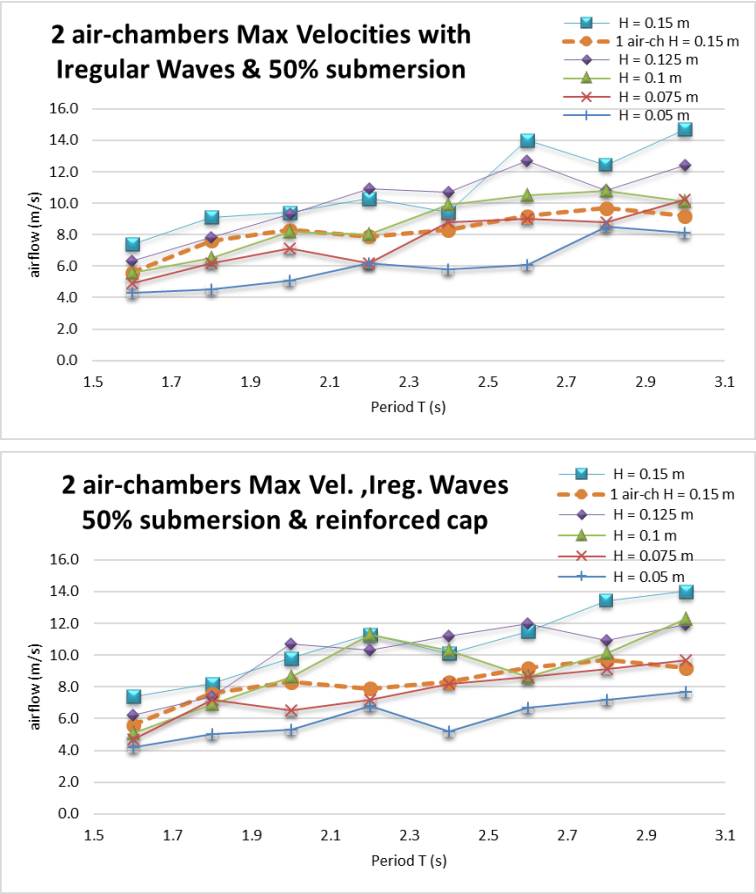

Figure 6.11: Performance with 2 air-chambers with irregular waves and 50% submersion. *(top)* normal cap; *(bottom)* reinforced cap.

during the design stage.

Wave-flume tests were conducted with a plurality of parameters to observe its effect on the performance under a wide variety of sea conditions. The tests performed provide valuable insights on the design of the UFCAP WEC.

Figures 6.9 and 6.10 support in the evaluation the submersion effect, it is interesting that an incremental trend line is observed in most of the Figure 6.9 curves, as the period increases, the airflow velocity increments also. This is congruent with the energy flux carried by the waves defined simplistic for shallow waters by eq.

$$\dot{F} = \frac{1}{64\pi}\rho g^2 H^2 T \tag{6.12}$$

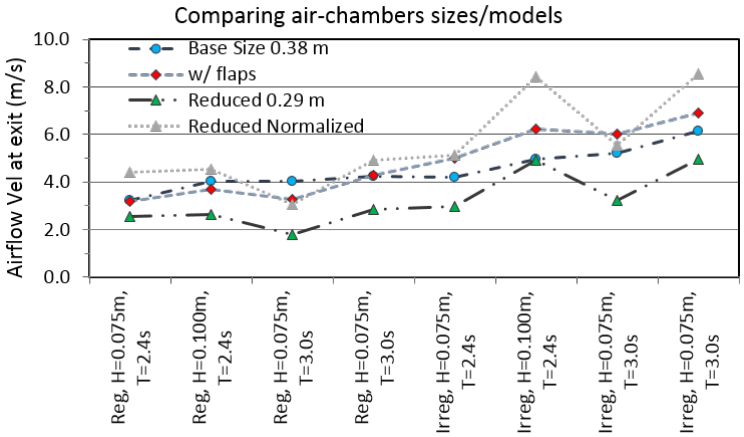

Figure 6.12: Three air-chamber models compared.

where period T is proportional to energy flux F.

The cap deformation, and the reduced surface level at the interior of the air-chamber are indicators that some compression is happening. This is happening basically due to the small conduit diameter relative to the air-chamber size. Therefore, the performed tests, suggest to increment the chambers conduit diameter to improve performance. For a given air-chamber size, constant wave condition, there is a minimum critical conduit diameter. Below this value, the time is not enough for the whole mass of air to flow through the conduit. Therefore, when the pumping is incremented (Period Reduced), a detrimental on the performance is observed since the wave amplitude inside the air-chamber is reduced and some wave cancellation due to phase superposition might occur.

In other words, after some larger values of periods, the airspeed no longer increases. In conclusion, the submersion parameter need to be considered along with the local weather when designing a UFCAP WEC. It is noted that from the high value of reflection coefficients, the model was deemed to be too large for the wave flume. This created additional wave reflections that possibly distorted the results. The check-valve leakage was observed to be also large, and then check-valve sealing needs to be

improved in order to improve the overall performance of the device.

The current capture efficiency of the device is on order of 1-3% depending on the wave state. It is still low compared to other OWC devices, but it can be incremented with the suggested redesigns (conduit size increment, streamlined shapes, reduce check valve leakage mainly). Conversely, its manufacturing, implementation, and overall cost, can be seen as the main advantage of the device.

Chapter 7

Conclusions and Future Work

A Wave Energy Converter (WEC) has been designed, built and tested in a controlled environment wave channel and also in a near-shore ocean setting. The present work focused in identifying design parameters and closing the technological gaps to implement a real WEC to produce clean energy. Such a WEC requires to be produced, installed, with current local technology and products; be simple to operate and very important, not costly. First, the problems from implemented WECs were identified in the literature, and a specific WEC was selected which could solve both, the general problems in the literature, and the specific problems such as local available technology and low-cost. While most of their components were standard, the development of its non-commercial components such as the check-valves, turbine, and the overall WEC was necessary and performed in the present work. Analytical, numerical models as well as wave-flume and ocean-tests, have been presented.

A scaling criterion which complements Froude's to scale WEC models has been proposed and included in section 6.1. It is a more robust scaling method, and discloses similarity errors that had not been pointed-out or detected before. The information may explain results variations in previous works due to scaling that would not had

been visualized otherwise.

There is still large variation in the cost of wave energy between different WECs and locations [23, 126]. The UFCAP WEC ocean prototype cost $3,000 USD, which is only a fraction of the more complex WEC prototypes. Based on the cost projections in Table A.1, the UFCAP WEC has the potential to bring cost of energy to a fraction of other WECs and below the cost of wind-energy. The device can also be easily installed as demonstrated during the ocean tests. Being an Oscillating Water Column (OWC) and based on a different operating principle compared to other reported devices, it utilizes a common fixed pitch turbine, which is less complex and expensive to a comparable Wells Turbine, that is the current standard. The proposed WEC may include different air-chambers or point absorbers, while still utilizing a single central Turbine for several of these air-chambers. The cost has been brought down by an integral approach, which include the cost not only of the product but also from the installation and O&M.

The solution has been found through an integral overview of the problem which include practical issues such as design for manufacturing and installation as well as a deep analysis on the state-of-the-art technology and its problems, and tools such as CAD modeling, CFD analysis, experimental testing were used during the development stage of the components. The WEC has been evaluated numerically, a prototype built and tested in a Wave-Flume, and a larger prototype built and tested at the ocean. Other WEC may be more efficient, but no current technology in WECs is less expensive and easy to construct and install, than the developed in this work. The presented ocean deployments are a proof of it.

The new check-valves were designed specifically for the WEC. They required to fulfill a difficult flow regime including very large flowrate at very low pressures. Any pressure loss may decrease the flowrate greatly and with this, reduce seriously the

WEC overall performance. It was mandatory then to use a check valve with the least amount of pressure-drop possibly in both, operation and opening. The necessary pressure to open a check-valve is known as the crack-pressure of the valve. Available check-valves for large flowrates are usually designed for either liquids, or medium to high pressure gases. A significant reduction of crack-pressure of 150 times was achieved with respect to commercial valves. Such a great reduction was achieved by the implementation of counter-weights at the gates which reduces the necessary torque to move them. Counterweights allow also to work in any orientation which is a desirable feature when the slightest pressure loss could affect greatly the performance. Additionally, the pressure drop was minimized by a unique design of the gates, which reduce the stroke, and the shadow when opened. A reduced stroke also permits to open and close more rapidly. According to the numerical analysis performed on developed check-valve models and commercial models can be concluded that it is more recommendable the use of the developed check-valves against the commercial models due to a pressure-drop improvement.

Numerical analysis, and experimental tests suggest that the conduit diameter may be increased to increase efficiency around 1.8 times. An optimization will be desirable as a future work to find the best value for this critical characteristic. The knowledge on the full behavior from this WEC device is far from being complete, but the present study contributed uniquely to widening it. The experience of the deployments at the ocean throw valuable experience at installation as well as in product development by identifying new failure modes which can now be addressed in the next stage of design.

Lighting LEDs out of pure ocean energy with a cost-effective and practical device is a remarkable achievement which contributed to create alliances with local team players and the future continuation of the project by a leader university and R&D consortium integrated by more than 40 members (Research Centers, universities, and

industries), which will likely make it a competitive device and potentially bring it into a real Full Size Device generating clean energy.

A Near-shore device has the disadvantage of having a smaller wave resource available. However, wind energy has demonstrated that it is more cost-feasible to waste excess energy during faster winds, rather than over dimension the device building a larger wind-turbine, able to catch those less frequent faster winds. Hence, a smaller, less expensive device may be created for near-shore waves which might still be cost feasible. Underwater cable is expensive, depending on its characteristics, it cost may range between $282,000 - 939,000 Euros [23], other sources mention even higher levels or approximated to 10% of total project cost [126]. A further possibility of the present device that might be evaluated in a future work, is utilizing the air-conduits to bring the energy, and turbine to land, replacing the electrical cable by air conduits to potentially obtain cost savings. Future work must include optimization of the device by numerical work Wave-Flume test

Phase Control strategies have demonstrated to greatly improve efficiency and are a increasing field of study among the WECs [127]. A further phase control mechanism and strategy will be important in future work to improve device performance. Turbine is an essential part for the good performance of the UFCAP WEC. Turbine development is necessary given the special flow characteristics. A wider range of airflow velocities must be considered for its design, rather than maximize performance for a target airflow velocity since the wave resource has variations, and the airflow is varying from wave to wave.

In summary, this work presents a WEC with important economical and implementation advantages and unique studies on the device, suggestion for redesign to improve performance, and field experience at ocean to support further deployments. However, much work is still to be done to fully characterize and control, to bring

Ocean WECs to a competitive stage among the renewable energies.

Appendix A

Cost Projections

Table A.1: Predicted Cost of UFCAP vs. WECs

Device	Rating	US$/kW	US$MW-hr	Cost*
UFCAP	10 kW	$ 19,230.77	$ 1,100.00	$ 192,308.00
UFCAP	500 kW	$ 1,892.31	$ 150.00	$ 946,154.00
UFCAP	2 MW	$ 1,361.54	$ 110.00	$ 2,723.077.00
UFCAP	$\geq$ 2 MW	$\leq$ $ 1,100.00	$ 100.00	**
Pelamis	2.25 MW	$ 5,466.67	$ 350.00	$ 12,300.00
Eolic***	2.5 MW	$ 2,000	$ 100.00	$ 5'000,000.00
Others****	750 kW	$ 8,000	$ 1,971.00	$ 6'000,000.00

* Costs include only the device (i.e. no transmission, studies, etc.). Prices quoted in Mexico in 2010. Exchange rate 13MXN=1 USD.

** Depends on rated size.

*** Wind Farm Cost in North America [87].

**** Cost from a real quoted project from an Australian Firm to the Mexican Federal Electricity Commission. (personnel interview 2008).

Appendix B

Turbine information

Space intentionally blank

Table B.1: Airfoils utilized in similar industry applications

WinTurbine other families	Wind Turbine NACA family	NACA in Helicopters	NACA in airplane wings
230XX	230XX	6-H-10	2412
RIS-A1-21	63-series	6-H-15	2414
RIS-A1-24	63-215	6-H-20	2415
RISO-1	63-218	8-H-12	6409
63-415-Ris-D	63-221	23012	
FFA-W3-XXX	63-415	FX 69-H-098	
FX66-s-196 V1	63-418		
FX 63-137	63-421		
E387	63-425		
S822			
S823			
S834			
SD2030			
SH3055			
A18			
BW-3			
GOE 417a			
SD7032			
SD7062			
SG6040			
SG6042			
SG6043			
USNPS-4			
RIS-A1-18			

Table B.2: Coordinates airfoil J1-1, actual size and orientation

X (mm)	Y (mm)	X (mm)	Y (mm)
-3.377	5.200	-3.77	5.200
-3.308	5.334	-3.275	5.103
-3.266	5.366	-3.231	5.088
-3.226	5.395	-3.186	5.075
-3.052	5.483	-3.015	5.042
-2.685	5.602	-2.686	4.988
-2.302	5.659	-2.372	4.920
-1.911	5.667	-2.068	4.837
-1.134	5.547	-1.494	4.611
-0.396	5.268	-0.965	4.307
0.274	4.861	-0.477	3.933
0.868	4.362	-0.029	3.505
1.387	3.798	0.391	3.031
1.809	3.170	0.760	2.506
2.160	2.511	1.100	1.951
2.452	1.833	1.417	1.373
2.686	1.141	1.710	0.772
2.870	0.439	1.978	0.152
3.011	-0.267	2.223	-0.484
3.115	-0.975	2.447	-1.134
3.189	-1.683	2.651	-1.794
3.241	-2.390	2.836	-2.464
3.275	-3.096	3.002	-3.141
3.301	-3.799	3.150	-3.823
3.330	-4.501	3.176	-4.510

Table B.3: Coordinates airfoil J1-2, actual size and orientation

X (mm)	Y (mm)	X (mm)	Y (mm)
0.052	-0.517	8.814	-10.504
0.260	-1.012	8.444	-10.124
0.500	-1.492	8.090	-9.728
0.760	-1.961	7.745	-9.325
1.035	-2.422	7.407	-8.915
1.324	-2.874	7.076	-8.501
1.625	-3.318	6.749	-8.082
1.925	-3.738	6.427	-7.661
2.247	-4.166	6.107	-7.237
2.594	-4.604	5.789	-6.812
2.938	-5.015	5.472	-6.386
3.292	-5.419	5.156	-5.960
3.650	-5.811	4.839	-5.534
4.026	-6.205	4.521	-5.109
4.396	-6.579	4.203	-4.684
4.793	-6.965	3.883	-4.261
5.186	-7.336	3.559	-3.840
5.578	-7.696	3.232	-3.422
5.972	-8.048	2.902	-3.007
6.375	-8.402	2.568	-2.594
6.782	-8.752	2.229	-2.185
7.190	-9.101	1.887	-1.780
7.603	-9.450	1.540	-1.378
8.010	-9.793	1.188	-0.981
8.414	-10.147	0.828	-0.591

Appendix C

Ocean Physical Model

C.1 Model Modifications

After Deployment I, the following modifications to the model were made: 1. Six additional check valves were added on the manifolds to prevent back flow. This measure was taken due to the numerical simulations which indicated backflow presence. Calculated air speed at turbine with back flow was about 4m/s while without was above 20m/s.

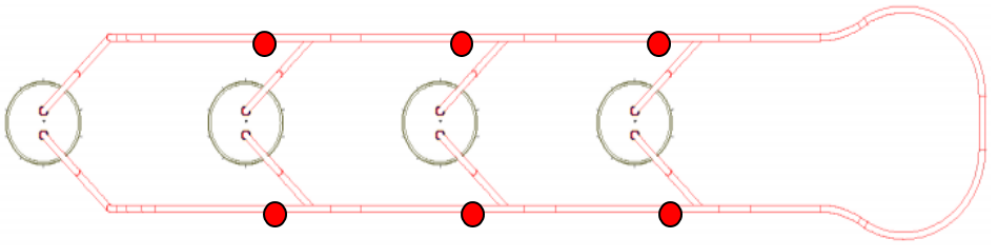

Figure C.1: Additional check-valves position.

Simplified Mooring. The plurality of sand pockets each with an individual cord was replaced by a single metal gasket filled with sand costal. This process largely simplifies the installation and removal procedures. Additionally, a single tether holds

the air-chamber conversely with 12 of them. Underwater diver tasks are simpler.

Figure C.2: Mooring metal basket and sand weights.

Additional sealing in the turbine region, due to some leakage observed last time. 2. Venturi Tube reinforced and re-sealed. 3. Distance among air-chambers was changed from 27m to 20m. Distance was reduced to allow larger waves without imposing a large stress on the conduits. During first trial conduits were broken due to large stresses on air chamber 1. 4. Floating valves were removed (they mainly caused mal-function during previous deployment). 5. Extra small boat was used to manage control board. This was found to be useful and habilitate working in parallel. 6. Installation procedure (sequence and manage of conduits, etc.) was optimized. The second trial was way more efficient and fast.

Appendix D

Analytical Model

D.1 Iterative code

```
clear all;
den_water = 1027;
g = 9.81;
deltaPck = 1500;
Patm=101325;

    Tmin=5; Tmax=14; deltaT=0.5; Wmin=1; Wmax=3; deltaW=0.2; e = 0.0001;
    N = 65;
Rcent_cond = 1.0;
deltaX = 120;
Rch = 1.0;
den_air = 4.2;
kvisc_air = 0.000004;
```

```
    mu = den_air*kvisc_air; Acent_cond = pi*Rcent_cond2̂; Ach = pi*Rch2̂;
    for j = 1 : 1: (1/deltaT)*(Tmax-Tmin)+1
for i= 1 : 1 :(1/deltaW)*(Wmax-Wmin)+1
PR_PS(i,j) = 1000;
Phi(i,j) = 1;
phi(i,j) = 2;
ach(i,j) = 2;
deltaPT(i,j)=2;
deltaPcond(i,j)=0;
Plosses(i,j)=2;
deltaPNet(i,j)=2;
P4_P1(i,j)=2;

    Wave_height(i)= Wmin +(i-1)*deltaW;
T(j)= Tmin +(j-1)*deltaT;
Pw2_Pw1(i) = den_water*g*Wave_height(i);
end
end

    for j = 1 : 1: (1/deltaT)*(Tmax-Tmin)+1
for i= 1 : 1 : (1/deltaW)*(Wmax-Wmin)+1

    for itera = 1: 1: 90 phi(i,j) = Phi(i,j);
    ach(i,j) = (Pw2_Pw1(i) - PR_PS(i,j))/(2*g*(den_water + den_air)); Phi(i,j) =
N*Ach*4*ach(i,j)/T(j); deltaPT(i,j) = den_air*Phi(i,j)2̂/(pi2̂*Rcent_cond4̂); Plosses(i,j)
= 2*deltaPck + 2*deltaPcond(i,j) + deltaPT(i,j); deltaPNet(i,j) = Phi(i,j)*8*mu*deltaX/(pi*Rcent
```

P4_P1(i,j) = deltaPNet(i,j) + Plosses(i,j); PR_PS(i,j) = P4_P1(i,j); if (abs(Phi(i,j)-phi(i,j)) ¡ e)

break

end

end

vel(i,j) = Phi(i,j)/Acent_cond;

P(i,j) = 0.5 * den_air * vel(i,j)$\hat{3}$ * Acent_cond/1000; if (abs(Phi(i,j)-phi(i,j)) ¿ 100*e)

P(i,j) = -0;

end

end

end

itera

Bibliography

[1] M. I. Yuce and A. Muratoglu, "Hydrokinetic energy conversion systems: A technology status review," *Renewable and Sustainable Energy Reviews*, vol. 43, pp. 72–82, 2015.

[2] H. Fernandez, G. Iglesias, R. Carballo, A. Castro, J. A. Fraguela, F. Taveira-Pinto, and M. Sanchez, "The new wave energy converter WaveCat: Concept and laboratory tests," *Marine Structures*, vol. 29, no. 1, pp. 58–70, 2012.

[3] B. Drew, A. Plummer, and M. N. Sahinkaya, "A review of wave energy converter technology," *Journal of Power and Energy*, vol. 223, pp. 887–902, 2009.

[4] A. Falcão, J. Henriques, and L. Gato, "Rotational speed control and electrical rated power of an oscillating-water-column wave energy converter," *Energy*, vol. 120, pp. 253–261, 2016.

[5] K. Thiruvenkatasamya9 and S. Neelamanib, "On the efficiency of wave in array energy caissons," *Applied Ocean Research*, vol. 19, pp. 61–72, 1997.

[6] Z. B.-S. H. H. S. K. H. Liu, "Practical Simulation of Oscillating Water Column Chamber for Wave Energy Conversion," *International Journal of Green Energy*, vol. 7, no. April 2015, pp. 337–346, 2010.

[7] J. Falnes, "A review of wave-energy extraction," *Marine Structures*, vol. 20, no. 4, pp. 185–201, 2007.

[8] I. E. Agency, "Status Research and Development Priorities 2003," tech. rep., IEA, 2003.

[9] A. F. d. O. Falcao, "Wave energy utilization: A review of the technologies," *Renewable and Sustainable Energy Reviews*, vol. 14, no. 3, pp. 899–918, 2010.

[10] K. L. Guiberteau, Y. Liu, J. Lee, and T. A. Kozman, "Investigation of Developing Wave Energy Technology In the Gulf of Mexico," *Distributed Generation & Alternative Energy Journal*, vol. 27, no. 4, pp. 36–52, 2012.

[11] K. Ruehl and D. Bull, "Wave Energy Development Roadmap: Design to commercialization," *OCEANS 2012 MTS/IEEE: Harnessing the Power of the Ocean*, 2012.

[12] J. H. Wilson and A. Beyene, "California Wave Energy Resource Evaluation," in *Volume 5: Ocean Space Utilization; Polar and Arctic Sciences and Technology; The Robert Dean Symposium on Coastal and Ocean Engineering; Special Symposium on Offshore Renewable Energy*, vol. v 5, pp. 549–562, ASME, 2007.

[13] A. Clément, P. Mccullen, A. Fiorentino, F. Gardner, K. Hammarlund, G. Lemonis, T. Lewis, K. Nielsen, S. Petroncini, P. Schild, B. Sjo, and T. Thorpe, "Wave energy in Europe: current status and perspectives," *Renewable and Sustainable Energy Reviews*, vol. 6, pp. 405–431, 2002.

[14] R. Prest, T. Daniell, and B. Ostendorf, "Using GIS to evaluate the impact of exclusion zones on the connection cost of wave energy to the electricity grid," *Energy Policy*, vol. 35, no. 9, pp. 4516–4528, 2007.

[15] M. Previsic, "Wave Power Technologies Paper 05 GM 0542," in *HARNESSING THE UNTAPPED ENERGY POTENTIAL OF THE OCEANS: TIDAL, WAVE, CURRENTS AND OTEC* (Energy Development and Power Generation Committee, ed.), (San Francisco), pp. 12–16, IEEE POWER ENGINEERING SOCIETY, 2005.

[16] A. F. O. Falc??o and J. C. C. Henriques, "Oscillating-water-column wave energy converters and air turbines: A review," *Renewable Energy*, vol. 85, pp. 1391–1424, 2016.

[17] Iea, "World Energy Outlook 2006," *Outlook*, p. 600pp, 2006.

[18] G. J. Dalton, R. Alcorn, and T. Lewis, "Case study feasibility analysis of the Pelamis wave energy convertor in Ireland, Portugal and North America," *Renewable Energy*, vol. 35, no. 2, pp. 443–455, 2010.

[19] J. Rodriguez, *The Unidirectional Flow Collective Air Pumps A Novel Wave Energy Converter*. Master of applied science thesis, University of Victoria, 2006.

[20] S. Astariz and G. Iglesias, "The economics of wave energy: A review," *Renewable and Sustainable Energy Reviews*, vol. 45, pp. 397–408, 2015.

[21] L. Castro-Santos, G. P. Garcia, A. Estanqueiro, and P. A. Justino, "The Levelized Cost of Energy (LCOE) of wave energy using GIS based analysis: The case study of Portugal," *International Journal of Electrical Power & Energy Systems*, vol. 65, pp. 21–25, 2015.

[22] N. Farrell, C. O. Donoghue, and K. Morrissey, "Quantifying the uncertainty of wave energy conversion device cost for policy appraisal: An Irish case study," *Energy Policy*, vol. 78, pp. 62–77, 2015.

[23] M. O'Connor, T. Lewis, and G. Dalton, "Techno-economic performance of the Pelamis P1 and Wavestar at different ratings and various locations in Europe," *Renewable Energy*, vol. 50, pp. 889–900, 2013.

[24] R. E. Bedard, "Ocean Wave Power / Energy Economics."

[25] I. Webb, C. Seaman, and G. Jackson, "Oscillating water column wave energy converter evaluation report," *the Carbon Trust*, 2005.

[26] J. Fievez and K. O. Brien, "Progress toward the Worldwide Deployment of the CETO Wave Energy Technology," *4th International Conference on Ocean Energy*, pp. 1–5, 2012.

[27] A. F. O. Falcão, J. C. C. Henriques, and J. J. Cândido, "Dynamics and optimization of the OWC spar buoy wave energy converter," *Renewable Energy*, vol. 48, pp. 369–381, 2012.

[28] J. Cruz, *Ocean Wave Energy*. Springer Berlin Heidelberg, 2002.

[29] E. Friis-Madsen, H. C. Sørensen, and S. Parmeggiani, "The development of a 1 . 5 MW Wave Dragon North Sea Demonstrator," *4th International Conference on Ocean Energy*, pp. 1–5, 2012.

[30] J. P. Kofoed, P. Frigaard, E. Friis-Madsen, and H. C. Sørensen, "Prototype testing of the wave energy converter wave dragon," *Renewable Energy*, vol. 31, no. 2, pp. 181–189, 2006.

[31] J. Tedd and J. Peter Kofoed, "Measurements of overtopping flow time series on the Wave Dragon, wave energy converter," *Renewable Energy*, vol. 34, no. 3, pp. 711–717, 2009.

[32] N. Delmonte, D. Barater, F. Giuliani, and P. Cova, "Oscillating Water Column Power Conversion : a Technology Review," *Energy Conversion Congress and Exposition (ECCE), 2014 IEEE*, pp. 1852–1859, 2014.

[33] P. Filianoti and S. M. Camporeale, "A linearized model for estimating the performance of submerged resonant wave energy converters," *Renewable Energy*, vol. 33, no. 4, pp. 631–641, 2008.

[34] UBelfast, "Islay limpet wave power plant," *Control*, no. April, pp. 1–62, 2002.

[35] D. Evans and R. Porter, "Hydrodynamic characteristics of an oscillating water column device," *Applied Ocean Research*, vol. 17, no. 3, pp. 155–164, 1995.

[36] M. a. Srokosz and D. V. Evans, "A theory for wave-power absorption by two independently oscillating bodies," *Journal of Fluid Mechanics*, vol. 90, no. 02, p. 337, 1976.

[37] C. B. Boake, T. J. T. Whittaker, M. Folley, and H. Ellen, "Overview and Initial Operational Experience of the LIMPET Wave Energy Plant," *Proceedings of The 12th International Offshore and Polar Engineering Conference*, vol. 3, no. January, pp. 586–594, 2002.

[38] J. Fernández chozas, "Estudio de Plantas de Produccion de Energias Renovables con Aprovechamiento de la Energia del Mar." Universidad Politecnica de Madrid, 2008.

[39] J. Rodriguez and A. Suleman, "Apparatus for converting ocean wave energy into mechanical energy." Canadian Intellectual Property Office. CA 2692188, 2006.

[40] A. Fleming, I. Penesis, G. MacFarlane, N. Bose, and T. Denniss, "Energy balance analysis for an oscillating water column wave energy converter," *Ocean Engineering*, vol. 54, pp. 26–33, 2012.

[41] B. Pereiras, F. Castro, A. el Marjani, and M. A. Rodríguez, "An improved radial impulse turbine for OWC," *Renewable Energy*, vol. 36, no. 5, pp. 1477–1484, 2011.

[42] A. Thakker and R. Abdulhadi, "The performance of Wells turbine under bidirectional airflow," *Renewable Energy*, vol. 33, no. 11, pp. 2467–2474, 2008.

[43] K. Mala, J. Jayaraj, V. Jayashankar, T. M. Muruganandam, S. Santhakumar, M. Ravindran, M. Takao, T. Setoguchi, K. Toyota, and S. Nagata, "A twin unidirectional impulse turbine topology for OWC based wave energy plants - Experimental validation and scaling," *Renewable Energy*, vol. 36, no. 1, pp. 307–314, 2011.

[44] M. Torresi, S. M. Camporeale, P. D. Strippoli, and G. Pascazio, "Accurate numerical simulation of a high solidity Wells turbine," *Renewable Energy*, vol. 33, no. 4, pp. 735–747, 2008.

[45] M. Amundarain, M. Alberdi, A. J. Garrido, I. Garrido, and J. Maseda, "Wave energy plants: Control strategies for avoiding the stalling behaviour in the Wells turbine," *Renewable Energy*, vol. 35, no. 12, pp. 2639–2648, 2010.

[46] T. H. Kim, T. Setoguchi, K. Kaneko, and S. Raghunathan, "Numerical investigation on the effect of blade sweep on the performance of Wells turbine," *Renewable Energy*, vol. 25, no. 2, pp. 235–248, 2002.

[47] Z. Taha, Sugiyono, and T. Sawada, "A comparison of computational and experimental results of Wells turbine performance for wave energy conversion," *Applied Ocean Research*, vol. 32, no. 1, pp. 83–90, 2010.

[48] M. Folley, R. Curran, and T. Whittaker, "Comparison of LIMPET contra-rotating wells turbine with theoretical and model test predictions," *Ocean Engineering*, vol. 33, no. 8-9, pp. 1056–1069, 2006.

[49] S. Ceballos, J. Rea, E. Robles, I. Lopez, J. Pou, and D. O'Sullivan, "Control strategies for combining local energy storage with wells turbine oscillating water column devices," *Renewable Energy*, vol. 83, pp. 1097–1109, 2015.

[50] M. a. Srokosz and D. V. Evans, "A theory for wave-power absorption by two independently oscillating bodies," *Journal of Fluid Mechanics*, vol. 90, no. 02, p. 337, 1979.

[51] A. Brendmo, J. Falnes, and P. M. Lillebekken, "Linear modelling of oscillating water columns including viscous loss," *Applied Ocean Research*, vol. 18, no. 2-3, pp. 65–75, 1996.

[52] A. Sarmento and A. De O. Falcao, "Wave Generation by an Oscillating Surface-Pressure and Its Application in Wave-Energy Extraction," *Journal of Fluid Mechanics*, vol. 150, no. May, pp. 467–485, 1985.

[53] J. Falnes and P. McIver, "Surface wave interactions with systems of oscillating bodies and pressure distributions," *Applied Ocean Research*, vol. 7, no. 4, pp. 225–234, 1985.

[54] D. Evans and R. Porter, "Efficient calculation of hydrodynamic properties of OWC-type devices," *Journal of Offshore Mechanics and Arctic Engineering*, vol. 119, pp. 210–218, nov 1997.

[55] Z. Deng, Z. Huang, and A. W. K. Law, "Wave power extraction from a bottom-mounted oscillating water column converter with a V-shaped channel," *Proceedings of the Royal Society A: Mathematical, Physical and Engineering Sciences*, vol. 470, no. 2167, pp. 20140074–20140074, 2014.

[56] A. Kamath, H. Bihs, and Ø. A. Arntsen, "Numerical modeling of power take-off damping in an oscillating water column device," *International Journal of Marine Energy*, vol. 10, pp. 1–16, 2015.

[57] Y. Luo, J. R. Nader, P. Cooper, and S. P. Zhu, "Nonlinear 2D analysis of the efficiency of fixed Oscillating Water Column wave energy converters," *Renewable Energy*, vol. 64, pp. 255–265, 2014.

[58] U. entürk and A. Özdamar, "Wave energy extraction by an oscillating water column with a gap on the fully submerged front wall," *Applied Ocean Research*, vol. 37, pp. 174–182, 2012.

[59] B. Bouali and S. Larbi, "Sequential optimization and performance prediction of an oscillating water column wave energy converter," *Ocean Engineering*, vol. 131, no. May 2015, pp. 162–173, 2017.

[60] T. K. A. Brekken, K. Rhinefrank, A. Von Jouanne, A. Schacher, J. Prudell, and E. Hammagren, "Scaled development of a novel wave energy converter including numerical analysis and high-resolution tank testing," *Proceedings of the IEEE*, vol. 101, no. 4, pp. 866–875, 2013.

[61] M. Meier, G. Yadigaroglu, and B. L. Smith, "A novel technique for including surface tension in PLIC-VOF methods," *European Journal of Mechanics, B/Fluids*, vol. 21, no. 1, pp. 61–73, 2002.

[62] G. Payne, "Guidance for the experimental tank testing of wave energy converters," *SuperGen Marine, University of Edinburgh*, 2008.

[63] M. T. Morris-thomas and R. J. Irvin, "An Investigation Into the Hydrodynamic Efficiency of an," vol. 129, no. 7491, pp. 273–278, 2017.

[64] L. Wan, Z. Gao, T. Moan, and C. Lugni, "Experimental and numerical comparisons of hydrodynamic responses for a combined wind and wave energy converter concept under operational conditions," *Renewable Energy*, vol. 93, pp. 87–100, 2016.

[65] J. Fairhurst and J. L. V. Niekerk, "International Journal of Marine Energy Modelling , simulation and testing of a submerged oscillating water column," *International Journal of Marine Energy*, vol. 16, pp. 181–195, 2016.

[66] R. P. F. Gomes, J. C. C. Henriques, L. M. C. Gato, and A. F. O. Falc??o, "Wave power extraction of a heaving floating oscillating water column in a wave channel," *Renewable Energy*, vol. 99, pp. 1262–1275, 2016.

[67] A. F. O. Falcão and J. C. C. Henriques, "Model-prototype similarity of oscillating-water-column wave energy converters," *International Journal of Marine Energy*, vol. 6, pp. 18–34, 2014.

[68] K. Ram, M. Faizal, M. Ahmed, and Y. Lee, "Experimental studies on the flow characteristics in an oscillating water column device," *Journal of Mechanical Science and Technology*, vol. 24, no. 10, pp. 2043–2050, 2010.

[69] K. Rezanejad, C. Guedes Soares, I. López, and R. Carballo, "Experimental and Numerical Investigation of the Hydrodynamic Performance of an Oscillating Water Column Wave Energy Converter," *Renewable Energy*, vol. 106, 2017.

[70] D. Z. Ning, R. Q. Wang, Q. P. Zou, and B. Teng, "An experimental investigation of hydrodynamics of a fixed OWC Wave Energy Converter," *Applied Energy*, vol. 168, pp. 636–648, 2016.

[71] F. X. Correia da Fonseca, R. P. F. Gomes, J. C. C. Henriques, L. M. C. Gato, and A. F. O. Falc??o, "Model testing of an oscillating water column spar-buoy wave energy converter isolated and in array: Motions and mooring forces," *Energy*, vol. 112, pp. 1207–1218, 2016.

[72] S. K. Patel, K. Ram, and M. R. Ahmed, "Effect of turbine section orientation on the performance characteristics of an oscillating water column device," *Experimental Thermal and Fluid Science*, vol. 44, pp. 642–648, 2013.

[73] J. C. C. Henriques, R. P. F. Gomes, L. M. C. Gato, A. F. O. Falcão, E. Robles, and S. Ceballos, "Testing and control of a power take-off system for an oscillating-water-column wave energy converter," *Renewable Energy*, vol. 85, pp. 714–724, 2016.

[74] J. C. C. Henriques, L. M. C. Gato, A. F. O. Falcão, E. Robles, and F. X. Faÿ, "Latching control of a floating oscillating-water-column wave energy converter," *Renewable Energy*, vol. 90, pp. 229–241, 2016.

[75] Y. Dai, Y. Chen, and L. Xie, "A study on a novel two-body fl oating wave energy converter," *Ocean Engineering*, vol. 130, no. July 2015, pp. 407–416, 2017.

[76] T. Vyzikas, S. Deshoulières, M. Barton, O. Giroux, D. Greaves, and D. Simmonds, "Experimental investigation of different geometries of fixed oscillating water column devices," *Renewable Energy*, vol. 104, pp. 248–258, 2017.

[77] A. N. Fleming and G. J. Macfarlane, "Experimental flow field comparison for a series of scale model oscillating water column wave energy converters," *Marine Structures*, vol. 52, pp. 108–125, 2017.

[78] T. Kinoshita and W. Kato, "Fundamental Research on Oscillating Water Column Wave Power Absorbers," vol. 107, no. March 1985, 2017.

[79] Y. Saadat, N. Fernandez, A. Samimi, M. R. Alam, M. Shakeri, and R. Ghorbani, "Investigating of Helmholtz wave energy converter," *Renewable Energy*, vol. 87, pp. 67–76, 2016.

[80] S. Ogai, S. Umeda, and H. Ishida, "An experimental study of compressed air generation using a pendulum wave energy converter," *Journal of Hydrodynamics, Ser. B*, vol. 22, no. 5, pp. 290–295, 2010.

[81] E. Renzi and F. Dias, "Hydrodynamics of the oscillating wave surge converter in the open ocean," *European Journal of Mechanics, B/Fluids*, vol. 41, pp. 1–10, 2013.

[82] D. G. Dorrell, S. S. Ngu, and C. Cossar, "Comparison of permanent magnet generators for a very low speed renewable energy application," *Proceedings - 2012 20th International Conference on Electrical Machines, ICEM 2012*, pp. 115–121, 2012.

[83] L. Szabo, C. Oprea, I. A. Viorel, and K. A. Biro, "Novel Permanent Magnet Tubular Linear Generator for Wave Energy Converters," *2007 IEEE International Electric Machines Drives Conference*, vol. 2, pp. 983–987, 2007.

[84] R. Vermaak and M. J. Kamper, "Design aspects of a novel topology air-cored permanent magnet linear generator for direct drive wave energy converters,"

IEEE Transactions on Industrial Electronics, vol. 59, no. 5, pp. 2104–2115, 2012.

[85] M. A. Mueller, H. Polinder, and N. Baker, "Current and novel electrical generator technology for wave energy converters," *Proceedings of IEEE International Electric Machines and Drives Conference, IEMDC 2007*, vol. 2, no. 1, pp. 1401–1406, 2007.

[86] D. L. O'Sullivan and A. W. Lewis, "Generator selection for offshore oscillating water column wave energy converters," *2008 13th International Power Electronics and Motion Control Conference, EPE-PEMC 2008*, pp. 1790–1797, 2008.

[87] I. Renewable Energy Agency, "Renewable Energy Cost Analysis: Wind Power," 2012.

[88] R. Henderson, "Design, simulation, and testing of a novel hydraulic power take-off system for the Pelamis wave energy converter," *Renewable Energy*, vol. 31, no. 2, pp. 271–283, 2006.

[89] M. F. P. Lopes, J. Hals, R. P. F. Gomes, T. Moan, L. M. C. Gato, and A. F. d. O. Falcão, "Experimental and numerical investigation of non-predictive phase-control strategies for a point-absorbing wave energy converter," *Ocean Engineering*, vol. 36, no. 5, pp. 386–402, 2009.

[90] Camara de Diputados del H. Congreso de la Union, "Ley para el aprovechamiento sustentable de energía 2008." http://dof.gob.mx/nota_detalle.php?codigo=5070928&fecha=28/11/2008, 2008.

[91] Camara de Diputados del H. Congreso de la Union, "Ley de Promocion y Desarrollo de los bioenergeticos. 2008." http://www.diputados.gob.mx/LeyesBiblio/pdf/LPDB.pdf, 2008.

[92] Camara de Diputados del H. Congreso de la Union, "Ley para el aprovechamiento de energías renovables y el financiamiento de la transición energetica 2008." http://www.diputados.gob.mx/LeyesBiblio/abro/laerfte/LAERFTE_orig_28nov08.pdf.

[93] Camara de Diputados del H. congreso de la Union, "Ley de Transicion energetica 2015.." http://www.diputados.gob.mx/LeyesBiblio/pdf/LTE.pdf, 2015.

[94] B. W. Karney and A. R. Simpson, "In-line check valves for water hammer control," *Journal of Hydraulic Research*, vol. 45, no. 4, pp. 547–554, 2007.

[95] J. Cassata, Z. Feng, S. Dasgupta, and R. Samways, "Prevent overpressure failures on heat exchangers," *Hydrocarbon Processing*, vol. 77, p. p, nov 1998.

[96] Stojkov Brent T., "Valve Primer," *Industrial Press*, 2010.

[97] K. L. McElhaney, "Analysis of check valve performance characteristics based on valve design," *Nuclear Engineering and Design*, vol. 197, no. 1, pp. 169–182, 2000.

[98] D. E. Albrecht Jr., "Slip-in and thread-in check valve elements," *Fluid Power Journal*, vol. 13, no. 9, pp. 14–15, 2006.

[99] K. Ou and M. Chiao, "A passive check valve using microspheres for low pressure and low flow rate applications," *2011 16th International Solid-State Sensors, Actuators and Microsystems Conference, TRANSDUCERS'11*, pp. 1785–1788, 2011.

[100] H. Tu, E. Kim, and Y. Xu, "An in-channel micro check valve fabricated using a simple two-mask process," *Proceedings of IEEE Sensors*, vol. 2, pp. 1–4, 2012.

[101] J. Burger, M. van der Wekken, E. Berenschot, H. Holland, H. ter Brake, H. Rogalla, J. Gardeniers, and M. Elwenspoek, "High pressure check valve for application in a miniature cryogenic sorption cooler," *Technical Digest. IEEE International MEMS 99 Conference. Twelfth IEEE International Conference on Micro Electro Mechanical Systems (Cat. No.99CH36291)*, 1999.

[102] G. Bryans and R. Payne, "FPMC2015-9597 COMPONENT ANALYSIS FOR HYDROSTATIC TRANSMISSION FOR WAVE ENERGY APPLICATION SIMULATION AND VALIDATION," pp. 1–10, 2017.

[103] H. Sugiyama, K. Ohtani, Y. Sasaki, H. Musha, K. Mizobata, T. Ohishi, and T. Miwa, "Dynamic characteristics of a check valve for drain pumps," *Proceedings of the ASME/JSME Joint Fluids Engineering Conference*, vol. 2 D, pp. 2851–2856, 2003.

[104] J. R. Valdés, J. M. Rodríguez, R. Monge, J. C. Peña, and T. Pütz, "Numerical simulation and experimental validation of the cavitating flow through a ball check valve," *Energy Conversion and Management*, vol. 78, pp. 776–786, 2014.

[105] T. T. Veenstra, G. C. F. Venhorst, J. F. Burger, H. J. Holland, H. J. M. Brake, A. Sirbi, and H. Rogalla, "Development of a stainless steel check valve for cryogenic applications," vol. 47, pp. 121–126, 2007.

[106] Y. Rao, L. Yu, S. Fu, and F. Zhang, "Annals of Nuclear Energy Development of a butterfly check valve model under natural circulation conditions," *Annals of Nuclear Energy*, vol. 76, pp. 166–171, 2015.

[107] A. Hansen, H. Pedersen, and T. Andersen, "Design of bidirectional check valve for discrete fluid power force system for wave energy converters," *ASME/BATH 2013 Symposium on Fluid Power and Motion Control, FPMC 2013*, 2013.

[108] A. H. Hansen, H. C. Pedersen, and T. O. Andersen, "Model based feasibility study on bidirectional check valves in wave energy converters," *International Journal of Marine Energy*, vol. 5, pp. 1–23, 2014.

[109] W. Al-Faqheri, F. Ibrahim, T. H. G. Thio, M. M. Aeinehvand, H. Arof, and M. Madou, "Development of novel passive check valves for the microfluidic CD platform," *Sensors and Actuators, A: Physical*, vol. 222, pp. 245–254, 2015.

[110] Val-Matic Specification, "Surgebuster Swing Check Valve." http://www.valmatic.com/drawings/VM-7200-S_12-2-14.pdf.

[111] Val-Matic Specification, "Dual Disc Check Valve." http://www.valmatic.com/drawings/VM-8802-S_7-5-11.pdf.

[112] B. E. Dallstream, "Swing Check Valve Design Criteria and CFD Validation," pp. 1–9, 2017.

[113] S. L. S. L. Dixon, *Fluid mechanics, thermodynamics of turbomachinery*. Elsevier-Butterworth-Heinemann, 2005.

[114] W. Braitsch and H. Haas, "2.7 Turbines for hydroelectric power," in *Renewable Energy*, pp. 197–222, Springer Berlin Heidelberg.

[115] H. Martins-Rivas and C. C. Mei, "Wave power extraction from an oscillating water column at the tip of a breakwater," *Journal of Fluid Mechanics*, vol. 626, p. 395, 2009.

[116] T. Burton, N. Jenkins, D. Sharpe, and E. Bossanyi, *Wind Energy Handbook*. Chichester, UK: John Wiley & Sons, Ltd, may 2011.

[117] H. Cohen, G. F. C. G. F. C. Rogers, and H. I. H. Saravanamuttoo, *Gas turbine theory*. Longman Scientific & Technical, 1987.

[118] UIUC Applied Aerodynamics Group, "UIUC Airfoil Coordinates Database."

[119] M. A. Bhinder, C. G. Mingham, D. M. Causon, M. T. Rahmati, G. A. Aggidis, and R. V. Chaplin, "Numerical and experimental study of a point absorbing wave energy converter in regular waves," *Clean Electrical Power, 2009 International Conference on*, pp. 599–603, 2009.

[120] K. Lynch, J. Murphy, L. Serri, and D. Airoldi, "Site Selection Methodology for Combined Wind and Ocean Energy Technologies In Europe," *4th International Conference on Ocean Energy*, 2012.

[121] C. E. Choi, C. W. W. Ng, S. C. H. Au-Yeung, and G. R. Goodwin, "Froude characteristics of both dense granular and water flows in flume modelling," *Landslides*, 2015.

[122] H. Cavitation, "General Modelling and Scaling Laws," *Methods*, no. 1.

[123] CFE, "Rosarito Proyecto Oleaje (1994-2009)," 2010.

[124] P. Boccotti, P. Filianoti, V. Fiamma, and F. Arena, "Caisson breakwaters embodying an OWC with a small opening-Part II: A small-scale field experiment," *Ocean Engineering*, vol. 34, no. 5-6, pp. 820–841, 2007.

[125] P. Boccotti, "Comparison between a U-OWC and a conventional OWC," *Ocean Engineering*, vol. 34, no. 5-6, pp. 799–805, 2007.

[126] G. J. Dalton, R. Alcorn, and T. Lewis, "A 10 year installation program for wave energy in Ireland: A case study sensitivity analysis on financial returns," *Renewable Energy*, vol. 40, no. 1, pp. 80–89, 2012.

[127] G. Nunes, D. Valério, P. Beirão, and J. Sá da Costa, "Modelling and control of a wave energy converter," *Renewable Energy*, vol. 36, no. 7, pp. 1913–1921, 2011.